

NONCLASSICAL PROPERTIES OF LIGHT IN  
ATOM-CAVITY INTERACTION SCHEME WITH TIME-  
AND INTENSITY-DEPENDENT COUPLING

NOR HAZMIN SABRI

PHYSICS DEPARTMENT, FACULTY OF SCIENCE  
UNIVERSITY OF MALAYA  
KUALA LUMPUR

2013

NONCLASSICAL PROPERTIES OF LIGHT IN  
ATOM-CAVITY INTERACTION SCHEME WITH TIME-  
AND INTENSITY-DEPENDENT COUPLING

NOR HAZMIN SABRI

THESIS SUBMITTED IN FULFILMENT  
OF THE REQUIREMENTS  
FOR THE DEGREE OF DOCTOR OF PHILOSOPHY

PHYSICS DEPARTMENT, FACULTY OF SCIENCE  
UNIVERSITY OF MALAYA  
KUALA LUMPUR

2013

**UNIVERSITI MALAYA**  
**ORIGINAL LITERARY WORK DECLARATION**

Name of Candidate: Nor Hazmin bt. Sabri (I.C./Passport No.:800627085438)

Registration/Matrix No.: SHC100078

Name of Degree: Doctor of Philosophy

Title of Project Paper/Research Report/Dissertation/Thesis ("this Work"):

Nonclassical Optical Properties of Light in Atom-Cavity Interaction Scheme with Time- and Intensity-Dependent Coupling

Field of Study: Theoretical Physics, Quantum Optics, Atom & Molecular Physics

I do solemnly and sincerely declare that:

- (1) I am the sole author/writer of this Work;
- (2) This work is original;
- (3) Any use of any work in which copyright exists was done by way of fair dealing and for permitted purposes and any excerpt or extract from, or reference to or reproduction of any copyright work has been disclosed expressly and sufficiently and the title of the Work and its authorship have been acknowledged in this Work;
- (4) I do not have any actual knowledge nor do I ought reasonably to know that the making of this work constitutes an infringement of any copyright work;
- (5) I hereby assign all and every rights in the copyright to this Work to the University of Malaya ("UM"), who henceforth shall be owner of the copyright in this Work and that any reproduction or use in any form or by any means whatsoever is prohibited without the written consent of UM having been first had and obtained;
- (6) I am fully aware that if in the course of making this Work I have infringed any copyright whether intentionally or otherwise, I may be subject to legal action or any other action as may be determined by UM.

Candidate's Signature

Date

Subscribed and solemnly declared before,

Witness's Signature

Date

Name: Nor Hazmin binti Sabri

Designation:

## ABSTRACT

### **Nonclassical Properties of Light in Atom-Cavity Interaction Scheme with Time- and Intensity-Dependent Coupling**

The nonclassical properties of light and atomic dynamics are studied. The system considered are two level atom interact with a quantized field in a high quality cavity, which is recognized as the Jaynes-Cumming Model. The time- and intensity-dependent atom-field coupling are applied to the system, with different initial field states and initial atomic states. We also extend the system for three level atom in a cavity, and include the dissipative mechanism in the system. We consider the laser driven three level atom in a cavity coupled to a reservoir. Interesting effects of the transient coupling are analyzed through the collapse-revival pattern in population inversion, while the nonclassicality of cavity field is studied through the features in the evolution of Wigner function. The inversion of initial superposed atomic state seems to be independent of initial classical fields but can be stimulated by the Schrodinger cat field. In two level system, the oscillatory coupling coefficient can prolong the occurrence of collapse, in analogy to the Zeno effect. The intensity atom-field coupling duration is an important parameter for controlling atomic inversion and producing frozen nonclassical light in the cavity after the atom-field coupling ceases. The theory developed will provide useful physical insights for future experimental work and enhance significant knowledge on the nonclassicality of light in matter-wave interaction. The research results will particularly benefit quantum information technology.

## ABSTRAK

### **Ciri-ciri Kuantum bagi Cahaya dalam Interaksi Antara Cahaya-Jasad dengan Fungsi Gandingan Bersandarkan Masa dan Keamatan Cahaya**

Ciri-ciri optik yang melangkaui interpretasi klasik iaitu sifat kuantum, dikaji bagi memahami dinamik cahaya dan atom. Sistem kuantum yang dipertimbangkan dalam kajian ini ialah sistem atom dua aras yang berinteraksi dengan medan cahaya terkuantum dalam rongga berkualiti tinggi, yang juga dikenali sebagai model Jaynes-Cumming. Gandingan atom-cahaya bersandarkan masa dan keamatan diaplikasikan keatas sistem, dengan keadaan awalan medan cahaya dan keadaan awalan atom yang berbeza. Kami juga mempraktikkan kaedah yang sama keatas sistem yang lebih kompleks iaitu sistem atom tiga aras yang juga diletakkan dalam rongga, dan mengambilkira mekanisma pereputan. Atom tiga aras ini di pandu oleh laser dalam rongga tertutup dan berinteraksi dengan takungan sinaran. Kesan yang menarik dalam gandingan transien dianalisis melalui corak runtuh-pulih dalam songsangan populasi, manakala kekuantuman medan rongga dikaji melalui sifat medan dalam evolusi fungsi Wigner. Songsangan bagi atom berkeadaan superposisi kelihatan tidak bersandar kepada medan klasikal tetapi boleh dirangsang dengan menggunakan medan Schrodinger cat. Dalam sistem dua aras, koefisien gandingan ayunan boleh memanjangkan keadaan keruntuhan, sebagai analogi kepada kesan Zeno. Tempoh keamatan gandingan atom-medan merupakan parameter yang penting untuk mengawal songsangan atomik dan menghasilkan cahaya kuantum yang terbeku dalam rongga selepas gandingan atom-medan terhenti. Teori yang dibangunkan akan menyediakan pengetahuan fizikal yang berguna untuk kajian bereksperimen dan sekaligus meningkatkan serta menambah ilmu yang bermanfaat dalam kajian interaksi jasad-gelombang dan sifatnya yang melangkaui interpretasi klasik. Hasil kajian ini adalah bermanfaat untuk teknologi kuantum informasi khususnya.

## ACKNOWLEDGEMENTS

In the name of Allah, the most gracious and the most merciful. I would like to thank all people around me for their support. First and foremost, I owe a great deal to my supervisor, Assoc. Prof. Dr. Raymond Ooi, for his outstanding guidance and thoughtful ideas. His enthusiasm in research and his relentless curiosity, have motivated and inspired me during those years that I had the opportunity to be his student. I would like to appreciate my true love, Roslan Umar, the most understanding, patient and tolerant person for being by my side along this journey and always there to lend me his shoulder to rely on. I am thankful for having such a wonderful kids, Muqri Wafa and Irdina Wafa, and also the unforgotten deceased daughter, Syafiqatul Wafa for cheering up my life. Not to forget my helpful and caring mother, Naimah, for her unconditional love, patience and inspiration. An appreciation also goes to my father and mother in law, Umar and Eshah for their neverending du'a. I would also like to thank my whole family for their endless support. During the completion of this work, I had the privilege of working with many inspiring colleagues, in particular with Poh Choo and Aini for their helpful discussion and endless assistance, Wai Loon and Kai Shuen for always be there for me, Ka Chun, Kam Seng, Khoo, Faisal and Lee Choo Yong for the support; their contributions to this work is gratefully acknowledged. I had a very colorful life with them and have always enjoyed the friendly atmosphere of the group, and it was a privilege for me to work with such an outstanding group of people. The warmest gratitude goes to several parties; Universiti Malaysia Terengganu, Ministry of Higher Education, and University Malaya for their financial support and great help. Beyond these specific acknowledgments, I would like to thank all the people involved in this work whether directly or indirectly gave the support until this work is successfully completed.

## TABLE OF CONTENTS

<b>ORIGINAL LITERARY WORK DECLARATION</b>	<b>ii</b>
<b>ABSTRACT</b>	<b>iii</b>
<b>ACKNOWLEDGEMENTS</b>	<b>v</b>
<b>TABLE OF CONTENTS</b>	<b>vi</b>
<b>LIST OF FIGURES</b>	<b>viii</b>
<b>LIST OF TABLES</b>	<b>xi</b>
<b>LIST OF APPENDICES</b>	<b>xii</b>
<b>CHAPTER 1: INTRODUCTION TO QUANTUM OPTICS</b>	<b>1</b>
1.1 Introduction	1
1.2 Operators and States	1
1.2.1 Atomic Operators	2
1.2.2 Field Operator	3
1.2.3 Fock State and Vacuum State	4
1.2.4 Coherent States	5
1.2.5 Cat State	5
1.3 The Density Matrix	6
1.3.1 Optical Bloch Equation	7
1.4 Master Equation	11
1.4.1 Atomic Damping	11
1.4.2 Field damping	16
1.5 Conclusion	17
<b>CHAPTER 2: LIGHT-MATTER INTERACTION</b>	<b>18</b>
2.1 Introduction	18
2.2 Semiclassical Atom-Field Theory	19
2.2.1 Two-level Atom	19
2.2.2 Three-level Atom	25
2.3 Full Quantum Treatment	28
2.3.1 The Jaynes-Cumming Model	28
2.3.2 Three-Level Atom	35
2.4 Conclusion	38
<b>CHAPTER 3: NONCLASSICAL PROPERTIES OF LIGHT</b>	<b>39</b>
3.1 Introduction	39
3.2 Literature Review	40
3.3 Squeezed Light	41
	vi

3.4	Photon Anti-bunching	43
3.5	Wigner Function	44
3.6	Entropy	45
3.7	Conclusion	48
<b>CHAPTER 4: TIME- &amp; INTENSITY-DEPENDENT TWO-LEVEL ATOM</b>		<b>49</b>
4.1	Introduction	49
4.2	Related Studies	50
4.3	Dynamics of the JCM with time- and intensity-dependent coupling	52
4.3.1	Atomic inversion and coherence	55
4.3.2	Wigner function	56
4.3.3	Coupling Function Properties	57
4.3.4	Initial State of Atom and Field	59
4.4	Transient Effects in Cavity Coupling	62
4.4.1	Constant Coupling Case	63
4.4.2	Sinusoidal Coupling Function	67
4.4.3	'Hat' Pulse Function	70
4.5	Extracting Nonclassical Photons	73
4.6	Conclusions	74
<b>CHAPTER 5: ENTROPY OF A THREE-LEVEL ATOM WITH DAMPING</b>		<b>77</b>
5.1	Introduction	77
5.2	Past Researches	78
5.3	$\Lambda$ -type Three-Level Atom	80
5.4	Inversion and Entropy	86
5.5	Conclusion	89
<b>CHAPTER 6: CONCLUSION AND OUTLOOK</b>		<b>101</b>
6.1	Introduction	101
6.2	Research Significances	101
6.3	Future works	102
<b>APPENDICES</b>		<b>104</b>
<b>REFERENCES</b>		<b>123</b>



## LIST OF FIGURES

Figure 1.1	$u(t)$ vs $t$ for Bloch equation	8
Figure 1.2	$v(t)$ vs $t$ for Bloch equation	8
Figure 1.3	$w(t)$ vs $t$ for Bloch equation	9
Figure 1.4	$u(t)$ , $v(t)$ and $w(t)$ vs $t$ for Bloch equation	9
Figure 2.1	A single two-level atom placed inside a cavity	20
Figure 2.2	Three type three-level atom configuration with (i) $\Lambda$ -type, (ii) $V$ -type, and (iii) $\Xi$ configuration	26
Figure 2.3	$\Lambda$ -type three-level atom interact with two fields frequency $\omega_1$ and $\omega_2$ .	26
Figure 2.4	Collapse and Revival pattern for an inversion of the JCM for photon number $n=150$	33
Figure 3.1	Quadrature-squeezed state compared with vacuum state	42
Figure 3.2	Hanbury Brown-Twiss experiment to demonstrate the phenomena of anti-bunching using photon detector	43
Figure 3.3	Field entropy for two level atom interact with a single mode field(without damping effect) in time duration $gt = 0$ to $gt = 30$ .	47
Figure 3.4	Field entropy for two level atom interact with a single mode field(without damping effect) in time duration $gt = 0$ to $gt = 100$ .	47
Figure 3.5	Atom entropy for two level atom interact with a single mode field(without damping effect) in time duration $gt = 0$ to $gt = 100$ .	48
Figure 4.1	Research methodology for JCM with time- and intensity-dependent coupling	50
Figure 4.2	A two-level atom coupled to a quantized cavity field in arbitrary state. The cavity has negligible loss within the timescale of the atomic dynamics. Transient couplings realized by: a) transiting atom modelled by a "hat" function, and b) atom oscillating back and forth through the cavity modelled by sinusoidal function.	52
Figure 4.3	Wigner evolution and Inversion plot of $g(t) = g$ for initial coherent state and Schrodinger cat state	64
Figure 4.4	Comparison of inversion plots of $g(t) = g$ for intensity independent coupling between initial (i) coherent state and (ii) Schrodinger cat state.	65
Figure 4.5	Comparison of inversion plots of $g(t) = g$ for intensity dependent coupling between initial (i) coherent state and (ii) Schrodinger cat state.	66
Figure 4.6	Comparison of inversion plots of $g(t) = g \sin^2(xgt)$ for intensity independent coupling between initial (i) coherent state and (ii) Schrodinger cat state.	67
Figure 4.7	Comparison of inversion plots of $g(t) = g \sin^2(xgt)$ for intensity dependent coupling between initial (i) coherent state and (ii) Schrodinger cat state.	69
Figure 4.8	(i)Inversion and Wigner plot for intensity independent hat coupling function for initial coherent state at time (ii) $gt = 0$ and (iii) $gt = 10$	71

Figure 4.9	(i) Inversion and Wigner plot for intensity independent hat coupling function for initial Schrodinger cat state at time (ii) $gt = 0$ and (iii) $gt = 10$	72
Figure 4.10	The Inversion plots of hat coupling function for initial Schrodinger cat state for (ii) intensity independent case and (iii) intensity dependent case	76
Figure 5.1	Overall research overview	78
Figure 5.2	A $\Lambda$ -type three-level atom interact with a single mode field and driven by a laser	80
Figure 5.3	(i) Inversion and (ii) field entropy plot for $g = 2 \times 10^6 s^{-1}$ with $\alpha_0 = \sqrt{15}$ , and no damping mechanism considered for time duration $gt = 0$ until $gt = 15$	87
Figure 5.4	(i) Inversion, (ii) atom entropy and (iii) field entropy plot for $g = 2 \times 10^6 s^{-1}$ with $\alpha_0 = \sqrt{15}$ , $\Gamma_{ab} = \Gamma_{ac} = 10^7 s^{-1}$ for time duration $gt = 0$ until $gt = 3$	90
Figure 5.5	(i) Inversion, (ii) atom entropy and (iii) field entropy plots for $g = 2 \times 10^6 s^{-1}$ with $\alpha_0 = \sqrt{15}$ , and $\Gamma_{ab} = \Gamma_{ac} = 10^6 s^{-1}$ within time duration $gt = 0$ until $gt = 3$	91
Figure 5.6	(i) Inversion, (ii) atom entropy and (iii) field entropy plots for $g = 2 \times 10^6 s^{-1}$ with $\alpha_0 = \sqrt{15}$ , $\Gamma_{ab} = \Gamma_{ac} = 10^6 s^{-1}$ and $\gamma_F = 10^6 s^{-1}$ within time duration $gt = 0$ until $gt = 3$	92
Figure 5.7	(i) Inversion, (ii) atom entropy and (iii) field entropy plots for $g = 2 \times 10^6 s^{-1}$ with $\alpha_0 = \sqrt{15}$ , $\Gamma_{ab} = \Gamma_{ac} = 10^6 s^{-1}$ , $\gamma_F = 10^6 s^{-1}$ and $\Omega_p = 10^7 s^{-1}$ within time duration $gt = 0$ until $gt = 3$	93
Figure 5.8	(i) Inversion, (ii) atom entropy and (iii) field entropy plots for $g = 2 \times 10^6 s^{-1}$ with $\alpha_0 = \sqrt{15}$ , $\Gamma_{ab} = \Gamma_{ac} = 10^6 s^{-1}$ , $\gamma_F = 10^6 s^{-1}$ and $\Omega_p = 10^8 s^{-1}$ within time duration $gt = 0$ until $gt = 3$	94
Figure 5.9	(i) Inversion, (ii) field entropy plots for $g = 2 \times 10^6 s^{-1}$ with $\alpha_0 = \sqrt{3}$ , with no damping within time duration $gt = 0$ until $gt = 10$	95
Figure 5.10	(i) Inversion, (ii) atom entropy and (iii) field entropy plots for $g = 2 \times 10^6 s^{-1}$ with $\alpha_0 = \sqrt{3}$ , with $\Gamma_{ab} = \Gamma_{ac} = 10^7 s^{-1}$ within time duration $gt = 0$ until $gt = 10$	96
Figure 5.11	(i) Inversion, (ii) atom entropy and (iii) field entropy plots for $g = 2 \times 10^6 s^{-1}$ with $\alpha_0 = \sqrt{3}$ , $\Gamma_{ab} = \Gamma_{ac} = 10^6 s^{-1}$ with no field damping within time duration $gt = 0$ until $gt = 3$	97
Figure 5.12	(i) Inversion, (ii) atom entropy and (iii) field entropy plots for $g = 2 \times 10^6 s^{-1}$ with $\alpha_0 = \sqrt{3}$ , $\Gamma_{ab} = \Gamma_{ac} = 10^6 s^{-1}$ with $\gamma_F = 10^6 s^{-1}$ within time duration $gt = 0$ until $gt = 3$	98
Figure 5.13	(i) Inversion, (ii) atom entropy and (iii) field entropy plots for $g = 2 \times 10^6 s^{-1}$ with $\alpha_0 = \sqrt{3}$ , $\Gamma_{ab} = \Gamma_{ac} = 10^6 s^{-1}$ , $\gamma_F = 10^6 s^{-1}$ with $\Omega_p = 10^7 s^{-1}$ within time duration $gt = 0$ until $gt = 3$	99
Figure 5.14	Intuitive sequence of pulses for atom initially in level $ c\rangle$ (i) Inversion, (ii) atom entropy and (iii) field entropy plots for $g = 2 \times 10^6 s^{-1}$ with $\alpha_0 = \sqrt{3}$ , $\Gamma_{ab} = \Gamma_{ac} = 10^6 s^{-1}$ , $\gamma_F = 10^6 s^{-1}$ with $\Omega_p = 10^7 s^{-1}$ within time duration $gt = 0$ until $gt = 3$	100

Figure 5.15 Counter-intuitive sequence for atom initially at  $|c\rangle$  with (i) Inversion, (ii) atom entropy and (iii) field entropy plots for  $g = 2 \times 10^6 s^{-1}$ ,  $\alpha_0 = \sqrt{3}$ ,  $\Gamma_{ab} = \Gamma_{ac} = 10^6 s^{-1}$ ,  $\gamma_F = 10^6 s^{-1}$  and  $\Omega_p = 10^7 s^{-1}$  within time duration  $gt = 0$  until  $gt = 3$

100

## LIST OF TABLES

Table 2.1	Allowed and forbidden dipole transition in three-level atom	26
-----------	---	----

## LIST OF APPENDICES

Appendix A	List of Publications	105
Appendix B	Coupled Equation Derivation for Two-level Atom	106
Appendix C	Solving The Coupled Equation	109
Appendix D	Density Matrix Elements for Two-level Atom	112
Appendix E	Derivation of Inversion for Two-level Atom	116
Appendix F	Density Matrix Elements for Three-level Atom	120

## CHAPTER 1

### INTRODUCTION TO QUANTUM OPTICS

#### 1.1 Introduction

Quantum optics is a quantum interpretation of phenomenon involving light and its behaviour against the interaction with matter. The study involving light-matter interactions become very popular among scientists theoretically as well as experimentally due to its advantageous application for future technologies. This study is beneficial to the quantum information, laser science, quantum communication, quantum cryptography, teleportation and many more.

The study of quantum optics begins as early as 1801 by the double-slit experiment of Young (Fox, 2006). Around 1970, the first laboratory experiment observing the non-classicality of light such as photon antibunching lead to the enormously studies in this field. By the 1980s the theorists realized the possible interaction between single atoms and single modes of the electromagnetic field. This interaction is the simplest model to study the light-matter interaction which is called the Jaynes-Cumming model named after the founder. The transition dynamics of atom becomes wholly reversible (Gerry & Knight, 2004), as the atomic inversion shows the collapse-revival pattern, until coherence is eventually lost through a dissipative “decoherence” process. Nowadays, the theories expanded and it encompasses many new and interesting topics and now becomes cross disciplinary.

#### 1.2 Operators and States

A quantum system can be represented by a state vector denote as the ket  $|\psi\rangle$ . A pure state is described by a single state vector while in contrast a mixed state is an ensemble of several quantum states. If the system has  $n$  possible states, the linear superposition of states is given by

$$|\psi\rangle = \sum_n \lambda_n |\phi_n\rangle \quad (1.1)$$

where  $\lambda_n$  is amplitude written in a complex number form while its adjoint state is defined as

$$\langle \psi | = \sum_n \lambda_n^* \langle \phi_n | \quad (1.2)$$

The basis state  $|\phi_n\rangle$  are assumed orthonormal with  $\langle \phi_n | \phi_m \rangle = \delta_{nm}$  and complete  $\sum_n |\phi_n\rangle \langle \phi_n| = 1$ .

1. The coefficient  $\lambda_n$

$$\lambda_n = \langle \phi_n | \psi \rangle$$

is normalize according to

$$\langle \psi | \psi \rangle = \sum_n |\lambda_n|^2 = 1 \quad (1.3)$$

A complete description of one system must contain an operator. When an operator act on a state, it will produce another state which is generally is not normalize. The properties of a Hermitian operator, let say  $\hat{A}$  and its conjugate  $\hat{A}^\dagger$ , must comply

$$\begin{aligned} (\hat{A}^\dagger)^\dagger &= \hat{A} \\ (\hat{A} + \hat{B})^\dagger &= \hat{A}^\dagger + \hat{B}^\dagger \\ (\hat{A}\hat{B})^\dagger &= \hat{B}^\dagger \hat{A}^\dagger \\ (\lambda \hat{A})^\dagger &= \lambda^* \hat{A}^\dagger \end{aligned}$$

where  $\hat{B}$  is any other operator and  $\lambda$  is a complex number coefficient. Atomic operator and field operator which are commonly used in light-matter interaction will be discussed in the next section.

### 1.2.1 Atomic Operators

For atomic state, if we use  $|a\rangle$  as an excited state and  $|b\rangle$  as a ground state, the raising operator  $\hat{\sigma}_+$ , the lowering operator  $\hat{\sigma}_-$ , and the operator relation can be represented in Pauli matrices which are Hermitian and unitary in a set of three  $2 \times 2$  complex matrices as below

$$\hat{\sigma}_1 = \hat{\sigma}_+ + \hat{\sigma}_- = \begin{pmatrix} 0 & 1 \\ 1 & 0 \end{pmatrix} \quad (1.4)$$

$$\hat{\sigma}_2 = i(\hat{\sigma}_- - \hat{\sigma}_+) = \begin{pmatrix} 0 & -i \\ i & 0 \end{pmatrix} \quad (1.5)$$

$$\hat{\sigma}_3 = |a\rangle\langle a| - |b\rangle\langle b| = \begin{pmatrix} 1 & 0 \\ 0 & -1 \end{pmatrix} \quad (1.6)$$

where

$$\hat{\sigma}_+ = |a\rangle\langle b| = \begin{pmatrix} 0 & 1 \\ 0 & 0 \end{pmatrix} \quad (1.7)$$

$$\hat{\sigma}_- = |b\rangle\langle a| = \begin{pmatrix} 0 & 0 \\ 1 & 0 \end{pmatrix} \quad (1.8)$$

$$1 = |a\rangle\langle a| + |b\rangle\langle b| = \begin{pmatrix} 1 & 0 \\ 0 & 1 \end{pmatrix} \quad (1.9)$$

An atomic operator satisfy the spin 1/2 algebra which state that:

$$[\hat{\sigma}_-, \hat{\sigma}_+] = -\hat{\sigma}_z$$

$$[\hat{\sigma}_-, \hat{\sigma}_z] = 2\hat{\sigma}_-$$

Some basic operations on the operators can be done, for example

$$\hat{\sigma}_+ \hat{\sigma}_+ = \begin{pmatrix} 0 & 1 \\ 0 & 0 \end{pmatrix} \begin{pmatrix} 0 & 1 \\ 0 & 0 \end{pmatrix} = 0 \quad (1.10)$$

$$\hat{\sigma}_- \hat{\sigma}_- = \begin{pmatrix} 0 & 0 \\ 1 & 0 \end{pmatrix} \begin{pmatrix} 0 & 0 \\ 1 & 0 \end{pmatrix} = 0 \quad (1.11)$$

$$\hat{\sigma}_+ \hat{\sigma}_- = \begin{pmatrix} 0 & 1 \\ 0 & 0 \end{pmatrix} \begin{pmatrix} 0 & 0 \\ 1 & 0 \end{pmatrix} = \begin{pmatrix} 1 & 0 \\ 0 & 0 \end{pmatrix} \quad (1.12)$$

$$\hat{\sigma}_- \hat{\sigma}_+ = \begin{pmatrix} 0 & 0 \\ 1 & 0 \end{pmatrix} \begin{pmatrix} 0 & 1 \\ 0 & 0 \end{pmatrix} = \begin{pmatrix} 0 & 0 \\ 0 & 1 \end{pmatrix} \quad (1.13)$$

### 1.2.2 Field Operator

Since the system is considered in a fully quantum treatment, the operator of field is used. For field states, operator  $\hat{n}$  is defined as a number operator while  $|n\rangle$  is an energy eigenstate, where

$$\hat{n} = \hat{a}^\dagger \hat{a}$$



$$\hat{n}^\dagger = \left(\hat{a}^\dagger \hat{a}\right)^\dagger = \hat{a}^\dagger \hat{a} = \hat{n}$$

with  $\hat{a}^\dagger$  and  $\hat{a}$  are creation and annihilation operator respectively, for photon in the field where the definitions are

$$\begin{aligned}\hat{a} &= \sum_{n=0}^{\infty} \sqrt{n+1} |n\rangle \langle n+1| \\ \hat{a}^\dagger &= \sum_{n=0}^{\infty} \sqrt{n+1} |n+1\rangle \langle n|\end{aligned}\tag{1.14}$$

The action of operator  $\hat{a}$  and  $\hat{a}^\dagger$  on a basis  $|n\rangle$  and  $\langle n|$  (Barnett & Radmore, 1997) gives

$$\begin{aligned}\hat{a}|n\rangle &= \sqrt{n}|n-1\rangle \\ \hat{a}^\dagger|n\rangle &= \sqrt{n+1}|n+1\rangle \\ \langle n|\hat{a} &= \sqrt{n+1}\langle n+1| \\ \langle n|\hat{a}^\dagger &= \sqrt{n}\langle n-1| \\ \hat{a}^\dagger \hat{a}|n\rangle &= n|n\rangle \\ \hat{a} \hat{a}^\dagger|n\rangle &= (n+1)|n\rangle \\ \langle n|\hat{a}^\dagger \hat{a} &= \langle n|n \\ \langle n|\hat{a} \hat{a}^\dagger &= \langle n|n+1\end{aligned}\tag{1.15}$$

### 1.2.3 Fock State and Vacuum State

A single-mode field of frequency  $\nu$  with creation and annihilation operators  $\hat{a}^\dagger$  and  $\hat{a}$  has an energy eigenvalue  $E_n$  while the corresponding energy eigenstate is  $|n\rangle$  which satisfies

$$\begin{aligned}\hat{H}|n\rangle &= \hbar\nu \left(\hat{a}^\dagger \hat{a} + \frac{1}{2}\right)|n\rangle \\ &= E_n|n\rangle\end{aligned}\tag{1.16}$$

$\hat{a}^\dagger$  and  $\hat{a}$  has the commutation relation  $[\hat{a}, \hat{a}^\dagger] = 1$ . From the number state defined in previous section, we know that  $\hat{a}^\dagger \hat{a}|n\rangle = n|n\rangle$  the equation becomes

$$\begin{aligned}\hat{H}|n\rangle &= \hbar\nu \left(\hat{a}^\dagger \hat{a} + \frac{1}{2}\right)|n\rangle \\ &= \hbar\nu \left(n + \frac{1}{2}\right)|n\rangle\end{aligned}\tag{1.17}$$

So we get the energy eigenvalue for state  $|n\rangle$ , given by

$$E_n = \hbar\nu \left( n + \frac{1}{2} \right) \quad (1.18)$$

for  $n = 0, 1, 2, \dots, \infty$ . From the equation above, it is easy to show that the zero-point energy ( $n = 0$ ) still has a value of  $E_0 = \frac{1}{2}\hbar\nu$ . This state is called a vacuum state.

#### 1.2.4 Coherent States

Coherent state describes the quantum state of a laser, are the most familiar and important in quantum systems. It has a minimum-uncertainty state, which is generated by an ideal amplitude-stabilised gas laser. A single mode coherent state is given by Glauber displacement operator

$$\hat{D}(\alpha) = e^{(\alpha\hat{a}^\dagger - \alpha^*\hat{a})} \quad (1.19)$$

where  $\alpha = |\alpha|e^{i\theta}$  is a complex number which means there is a different coherent state for every possible choice of  $\alpha$ . Coherent state appears frequently in the field of quantum optics and plays an important role in the understanding the system of light-matter interactions. Using operator ordering theorem (Barnett & Radmore, 1997), the single mode coherent state  $|\alpha\rangle$  is given by

$$\begin{aligned} |\alpha\rangle &= \hat{D}(\alpha)|0\rangle \\ &= e^{-|\alpha|^2/2} e^{\alpha\hat{a}^\dagger} e^{-\alpha^*\hat{a}} |0\rangle \\ &= e^{-|\alpha|^2/2} e^{\alpha\hat{a}^\dagger} |0\rangle \\ &= e^{-|\alpha|^2/2} \sum_{n=0}^{\infty} \frac{\alpha^n}{\sqrt{n!}} |n\rangle \end{aligned} \quad (1.20)$$

Vacuum state is also a coherent state with  $\alpha = 0$ .

#### 1.2.5 Cat State

Another useful states in quantum information science is the cat state. It is named after Schrodinger cat state which predicts the probability of a cat inside a box being dead or alive after a while depending on the initial state. The same analogy applies to a quantum system which is very useful to explain the entanglement properties. Cat states are equal coherent superpositions of two different quantum states, named even and odd cat state. This state is important to be applied in quantum information processing, quantum

computing and quantum communication. For example, quantum error correction and entanglement purification have been studied using cat states to overcome the decoherence problem in dissipative environment (Jeong & Ralph, 2007).

If we denote an even cat state as  $|\alpha\rangle$  and its odd cat state as  $|- \alpha\rangle$ , the superposition of the cat state is

$$|\alpha_{cat}\rangle = |\alpha\rangle + |- \alpha\rangle \quad (1.21)$$

where  $|\alpha\rangle$  is coherent state in the Fock number basis as defined in the previous section

$$|\alpha\rangle = e^{-|\alpha|^2/2} \sum_{n=0}^{\infty} \frac{\alpha^n}{\sqrt{n!}} |n\rangle \quad (1.22)$$

$$|- \alpha\rangle = e^{-|\alpha|^2/2} \sum_{n=0}^{\infty} \frac{(-\alpha)^n}{\sqrt{n!}} |n\rangle \quad (1.23)$$

so  $|\alpha_{cat}\rangle$  becomes

$$\begin{aligned} |\alpha_{cat}^{(+)}\rangle &= |\alpha\rangle + |- \alpha\rangle \\ &= 2e^{-|\alpha|^2/2} \left( \frac{(-\alpha)^0}{\sqrt{0!}} |0\rangle + \frac{(-\alpha)^2}{\sqrt{2!}} |2\rangle + \dots \right) \end{aligned} \quad (1.24)$$

which only contains even terms. From here, we can also get the even cat states by

$$\begin{aligned} |\alpha_{cat}^{(-)}\rangle &= |\alpha\rangle - |- \alpha\rangle \\ &= 2e^{-|\alpha|^2/2} \left( \frac{(-\alpha)^1}{\sqrt{1!}} |1\rangle + \frac{(-\alpha)^3}{\sqrt{3!}} |3\rangle + \dots \right) \end{aligned} \quad (1.25)$$

### 1.3 The Density Matrix

The density matrix is introduced to describe an ensemble of several quantum states of a system which also defined as a mixed state. The density operator (Meystre & Sargent, 2007) is defined as

$$\hat{\rho} = |\psi\rangle \langle\psi| \quad (1.26)$$

If we have an observable operator represented by a Hermitian operator  $\langle\hat{O}\rangle$  with matrix elements  $O_{mn} = \langle m | \hat{O} | n \rangle$ , the mean value of  $O$  is

$$\begin{aligned} \langle\hat{O}\rangle &= \langle\psi| \hat{O} |\psi\rangle = \sum_{mn} C_m^* C_n O_{mn} \\ &= \sum_{mn} \rho_{mn} O_{mn} = Tr \{ \hat{\rho} \hat{O} \} \end{aligned} \quad (1.27)$$

The evolution equation of the density operator can then be derived as

$$\begin{aligned}\frac{d}{dt}\hat{\rho} &= \frac{d}{dt}(|\psi\rangle\langle\psi|) \\ &= \left(\frac{d}{dt}|\psi\rangle\right)\langle\psi| + |\psi\rangle\frac{d}{dt}\langle\psi| \end{aligned} \quad (1.28)$$

If we substitute the equation of motion  $i\hbar\frac{d}{dt}|\psi\rangle = \hat{H}|\psi\rangle$  and  $-i\hbar\frac{d}{dt}\langle\psi| = \langle\psi|\hat{H}$  into the above equation, we obtain

$$\begin{aligned}\frac{d}{dt}\hat{\rho} &= \frac{1}{i\hbar}\hat{H}|\psi\rangle\langle\psi| - \frac{1}{i\hbar}|\psi\rangle\langle\psi|\hat{H} \\ &= \frac{1}{i\hbar}\hat{H}\hat{\rho} - \frac{1}{i\hbar}\hat{\rho}\hat{H} \\ &= \frac{1}{i\hbar}\{\hat{H}\hat{\rho} - \hat{\rho}\hat{H}\} \\ &= \frac{1}{i\hbar}[\hat{H}, \hat{\rho}] \end{aligned} \quad (1.29)$$

called Liouville-Von-Neumann equation (Breuer & Petruccione, 2002).

### 1.3.1 Optical Bloch Equation

In the case of two-level atom, the density matrix  $\hat{\rho}$  is given by

$$\hat{\rho} = \rho_{aa}|a\rangle\langle a| + \rho_{ab}|a\rangle\langle b| + \rho_{ba}|b\rangle\langle a| + \rho_{bb}|b\rangle\langle b|$$

where  $\rho_{aa}$  ( $\rho_{bb}$ ) is the probability of the system being in upper state(lower state), while  $\rho_{ab}$  and  $\rho_{ba}$  are the atomic coherences which are an electric-dipole transition between two levels. In matrix notation, it can be presented as

$$\hat{\rho} = \begin{pmatrix} \rho_{aa} & \rho_{ab} \\ \rho_{ba} & \rho_{bb} \end{pmatrix} \quad (1.30)$$

The density matrix (Eq.1.30) can be written in a form of  $u$ ,  $v$ , and  $w$  as

$$\hat{\rho} = \frac{1}{2}(\mathbf{1} + u\sigma_1 + v\sigma_2 + w\sigma_3) \quad (1.31)$$

where

$$u = \rho_{ab} + \rho_{ba}$$

$$v = i(\rho_{ab} - \rho_{ba})$$

$$w = \rho_{aa} - \rho_{bb}$$

$$1 = \rho_{aa} + \rho_{bb}$$

The plot of time dependent Bloch equations  $u(t)$ ,  $v(t)$  and  $w(t)$  versus time  $t$ , are as shown in Fig.1.1, Fig.1.2 and Fig.1.3 respectively. The comparison between all plots is shown in Fig.1.4.

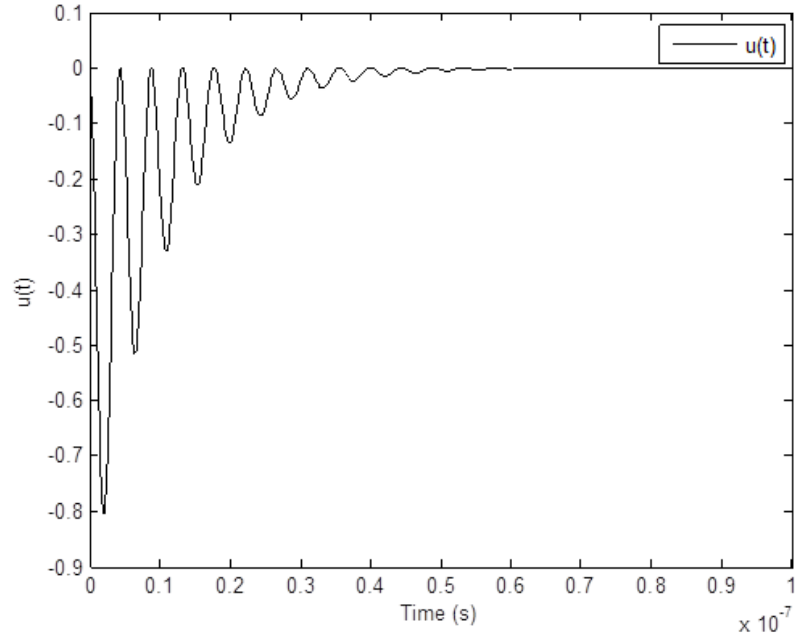


Figure 1.1:  $u(t)$  vs  $t$  for Bloch equation

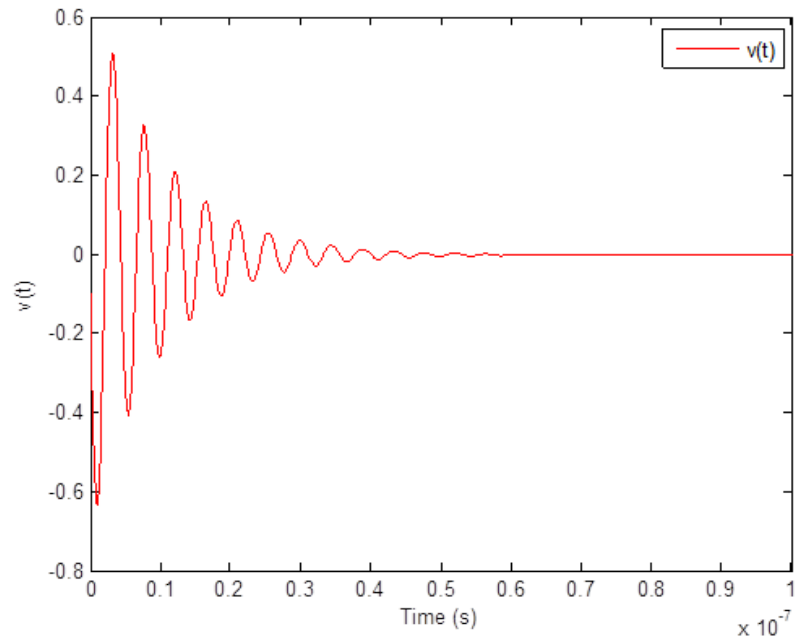


Figure 1.2:  $v(t)$  vs  $t$  for Bloch equation

The equivalence of Eq.1.30 and Eq.1.31 can be proved by substituting the term  $u$ ,  $v$ ,

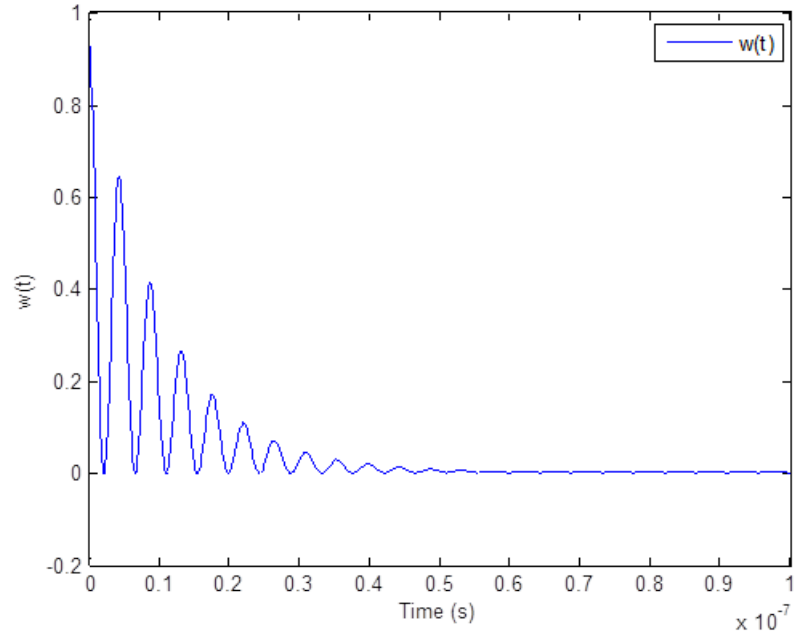


Figure 1.3:  $w(t)$  vs  $t$  for Bloch equation

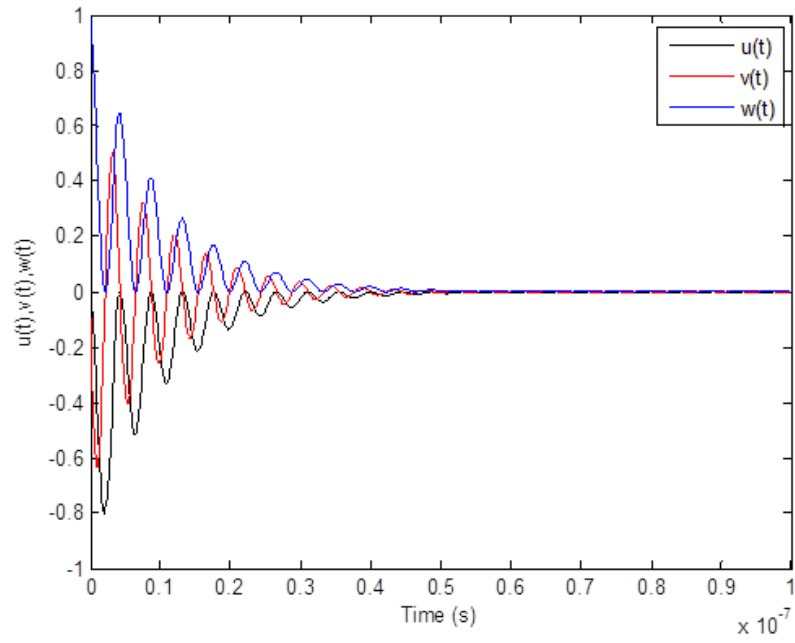


Figure 1.4:  $u(t)$ ,  $v(t)$  and  $w(t)$  vs  $t$  for Bloch equation

and  $w$  into Eq.1.31 and we get

$$\begin{aligned}
 \hat{\rho} &= \frac{1}{2}(\mathbf{1} + u\hat{\sigma}_1 + v\hat{\sigma}_2 + w\hat{\sigma}_3) \\
 &= \frac{1}{2}\{(\rho_{aa} + \rho_{bb})\begin{pmatrix} 1 & 0 \\ 0 & 1 \end{pmatrix} + (\rho_{ab} + \rho_{ba})\begin{pmatrix} 0 & 1 \\ 1 & 0 \end{pmatrix}
 \end{aligned} \tag{1.32}$$

$$\begin{aligned}
& +i(\rho_{ab} - \rho_{ba}) \begin{pmatrix} 0 & -i \\ i & 0 \end{pmatrix} + (\rho_{aa} - \rho_{bb}) \begin{pmatrix} 1 & 0 \\ 0 & -1 \end{pmatrix} \} \\
& = \begin{pmatrix} \rho_{aa} & \rho_{ab} \\ \rho_{ba} & \rho_{bb} \end{pmatrix}
\end{aligned}$$

$u$ ,  $v$ , and  $w$  can be defined as optical Bloch equations (Feynman, Jr., & Hellwarth, 1957) as first adapted to two-level atom which give

$$\frac{d}{dt}u = \Delta v - \frac{1}{T}u \quad (1.33)$$

$$\frac{d}{dt}v = -\Delta u - \frac{1}{T}v - \Omega w \quad (1.34)$$

$$\frac{d}{dt}w = \Omega v - \frac{1}{T}w \quad (1.35)$$

where  $T$  is relaxation time. The equation above can be transformed into matrix form,  $\frac{d}{dt}X = MX$  where

$$\begin{aligned}
X &= \begin{bmatrix} u \\ v \\ w \end{bmatrix} = \begin{bmatrix} \rho_{ab} + \rho_{ba} \\ i(\rho_{ab} - \rho_{ba}) \\ \rho_{aa} - \rho_{bb} \end{bmatrix} \\
M &= \begin{bmatrix} -\frac{1}{T} & \Delta & 0 \\ -\Delta & -\frac{1}{T} & -\Omega \\ 0 & \Omega & -\frac{1}{T} \end{bmatrix} \\
\frac{d}{dt} \begin{bmatrix} u \\ v \\ w \end{bmatrix} &= \begin{bmatrix} -\frac{1}{T} & \Delta & 0 \\ -\Delta & -\frac{1}{T} & -\Omega \\ 0 & \Omega & -\frac{1}{T} \end{bmatrix} \begin{bmatrix} u \\ v \\ w \end{bmatrix}
\end{aligned} \quad (1.36)$$

and to obtain its time evolution solution, it can be solved using Crank-Nicolson method

$$\begin{aligned}
X(t+dt) &= \frac{I + Mdt/2}{I - Mdt/2} X(t) \\
\begin{bmatrix} u(t+dt) \\ v(t+dt) \\ w(t+dt) \end{bmatrix} &= \frac{I + Mdt/2}{I - Mdt/2} \begin{bmatrix} u(t) \\ v(t) \\ w(t) \end{bmatrix}
\end{aligned}$$

## 1.4 Master Equation

If a physical system consists of several subsystems interact with each other, the system will undergo the dissipation due to several damping force, for example, a friction force or a heat transfer. This processes are irreversible and will reduce the total energy of the particular system since some part of the energy dissipate away as a consequences of the interaction. In quantum optics, master equation method is used to formulate this interaction when it involves damping mechanism in the microscopic scales such as cavity, laser and atomic interaction in laser system. The unitary time evolution operator method which will be discussed in section 2.3.1(b) in the next chapter can be used to solve a unitary system, which means there is no dissipative processes involved in the system.

To begin the master equation derivation, a system  $S$  interacting with reservoir  $R$  is considered via the interaction Hamiltonian  $\hat{V}$ , and the combined density operator is denoted by  $\hat{\rho}(t)$ . We assume that at initial time  $t$ , the two systems are uncorrelated so the initial state  $\hat{\rho}(0)$  is given by simple outer product (Yamamoto & Imamoglu, 1999)

$$\hat{\rho}(0) = \hat{\rho}_S(0) \otimes \hat{\rho}_R(0) \quad (1.37)$$

Liouville-von Neumann operator as derived in Eq.1.29 is given by

$$\begin{aligned} \frac{d}{dt}\hat{\rho}(t) &= \frac{1}{i\hbar} [\hat{V}(t), \hat{\rho}(t)] \\ \hat{\rho}(t) &= \frac{1}{i\hbar} \int_0^t dt' [\hat{V}(t'), \hat{\rho}(t')] \end{aligned} \quad (1.38)$$

The reduced density operator is given by

$$\begin{aligned} \frac{d}{dt}\hat{\rho}_S(t) &= \frac{1}{i\hbar} Tr_R [\hat{V}(t), \hat{\rho}(t)] \\ &= \frac{1}{i\hbar} Tr_R \left[ \hat{V}(t), \frac{1}{i\hbar} \int_0^t dt' [\hat{V}(t'), \hat{\rho}(t')] \right] \\ &= \left( \frac{1}{i\hbar} \right)^2 \int_0^t dt' Tr_R (\hat{V}(t), [\hat{V}(t'), \hat{\rho}(t')]) \end{aligned} \quad (1.39)$$

### 1.4.1 Atomic Damping

We consider a system of an atom placed inside a field reservoir. The interaction Hamiltonian is given by

$$\hat{V}_{AR}(t) = \hbar \sum_{\mathbf{k}} g_{\mathbf{k}} \left[ \hat{b}_{\mathbf{k}}^{\dagger} \sigma_{-} e^{-i(\omega - \nu_{\mathbf{k}})t} + \sigma_{+} \hat{b}_{\mathbf{k}} e^{i(\omega - \nu_{\mathbf{k}})t} \right] \quad (1.40)$$



where  $g_{\mathbf{k}}$  is a coupling between the atom and the multimode reservoir.  $\mathbf{k}$  is the total modes of the reservoir field.  $\hat{b}_{\mathbf{k}}$  and  $\hat{b}_{\mathbf{k}}^\dagger$  are the reservoir operators while  $\nu_{\mathbf{k}}$  is reservoir frequency.

The equation of motion of  $\hat{\rho}_{AR}(t)$  (density operator of combined atom and reservoir) is given by

$$i\hbar\dot{\rho}_{AR} = [\hat{V}_{AR}(t), \hat{\rho}_{AR}(t)] \quad (1.41)$$

where

$$\hat{\rho}_{AR}(t) = \hat{\rho}_{AR}(t_i) - \frac{i}{\hbar} \int_{t_i}^t [\hat{V}_{AR}(t'), \hat{\rho}_{AR}(t')] dt' \quad (1.42)$$

Substituting  $\hat{\rho}_{AR}(t)$  into  $i\hbar\dot{\rho}_{AR}$  yields

$$\begin{aligned} \dot{\rho}_{AR} = & -\frac{i}{\hbar} [\hat{V}_{AR}(t), \hat{\rho}_{AR}(t_i)] \\ & -\frac{1}{\hbar^2} \int_{t_i}^t [\hat{V}_{AR}(t), [\hat{V}_{AR}(t'), \hat{\rho}_{AR}(t')]] dt' \end{aligned} \quad (1.43)$$

If the interaction energy  $\hat{V}_{AR}(t)$  is zero, the system and reservoir are independent and the density operator  $\hat{\rho}_{AR}$  would factor as a direct product  $\hat{\rho}_{AR}(t) = \hat{\rho}_A(t) \otimes \hat{\rho}_R(t_i)$  where we assume the reservoir at equilibrium (Scully & Zubairy, 1997). Since  $\hat{V}_{AR}(t)$  is small, so the solution for Eq.1.43 is

$$\hat{\rho}_{AR}(t) = \hat{\rho}_A(t) \otimes \hat{\rho}_R(t_i) + \hat{\rho}_c(t) \quad (1.44)$$

where  $\hat{\rho}_c$  is of higher order of  $\hat{V}_{AR}$  with

$$Tr_R[\hat{\rho}_c(t)] = 0 \quad (1.45)$$

$$\begin{aligned} \dot{\rho}_A = & -\frac{i}{\hbar} Tr_R [\hat{V}_{AR}(t), \hat{\rho}_A(t_i) \otimes \hat{\rho}_R(t_i)] \\ & -\frac{1}{\hbar^2} Tr_R \int_{t_i}^t [\hat{V}_{AR}(t), [\hat{V}_{AR}(t'), \hat{\rho}_A(t') \otimes \hat{\rho}_R(t_i)]] dt' \end{aligned}$$

Substituting  $\hat{V}_{AR}$  into  $\dot{\rho}_A$  gives

$$\begin{aligned} \dot{\rho}_A = & -i \sum_{\mathbf{k}} g_{\mathbf{k}} \langle \hat{b}_{\mathbf{k}}^\dagger \rangle [\hat{\sigma}_-, \hat{\rho}_A(t_i)] e^{-i(\omega - \nu_{\mathbf{k}})t} \\ & - \int_{t_i}^t dt' \sum_{\mathbf{k}, \mathbf{k}'} g_{\mathbf{k}} g_{\mathbf{k}'} \{ (\hat{\sigma}_- \hat{\sigma}_- \hat{\rho}_A(t') - 2 \hat{\sigma}_- \hat{\rho}_A(t') \hat{\sigma}_- \\ & + \hat{\rho}_A(t') \hat{\sigma}_- \hat{\sigma}_-) e^{-i(\omega - \nu_{\mathbf{k}})t - i(\omega - \nu_{\mathbf{k}'})t'} \langle \hat{b}_{\mathbf{k}}^\dagger \hat{b}_{\mathbf{k}'}^\dagger \rangle \\ & + [\hat{\sigma}_- \hat{\sigma}_+ \hat{\rho}_A(t') - \hat{\sigma}_+ \hat{\rho}_A(t') \hat{\sigma}_-] e^{-i(\omega - \nu_{\mathbf{k}})t + i(\omega - \nu_{\mathbf{k}'})t'} \langle \hat{b}_{\mathbf{k}}^\dagger \hat{b}_{\mathbf{k}'} \rangle \\ & + [\hat{\rho}_A(t') \hat{\sigma}_- \hat{\sigma}_+ - \hat{\sigma}_+ \hat{\rho}_A(t') \hat{\sigma}_-] e^{-i(\omega - \nu_{\mathbf{k}})t + i(\omega - \nu_{\mathbf{k}'})t'} \langle \hat{b}_{\mathbf{k}'}^\dagger \hat{b}_{\mathbf{k}} \rangle \} \end{aligned} \quad (1.46)$$

$$\begin{aligned}
& + [\hat{\sigma}_+ \hat{\sigma}_- \hat{\rho}_A(t') - \hat{\sigma}_- \hat{\rho}_A(t') \hat{\sigma}_+] e^{i(\omega - \nu_{\mathbf{k}})t - i(\omega - \nu_{\mathbf{k}'})t'} \langle \hat{b}_{\mathbf{k}} \hat{b}_{\mathbf{k}'}^\dagger \rangle \\
& + [\hat{\rho}_A(t') \hat{\sigma}_+ \hat{\sigma}_- - \hat{\sigma}_- \hat{\rho}_A(t') \hat{\sigma}_+] e^{i(\omega - \nu_{\mathbf{k}})t - i(\omega - \nu_{\mathbf{k}'})t'} \langle \hat{b}_{\mathbf{k}'} \hat{b}_{\mathbf{k}}^\dagger \rangle \\
& - [\hat{\rho}_A(t') \hat{\sigma}_+ \hat{\sigma}_+ - \hat{\sigma}_+ \hat{\rho}_A(t') \hat{\sigma}_+] e^{i(\omega - \nu_{\mathbf{k}})t + i(\omega - \nu_{\mathbf{k}'})t'} \langle \hat{b}_{\mathbf{k}'} \hat{b}_{\mathbf{k}} \rangle \\
& - [\hat{\sigma}_+ \hat{\sigma}_+ \hat{\rho}_A(t') - \hat{\sigma}_+ \hat{\rho}_A(t') \hat{\sigma}_+] e^{i(\omega - \nu_{\mathbf{k}})t + i(\omega - \nu_{\mathbf{k}'})t'} \langle \hat{b}_{\mathbf{k}} \hat{b}_{\mathbf{k}'} \rangle \}
\end{aligned}$$

where expectation values  $\langle x, y \rangle$  where  $x, y = b_{\mathbf{k}}^\dagger, b_{\mathbf{k}'}^\dagger, b_{\mathbf{k}},$  or  $b_{\mathbf{k}'}$  refer to the initial state of the reservoir. In this section, thermal reservoir and squeezed vacuum reservoir will be considered.

#### 1.4.1 (a) Thermal Reservoir

Thermal reservoir operator is given by

$$\hat{\rho}_R = \prod_{\mathbf{k}} \left[ 1 - \exp\left(-\frac{\hbar \nu_{\mathbf{k}}}{k_B T}\right) \right] \exp\left(-\frac{\hbar \nu_{\mathbf{k}} \hat{b}_{\mathbf{k}}^\dagger \hat{b}_{\mathbf{k}}}{k_B T}\right) \quad (1.47)$$

where  $k_B$  is the Boltzmann constant,  $T$  is the temperature, and  $\bar{n}_{\mathbf{k}}$  is the thermal average boson number which is given by

$$\bar{n}_{\mathbf{k}} = \frac{1}{\exp\left(\frac{\hbar \nu_{\mathbf{k}}}{k_B T}\right) - 1}$$

By using Eq.1.46 and Eq.1.47, we obtain

$$\begin{aligned}
\dot{\rho}_A = & - \int_{t_i}^t dt' \sum_{\mathbf{k}, \mathbf{k}'} g_{\mathbf{k}}^2 \{ [\hat{\sigma}_- \hat{\sigma}_+ \hat{\rho}_A(t') - \hat{\sigma}_+ \hat{\rho}_A(t') \hat{\sigma}_-] \bar{n}_{\mathbf{k}} e^{-i(\omega - \nu_{\mathbf{k}})(t - t')} \\
& + [\hat{\sigma}_+ \hat{\sigma}_- \hat{\rho}_A(t') - \hat{\sigma}_- \hat{\rho}_A(t') \hat{\sigma}_+] (\bar{n}_{\mathbf{k}} + 1) e^{i(\omega - \nu_{\mathbf{k}})(t - t')} \} + H.c.
\end{aligned} \quad (1.48)$$

Now, using Weisskopf-Wigner approximation and the sum over  $\mathbf{k}$ ,

$$\sum_{\mathbf{k}} \longrightarrow 2 \frac{V}{(2\pi)^3} \int_0^{2\pi} d\phi \int_0^\pi d\theta \sin\theta \int_0^\infty dk k^2 \quad (1.49)$$

we obtain the reduced density operator,  $\rho_A(t)$  as

$$\begin{aligned}
\dot{\rho}_A(t) = & -\bar{n}_{th} \frac{\Gamma}{2} [\hat{\sigma}_- \hat{\sigma}_+ \hat{\rho}_A(t) - \hat{\sigma}_+ \hat{\rho}_A(t) \hat{\sigma}_-] \\
& - (\bar{n}_{th} + 1) \frac{\Gamma}{2} [\hat{\sigma}_+ \hat{\sigma}_- \hat{\rho}_A(t) - \hat{\sigma}_- \hat{\rho}_A(t) \hat{\sigma}_+] + H.c.
\end{aligned} \quad (1.50)$$

where

$$\begin{aligned}
\bar{n}_{th} & \equiv \bar{n}_{k_0} (k_0 = \omega/c) \\
\Gamma & = \frac{1}{4\pi\epsilon_0} \frac{4\omega^3 \mathcal{J}_{ab}^2}{3\hbar c^3}
\end{aligned}$$

$H.c.$  is the Hermitian conjugate and  $\Gamma$  is the atomic decay rate.

Thus, from Eq.1.48, we derived the equation of motion for the atomic density matrix elements as

$$\begin{aligned}\dot{\rho}_{aa} &= \langle a | \dot{\rho}_A | a \rangle \\ &= -(\bar{n}_{th} + 1)\Gamma\rho_{aa} + \bar{n}_{th}\Gamma\rho_{bb}\end{aligned}\quad (1.51)$$

$$\begin{aligned}\dot{\rho}_{ab} &= \dot{\rho}_{ba}^* \\ &= -\left(\bar{n}_{th} + \frac{1}{2}\right)\Gamma\hat{\rho}_{ab}\end{aligned}\quad (1.52)$$

$$\dot{\rho}_{bb} = -\bar{n}_{th}\Gamma\hat{\rho}_{bb} + (\bar{n}_{th} + 1)\Gamma\hat{\rho}_{aa}\quad (1.53)$$

Since we have considered the decay from the excited state  $|a\rangle$  to the ground state  $|b\rangle$  so that  $\dot{\rho}_{aa} + \dot{\rho}_{bb} = 0$  and  $\rho_{aa} + \rho_{bb} = 1$ .

For zero temperature, we easily get

$$\begin{aligned}\dot{\rho}_{aa} &= -\Gamma\rho_{aa} \\ \dot{\rho}_{ab} &= -\frac{\Gamma}{2}\rho_{ab} \\ \dot{\rho}_{bb} &= \Gamma\rho_{aa}\end{aligned}\quad (1.54)$$

#### 1.4.1 (b) Squeezed Vacuum Reservoir

The reduced density operator for squeezed vacuum reservoir (Puri & Agarwal, 2001) with squeezed parameter  $\xi$ , and the reference phase of squeezing field,  $\theta$ , is given by

$$\begin{aligned}\hat{\rho}_R &= |\xi\rangle\langle\xi| \\ &= \prod_{\mathbf{k}} S_{\mathbf{k}}(\xi) |0_{\mathbf{k}}\rangle\langle 0_{\mathbf{k}}| S_{\mathbf{k}}^\dagger(\xi)\end{aligned}\quad (1.55)$$

where the squeezed operator

$$S_{\mathbf{k}}(\xi) = \exp\left(\xi^* \hat{b}_{\mathbf{k}_0+\mathbf{k}} \hat{b}_{\mathbf{k}_0-\mathbf{k}} - \xi \hat{b}_{\mathbf{k}_0+\mathbf{k}}^\dagger \hat{b}_{\mathbf{k}_0-\mathbf{k}}^\dagger\right)\quad (1.56)$$

with

$$\begin{aligned}\hat{b}_{\mathbf{k}} &\equiv \hat{b}(ck) \\ \xi &= r \exp(i\theta) \\ v &= ck_0\end{aligned}$$

Using Eq.1.56, we obtain

$$\begin{aligned} S_{\mathbf{k}-\mathbf{k}_0}^\dagger \hat{b}_{\mathbf{k}} S_{\mathbf{k}-\mathbf{k}_0} &= \hat{b}_{\mathbf{k}} \cosh(r) - \hat{b}_{2\mathbf{k}_0-\mathbf{k}}^\dagger e^{i\theta} \sinh(r) \\ S_{\mathbf{k}-\mathbf{k}_0}^\dagger \hat{b}_{\mathbf{k}}^\dagger S_{\mathbf{k}-\mathbf{k}_0} &= \hat{b}_{\mathbf{k}}^\dagger \cosh(r) - \hat{b}_{2\mathbf{k}_0-\mathbf{k}} e^{-i\theta} \sinh(r) \end{aligned}$$

Thus, the expectation values are given by

$$\begin{aligned} \langle \hat{b}_{\mathbf{k}}^\dagger \hat{b}_{\mathbf{k}'} \rangle &= \prod_{\mathbf{q}} \langle 0_{\mathbf{q}} | S_{\mathbf{q}}^\dagger b_{\mathbf{k}}^\dagger S_{\mathbf{q}} S_{\mathbf{q}}^\dagger b_{\mathbf{k}'} S_{\mathbf{q}} | 0_{\mathbf{q}} \rangle \\ \langle \hat{b}_{\mathbf{k}} \rangle &= \langle \hat{b}_{\mathbf{k}}^\dagger \rangle = 0 \\ \langle \hat{b}_{\mathbf{k}}^\dagger \hat{b}_{\mathbf{k}'} \rangle &= \sinh^2(r) \delta_{\mathbf{k}\mathbf{k}'} \\ \langle \hat{b}_{\mathbf{k}} \hat{b}_{\mathbf{k}'}^\dagger \rangle &= \cosh^2(r) \delta_{\mathbf{k}\mathbf{k}'} \\ \langle \hat{b}_{\mathbf{k}} \hat{b}_{\mathbf{k}'} \rangle &= -e^{i\theta} \sinh(r) \cosh(r) \delta_{\mathbf{k}', 2\mathbf{k}_0-\mathbf{k}} \\ \langle \hat{b}_{\mathbf{k}}^\dagger \hat{b}_{\mathbf{k}'}^\dagger \rangle &= -e^{-i\theta} \sinh(r) \cosh(r) \delta_{\mathbf{k}', 2\mathbf{k}_0-\mathbf{k}} \end{aligned}$$

Substituting the expectation values into  $\dot{\rho}_A$  gives

$$\begin{aligned} \dot{\rho}_A &= -\frac{\Gamma}{2} \cosh^2(r) (\hat{\sigma}_+ \hat{\sigma}_- \hat{\rho}_A - 2 \hat{\sigma}_- \hat{\rho}_A \hat{\sigma}_+ + \hat{\rho}_A \hat{\sigma}_+ \hat{\sigma}_-) \\ &\quad -\frac{\Gamma}{2} \sinh^2(r) (\hat{\sigma}_- \hat{\sigma}_+ \hat{\rho}_A - 2 \hat{\sigma}_+ \hat{\rho}_A \hat{\sigma}_- + \hat{\rho}_A \hat{\sigma}_- \hat{\sigma}_+) \\ &\quad -\Gamma e^{-i\theta} \sinh(r) \cosh(r) \hat{\sigma}_- \hat{\rho}_A \hat{\sigma}_- \\ &\quad -\Gamma e^{i\theta} \sinh(r) \cosh(r) \hat{\sigma}_+ \hat{\rho}_A \hat{\sigma}_+ \end{aligned} \quad (1.57)$$

It is known that  $\hat{\sigma}_+ \hat{\sigma}_+ = \hat{\sigma}_- \hat{\sigma}_- = 0$  from Eq.1.10 and Eq.1.11, so the equations of motion (Scully & Zubairy, 1997) can be expressed as

$$\begin{aligned} \hat{\sigma}_x &= (\hat{\sigma}_- + \hat{\sigma}_+)/2 \\ \langle \dot{\sigma}_x \rangle &= -\frac{\Gamma}{2} e^{2r} \langle \hat{\sigma}_x \rangle \end{aligned} \quad (1.58)$$

$$\begin{aligned} \hat{\sigma}_y &= (\hat{\sigma}_- - \hat{\sigma}_+)/2i \\ \langle \dot{\sigma}_y \rangle &= -\frac{\Gamma}{2} e^{-2r} \langle \hat{\sigma}_y \rangle \end{aligned} \quad (1.59)$$

$$\begin{aligned} \hat{\sigma}_z &= (2\hat{\sigma}_+ \hat{\sigma}_- - 1) \\ \langle \dot{\sigma}_z \rangle &= -\Gamma [2 \sinh^2(r) + 1] \langle \hat{\sigma}_z \rangle - \Gamma \\ &= -\Gamma_z \langle \hat{\sigma}_z \rangle - \Gamma \end{aligned} \quad (1.60)$$

where  $\Gamma_z = \Gamma [2 \sinh^2(r) + 1]$ .

### 1.4.2 Field damping

Beside the atomic damping, the field can also be damped due to coupling with reservoir (Meystre & Sargent, 2007). The interaction Hamiltonian between the field and the reservoir is given by

$$\hat{V} = \hbar \sum_{\mathbf{k}} g_{\mathbf{k}} \left[ \hat{b}_{\mathbf{k}}^\dagger \hat{a} e^{-i(\nu - \nu_{\mathbf{k}})t} + \hat{a}^\dagger \hat{b}_{\mathbf{k}} e^{i(\omega - \nu_{\mathbf{k}})t} \right] \quad (1.61)$$

where  $\hat{b}_{\mathbf{k}}^\dagger$  and  $\hat{b}_{\mathbf{k}}$  are the field operators while  $\hat{a}^\dagger$  and  $\hat{a}$  are the reservoir operators. If  $\hat{b}_{\mathbf{k}}$  is in the mode of thermal equilibrium, we have

$$\dot{\rho} = -\frac{C}{2} \bar{n}_{th} \left( \hat{a} \hat{a}^\dagger \hat{\rho} - 2 \hat{a}^\dagger \hat{\rho} \hat{a} + \hat{\rho} \hat{a} \hat{a}^\dagger \right) \quad (1.62)$$

$$-\frac{C}{2} (\bar{n}_{th} + 1) \left( \hat{a}^\dagger \hat{a} \hat{\rho} - 2 \hat{a} \hat{\rho} \hat{a}^\dagger + \hat{\rho} \hat{a}^\dagger \hat{a} \right) \quad (1.63)$$

where  $C$  is the decay constant and  $\bar{n}_{th} \equiv \bar{n}_{k_0}$  is the mean number of quanta (at frequency  $\nu$ ). At  $T = 0$ ,  $\bar{n}_{th} = 0$  which gives

$$\dot{\rho} = -\frac{C}{2} \left( \hat{a}^\dagger \hat{a} \hat{\rho} - 2 \hat{a} \hat{\rho} \hat{a}^\dagger + \hat{\rho} \hat{a}^\dagger \hat{a} \right) \quad (1.64)$$

If all the losses are the transmission losses which actually represent the field outside the cavity (Scully & Zubairy, 1997),  $C$  may be related to the quality factor  $Q$  of the cavity as

$$C = \frac{\nu}{Q} \quad (1.65)$$

When  $\hat{b}_{\mathbf{k}}$  are initially in a squeezed vacuum, where

$$\begin{aligned} \hat{\rho}_R &= |\xi\rangle \langle \xi| \\ &= \prod_{\mathbf{k}} S_{\mathbf{k}}(\xi) |0_{\mathbf{k}}\rangle \langle 0_{\mathbf{k}}| S_{\mathbf{k}}^\dagger(\xi) \end{aligned} \quad (1.66)$$

the reduced density matrix is given as

$$\begin{aligned} \dot{\rho} &= -\frac{C}{2} (N+1) \left( \hat{a}^\dagger \hat{a} \hat{\rho} - 2 \hat{a} \hat{\rho} \hat{a}^\dagger + \hat{\rho} \hat{a}^\dagger \hat{a} \right) \\ &\quad -\frac{C}{2} N \left( \hat{a} \hat{a}^\dagger \hat{\rho} - 2 \hat{a}^\dagger \hat{\rho} \hat{a} + \hat{\rho} \hat{a} \hat{a}^\dagger \right) \\ &\quad +\frac{C}{2} M \left( \hat{a} \hat{a} \hat{\rho} - 2 \hat{a} \hat{\rho} \hat{a} + \hat{\rho} \hat{a} \hat{a} \right) \\ &\quad +\frac{C}{2} M^* \left( \hat{a}^\dagger \hat{a}^\dagger \hat{\rho} - 2 \hat{a}^\dagger \hat{\rho} \hat{a}^\dagger + \hat{\rho} \hat{a}^\dagger \hat{a}^\dagger \right) \end{aligned} \quad (1.67)$$

where

$$N = \sinh^2(r) \quad (1.68)$$

$$M = \cosh(r) \sinh(r) \exp(-i\theta)$$

$$|M| = [N(N+1)]^{1/2}$$

## 1.5 Conclusion

Fundamental and advanced mathematical methods are required to solve problems in quantum optics. The basic knowledge of operators and states play the biggest role as they can represent the system and provide useful information for further investigations. The understanding of basic quantum optics in this chapter will be used in the preceding chapters to solve the selected system and also the light properties of interest.

## CHAPTER 2

### LIGHT-MATTER INTERACTION

#### 2.1 Introduction

The heart of quantum optics lies in the interaction between light and matter. The understanding of the interaction is very important and the most essential part is to understand the behaviour of the system of interest, particularly the properties of light during the interaction. The study of light and matter began when scientists discovered that light would after all be affected by gravity although it does not have a mass (Fox, 2006). The light beam consists of photons that carry energies which contribute to the interaction between the light and the gravitational force.

In reality, because of the existence of electron and proton spins, the resonance line (the emission of the optical line) of an atom (e.g. Hydrogen) includes several neighbouring components, which are fine and hyperfine structure (Cohen-Tannoudji, Diu, & Laloe, 1977). The hyperfine structure refers to small shifts and splittings in the energy levels of atoms, molecules and ions due to the interaction between energy of the nucleus and internally generated electric and magnetic fields. In atoms, hyperfine structure occurs when the nuclear magnetic dipole moment interacts with the magnetic field generated by the electrons. It also occurs when the energy of the nuclear electric quadrupole moment interact with the electric field gradient due to the distribution of charge within the atom.

The resonance line of Hydrogen corresponds to an atomic transition between the ground state  $1s(n = 1; l = m = 0)$  and the excited state  $2p(n = 2; l = 1; m = +1, 0, -1)$ . When the atom is placed in a static magnetic field, the frequency and the polarization of the atomic lines are changed. This change is called the Zeeman effect and can be explained in the two- and three-level atom case discussed in this work.

For a moving atom, the ground state of a two-level atom is broadened and shifted when irradiated by a light beam. The light beam produces a displacement of the ground state as a whole (center-of-mass light shift) and it also can remove the Zeeman degeneracy of the level (Cohen-Tannoudji & Dupont-Roc, 1972). The difference of the center-

of-mass light shifts for two different hyperfine levels of an alkali-atom results in a modification of the hyperfine frequency of the ground state.

In the three-level atom (Fig.2.3) such as Raman system, the probe and driving fields have similar frequencies and propagation directions. Since both fields couple to the same upper level  $|a\rangle$ , they can have similar frequencies if the lower levels  $|b\rangle$  and  $|c\rangle$  are closely spaced in energy, which means, nearly degenerate. This is in fact the case for most of the alkali atoms-the workhorse of experimental quantum optics-whose electronic ground state contains a manifold of hyperfine and Zeeman levels (Lambropoulos & Petrosyan, 2007). A pair of such levels is then selected by properly adjusting the frequencies and polarizations of the probe and driving fields to serve as the lower metastable levels  $|b\rangle$  and  $|c\rangle$ .

Nowadays, the study of the light-matter interaction has a broader perspective and had been tailored to enhance laser technology, quantum information science to realize quantum computing and many other fields of study. All these must begin with an understanding of interaction in the subatomic scale as will be discussed in this chapter.

## 2.2 Semiclassical Atom-Field Theory

Semiclassical treatment is used when matter, for example an atom, is treated as a quantum system which can have certain levels of quanta; while light or electromagnetic wave is treated classically. Here the concept of photon is not applicable. In the next sub-section will discuss how to derive the final solution of the states for a system treated semiclassically.

### 2.2.1 Two-level Atom

A schematic view of a single two-level atom confined in a lossless cavity is shown in Fig.2.1 where  $|a\rangle, |b\rangle$  represents upper level and lower level state of the atom, respectively. This will cause an interaction between the atom and the field. The interaction exhibits interesting features to be discovered and provide space for scientists to investigate the nature of the light and understands its behaviour for a better future and to enhance the existing technology. One may begin to study the interaction by knowing that there are two ways to treat this interaction: semiclassical treatment and fully quantum treatment. It is



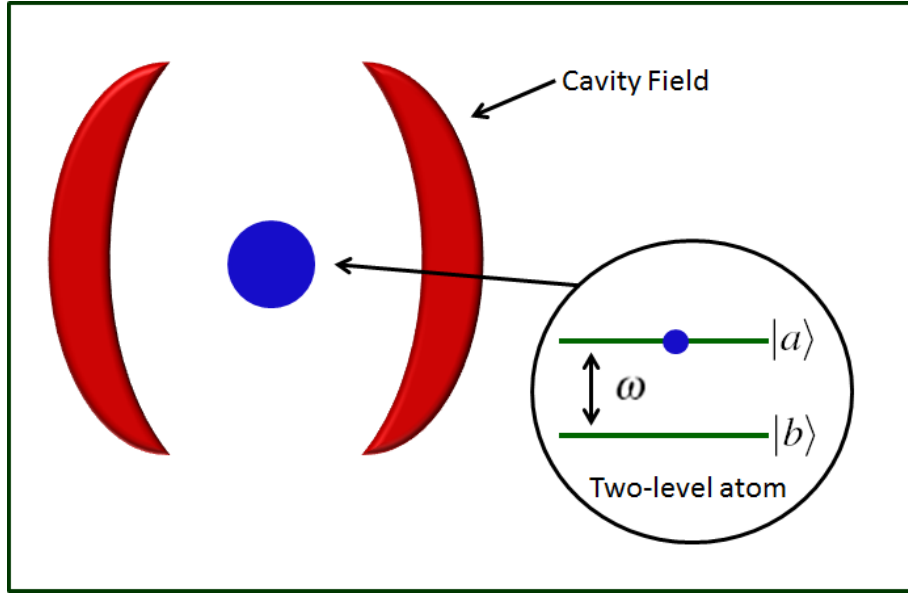


Figure 2.1: A single two-level atom placed inside a cavity

easier to begin with the semiclassical method in order to better understand the interaction mechanism.

Both levels  $|a\rangle$  and  $|b\rangle$  are the eigenstates of  $\hat{H}_0$  with eigenvalues of  $\hbar\omega_a$  and  $\hbar\omega_b$  respectively. The wavefunction of the two-level atom can be written as

$$|\psi(t)\rangle = C_a(t)|a\rangle + C_b(t)|b\rangle \quad (2.1)$$

where  $C_a$  and  $C_b$  are the probability amplitudes of finding the atom in states  $|a\rangle$  and  $|b\rangle$ , respectively. The corresponding Schrödinger Equation is

$$i\hbar \frac{d}{dt} |\psi(t)\rangle = \hat{H}(t) |\psi(t)\rangle \quad (2.2)$$

where

$$\hat{H} = \hat{H}_0 + \hat{V}$$

$\hat{H}_0$  and  $V$  represent the unperturbed and the interaction parts of the particular system.

Using completeness relation

$$|a\rangle \langle a| + |b\rangle \langle b| = 1 \quad (2.3)$$

we can write  $\hat{H}_0$  as

$$\begin{aligned} \hat{H}_0 &= (|a\rangle \langle a| + |b\rangle \langle b|) \hat{H}_0 (|a\rangle \langle a| + |b\rangle \langle b|) \\ &= \hbar\omega_a |a\rangle \langle a| + \hbar\omega_b |b\rangle \langle b| \end{aligned} \quad (2.4)$$

For semiclassical treatment, we assume the electric field,  $E(t)$ , is linearly polarized along the  $x$ -axis.  $\hat{V}$ , which is the dipole interaction, describe the interaction energy between atom and field and can be written by

$$\begin{aligned}
\hat{V} &= -e\hat{x}E(t) \\
&= -e(|a\rangle\langle a| + |b\rangle\langle b|)\hat{x}(|a\rangle\langle a| + |b\rangle\langle b|)E(t) \\
&= -(\wp_{ab}|a\rangle\langle b| + \wp_{ba}|b\rangle\langle a|)E(t) \\
&= -\wp_{ab}|a\rangle\langle b|\frac{1}{2}(e^{-i\nu t} + e^{i\nu t})E_x \\
&\quad -\wp_{ba}|b\rangle\langle a|\frac{1}{2}(e^{-i\nu t} + e^{i\nu t})E_x
\end{aligned} \tag{2.5}$$

where  $\wp_{ab} = \wp_{ba}^* = e\langle a|\hat{x}|b\rangle$  is the matrix element of the electric dipole moment,  $e$  is the electron charge,  $\hat{x} = D|a\rangle\langle b| + D^*|b\rangle\langle a|$  is the quantum mechanical position operator and  $E(t)$  is given as

$$\begin{aligned}
E(t) &= E_x \cos \nu t \\
&= \frac{1}{2}(e^{-i\nu t} + e^{i\nu t})E_x
\end{aligned}$$

with  $E_x$  is the field amplitude and  $\nu = ck$  is the frequency of the field. If the interaction equation is expanded, the term  $|a\rangle\langle b|e^{i\nu t}$  and  $|b\rangle\langle a|e^{-i\nu t}$  are fast rotating term, so they can be neglected which gives

$$\begin{aligned}
V &= -\wp_{ab}|a\rangle\langle b|\frac{1}{2}e^{-i\nu t}E_x - \wp_{ba}|b\rangle\langle a|\frac{1}{2}e^{i\nu t}E_x \\
&= -\frac{\hbar}{2}(\Omega_R|a\rangle\langle b|e^{-i\nu t} + \Omega_R^*|b\rangle\langle a|e^{i\nu t}) \\
&= -\frac{\hbar}{2}\Omega_R(|a\rangle\langle b|e^{-i\nu t} + |b\rangle\langle a|e^{i\nu t})
\end{aligned} \tag{2.6}$$

where we have assumed that the Rabi frequency  $\Omega_R = \Omega_R^*$  that is defined by

$$\Omega_R = \frac{|\wp_{ba}|E_x}{\hbar} \tag{2.7}$$

$$\wp_{ba} = |\wp_{ba}|\exp(i\phi) \tag{2.8}$$

where  $\phi$  is the phase of the dipole matrix elements

The total Hamiltonian becomes

$$\hat{H} = \hat{H}_0 + \hat{V} \tag{2.9}$$

$$\begin{aligned}
&= \hbar\omega_a |a\rangle \langle a| + \hbar\omega_b |b\rangle \langle b| \\
&\quad - \frac{\hbar}{2}\Omega_R (|a\rangle \langle b| e^{-i\nu t} + |b\rangle \langle a| e^{i\nu t})
\end{aligned}$$

By substituting Eq.2.1 and Eq.2.9 into the Schrodinger equation of Eq.2.2, we obtain for the left hand side

$$\begin{aligned}
i\hbar \frac{d}{dt} |\psi(t)\rangle &= i\hbar \frac{d}{dt} [C_a(t)|a\rangle + C_b(t)|b\rangle] \\
&= i\hbar \frac{d}{dt} C_a(t)|a\rangle + i\hbar \frac{d}{dt} C_b(t)|b\rangle
\end{aligned} \tag{2.10}$$

The eigenfunctions of the Hamiltonian are orthogonal (Fox, 2006) to each other and are normalized so that:

$$\int \psi_n^* \psi_{n'} d^3r = \delta_{nn'} \tag{2.11}$$

where  $\delta_{nn'}$  is the Kronecker delta function defined by

$$\begin{aligned}
\delta_{nn'} &= 1 & \text{if } n &= n' \\
\delta_{nn'} &= 0 & \text{if } n &\neq n'
\end{aligned}$$

This property is called orthonormality, so we have

$$\begin{aligned}
\langle a|a\rangle &= \langle b|b\rangle = 1 \\
\langle a|b\rangle &= \langle b|a\rangle = 0
\end{aligned}$$

Thus, the right hand side becomes

$$\begin{aligned}
\hat{H}(t)|\psi(t)\rangle &= (\hat{H}_0 + \hat{V}) [C_a(t)|a\rangle + C_b(t)|b\rangle] \\
&= \hat{H}_0[C_a(t)|a\rangle + C_b(t)|b\rangle] \\
&\quad + \hat{V}[C_a(t)|a\rangle + C_b(t)|b\rangle] \\
&= (\hbar\omega_a |a\rangle \langle a| + \hbar\omega_b |b\rangle \langle b|) C_a(t)|a\rangle \\
&\quad + (\hbar\omega_a |a\rangle \langle a| + \hbar\omega_b |b\rangle \langle b|) C_b(t)|b\rangle \\
&\quad - \frac{\hbar}{2}\Omega_R (|a\rangle \langle b| e^{-i\nu t} + |b\rangle \langle a| e^{i\nu t}) C_a(t)|a\rangle \\
&\quad - \frac{\hbar}{2}\Omega_R (|a\rangle \langle b| e^{-i\nu t} + |b\rangle \langle a| e^{i\nu t}) C_b(t)|b\rangle \\
&= \hbar\omega_a |a\rangle C_a(t) + \hbar\omega_b |b\rangle C_b(t) \\
&\quad - \frac{\hbar}{2}\Omega_R |b\rangle e^{i\nu t} C_a(t) - \frac{\hbar}{2}\Omega_R |a\rangle e^{-i\nu t} C_b(t)
\end{aligned} \tag{2.12}$$

The equation of motion becomes

$$\begin{aligned}
i\hbar \frac{d}{dt} C_a(t) |a\rangle + i\hbar \frac{d}{dt} C_b(t) |b\rangle = \\
\hbar \omega_a |a\rangle C_a(t) + \hbar \omega_b |b\rangle C_b(t) \\
-\frac{\hbar}{2} \Omega_R |b\rangle e^{i\nu t} C_a(t) - \frac{\hbar}{2} \Omega_R |a\rangle e^{-i\nu t} C_b(t)
\end{aligned} \tag{2.13}$$

then we project the resulting equation with  $\langle a|$  and  $\langle b|$  to obtain the equation of motion for amplitudes  $C_a$  and  $C_b$

$$\frac{d}{dt} C_a(t) = -\frac{i}{\hbar} \left[ \hbar \omega_a C_a(t) - \frac{\hbar}{2} \Omega_R e^{-i\nu t} C_b(t) \right] \tag{2.14}$$

$$\begin{aligned}
&= -i\omega_a C_a(t) + i\frac{\Omega_R}{2} e^{-i\nu t} C_b(t) \\
\frac{d}{dt} C_b(t) &= -\frac{i}{\hbar} \left[ \hbar \omega_b C_b(t) - \frac{\hbar}{2} \Omega_R e^{i\nu t} C_a(t) \right] \tag{2.15}
\end{aligned}$$

$$= -i\omega_b C_b(t) + i\frac{\Omega_R}{2} e^{i\nu t} C_a(t)$$

To solve  $C_a$  and  $C_b$ , the equation of motion for the slowly varying amplitudes,  $c_a = C_a e^{i\omega_a t}$  and  $c_b = C_b e^{i\omega_b t}$  are introduced, which reads,

$$\frac{d}{dt} c_a = \frac{d}{dt} [C_a e^{i\omega_a t}] \tag{2.16}$$

$$\begin{aligned}
&= \frac{d}{dt} C_a e^{i\omega_a t} + \frac{d}{dt} e^{i\omega_a t} C_a \\
&= i\frac{\Omega_R}{2} C_b(t) e^{i(\omega_a - \nu)t} \\
&= i\frac{\Omega_R}{2} c_b(t) e^{i(\omega - \nu)t}
\end{aligned}$$

$$\frac{d}{dt} c_b = i\frac{\Omega_R}{2} c_a e^{-i(\omega - \nu)t} \tag{2.17}$$

where  $\omega = \omega_a - \omega_b$  is the atomic transition frequency. The solution of 2.16 and 2.17 can be written as

$$\begin{aligned}
c_a &= \left( a_1 e^{i\Omega t/2} + a_2 e^{-i\Omega t/2} \right) e^{i\Delta t/2} \\
c_b &= \left( b_1 e^{i\Omega t/2} + b_2 e^{-i\Omega t/2} \right) e^{i\Delta t/2}
\end{aligned} \tag{2.18}$$

where  $\Delta = \omega - \nu$ , and  $\Omega = \sqrt{\Omega_R^2 + (\omega - \nu)^2}$ .

Coefficients  $a_1, a_2, b_1$  and  $b_2$  are constants of integration which are determined from the initial condition (Scully & Zubairy, 1997)

$$a_1 = \frac{1}{2\Omega} \left[ (\Omega - \Delta) c_a(0) + \Omega_R e^{-i\phi} c_b(0) \right]$$

$$\begin{aligned}
a_2 &= \frac{1}{2\Omega} \left[ (\Omega + \Delta) c_a(0) - \Omega_R e^{-i\phi} c_b(0) \right] \\
b_1 &= \frac{1}{2\Omega} \left[ (\Omega + \Delta) c_b(0) + \Omega_R e^{i\phi} c_a(0) \right] \\
b_2 &= \frac{1}{2\Omega} \left[ (\Omega - \Delta) c_b(0) - \Omega_R e^{i\phi} c_a(0) \right]
\end{aligned}$$

which gives

$$\begin{aligned}
c_a(t) &= \left[ c_a(0) \cos\left(\frac{\Omega t}{2}\right) - \frac{i\Delta}{\Omega} \sin\left(\frac{\Omega t}{2}\right) \right] e^{i\Delta t/2} \\
&\quad + c_b(0) i \frac{\Omega_R}{\Omega} e^{-i\phi} c_b(0) \sin\left(\frac{\Omega t}{2}\right) e^{i\Delta t/2}
\end{aligned} \tag{2.19}$$

$$\begin{aligned}
c_b(t) &= \left[ c_b(0) \cos\left(\frac{\Omega t}{2}\right) + \frac{i\Delta}{\Omega} \sin\left(\frac{\Omega t}{2}\right) \right] e^{-i\Delta t/2} \\
&\quad + c_b(0) i \frac{\Omega_R}{\Omega} e^{i\phi} c_a(0) \sin\left(\frac{\Omega t}{2}\right) e^{-i\Delta t/2}
\end{aligned} \tag{2.20}$$

The equations can also be written in density matrix form by introducing  $\rho_{nm} = c_n c_m^*$  to get four term of the elements which are

$$\begin{aligned}
\rho_{aa}(t) &= c_a(t) c_a^*(t) \\
\rho_{ab}(t) &= c_a(t) c_b^*(t) \\
\rho_{ba}(t) &= c_b(t) c_a^*(t) \\
\rho_{bb}(t) &= c_b(t) c_b^*(t)
\end{aligned}$$

As stated by (Eq.1.30) in previous chapter, the density matrix for two-level atom is in the form of

$$\hat{\rho}(t) = \begin{bmatrix} \rho_{aa}(t) & \rho_{ab}(t) \\ \rho_{ba}(t) & \rho_{bb}(t) \end{bmatrix} \tag{2.21}$$

So by substituting equations 2.16 and 2.17 and using the general differential rule, the time evolution density matrix for  $\rho_{aa}(t)$  is

$$\begin{aligned}
\frac{d}{dt} \rho_{aa}(t) &= \frac{d}{dt} [c_a(t) c_a^*(t)] \\
&= \left[ \frac{d}{dt} c_a(t) \right] c_a^*(t) + c_a(t) \left[ \frac{d}{dt} c_a^*(t) \right] \\
&= \left[ i \frac{\Omega_R}{2} c_b(t) e^{i\Delta t} \right] c_a^*(t) - c_a \left[ i \frac{\Omega_R}{2} c_b^*(t) e^{-i\Delta t} \right] \\
&= i \frac{\Omega_R}{2} \left[ e^{i\Delta t} \rho_{ba}(t) - e^{-i\Delta t} \rho_{ab}(t) \right]
\end{aligned} \tag{2.22}$$

while using the same method, the rest of the elements are given by

$$\frac{d}{dt} \rho_{ab}(t) = i \frac{\Omega_R}{2} [\rho_{bb}(t) - \rho_{aa}(t)] e^{i\Delta t} \tag{2.23}$$

$$\frac{d}{dt}\rho_{ba}(t) = \frac{d}{dt}\rho_{ab}^*(t) \quad (2.24)$$

$$= -i\frac{\Omega_R}{2}[\rho_{bb}(t) - \rho_{aa}(t)]e^{-i\Delta t}$$

$$\frac{d}{dt}\rho_{bb}(t) = -i\frac{\Omega_R}{2}\left[e^{i\Delta t}\rho_{ba}(t) - e^{-i\Delta t}\rho_{ab}(t)\right] \quad (2.25)$$

The probabilities of the atom being in state  $|a\rangle$  and  $|b\rangle$  at time  $t$  are given by  $|c_a(t)|^2$  and  $|c_b(t)|^2$ . The total probabilities of states are known as  $|c_a(t)|^2 + |c_b(t)|^2 = 1$ . If we

assume that atom is initially in the state  $|a\rangle$  then initial  $c_a(0) = 1$  and  $c_b(0) = 0$ . The inversion (Ooi, Hazmin, & Singh, 2012) is given by

$$n_{ab}(t) = |c_a(t)|^2 - |c_b(t)|^2 \quad (2.26)$$

$$= \left(\frac{\Delta^2 - \Omega_R^2}{\Omega^2}\right) \sin^2\left(\frac{\Omega t}{2}\right) + \cos^2\left(\frac{\Omega t}{2}\right)$$

Under the action of the incident field, a dipole moment is induced between the two atomic levels and is given by the expectation value of the dipole moment operator

$$P(t) = e\langle\psi(t)|r|\psi(t)\rangle = C_a^*C_b\mathcal{P}_{ab} + c.c. \quad (2.27)$$

$$= c_a^*c_b\mathcal{P}_{ab}e^{i\omega t} + c.c.$$

where *c.c.* stands for complex conjugate. For an atom initially in the upper level, we obtain

$$P(t) = 2\left\{Re\frac{i\Omega_R}{\Omega}\mathcal{P}_{ab}\left[\cos\left(\frac{\Omega t}{2}\right) + \frac{i\Delta}{\Omega}\sin\left(\frac{\Omega t}{2}\right)\right]\sin\left(\frac{\Omega t}{2}\right)e^{i\phi}e^{i\omega t}\right\} \quad (2.28)$$

The dipole moment therefore oscillates with the frequency of the incident field. When the atom is at resonance with the incident field ( $\Delta = 0$ ), we get  $\Omega = \Omega_R$  and  $W(t) = \cos(\Omega_R t)$ . The inversion oscillates between -1 and 1 at a frequency  $\Omega_R$

### 2.2.2 Three-level Atom

The three-level atom consists of three states, let say  $|a\rangle$ ,  $|b\rangle$  and  $|c\rangle$ . Several types have been recognized (Fleischhauer, Imamoglu, & Marangos, 2005) which are called V-type atom,  $\Lambda$ -type atom and  $\Xi$  configuration as shown in Fig.2.2

The allowed transition for each type of three-level atom are shown in table

Every single structure has its own properties and importance. We examine a  $\Lambda$ -type three-level atom (Berman & Ooi, 2012), where  $|a\rangle$  is an excited state while  $|b\rangle$  and  $|c\rangle$  are

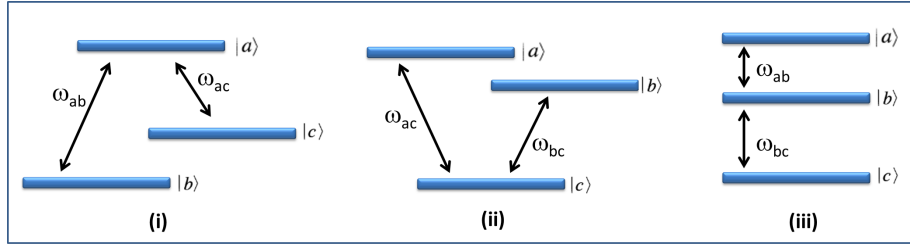


Figure 2.2: Three type three-level atom configuration with (i)  $\Lambda$ -type, (ii)  $V$ -type, and (iii)  $\Xi$  configuration

Table 2.1: Allowed and forbidden dipole transition in three-level atom

Atom Type	$ a\rangle \rightarrow  b\rangle$ transition	$ a\rangle \rightarrow  c\rangle$ transition	$ c\rangle \rightarrow  b\rangle$ transition
$V$ -type	Forbidden	Allowed	Allowed
$\Xi$ -type	Allowed	Forbidden	Allowed
$\Lambda$ -type	Allowed	Allowed	Forbidden

ground states coupled with the excited state  $|a\rangle$  that interacts with two field frequencies of  $\omega_1$  and  $\omega_2$  respectively as shown in Fig.2.3

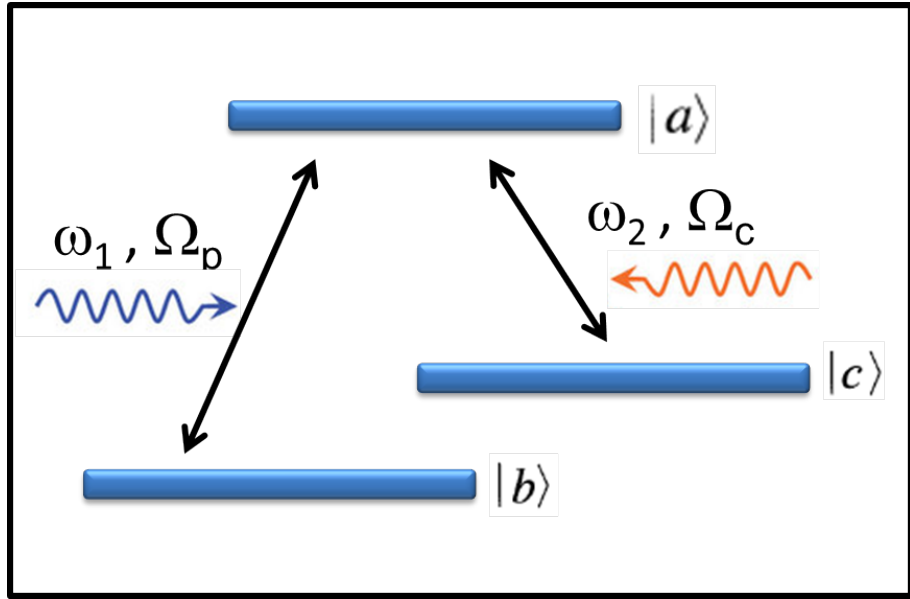


Figure 2.3:  $\Lambda$ -type three-level atom interact with two fields frequency  $\omega_1$  and  $\omega_2$ .

The Hamiltonian of the system is given by

$$\hat{H} = \hat{H}_0 + \hat{V} \quad (2.29)$$

where

$$\begin{aligned} \hat{H}_0 &= \hbar\omega_a |a\rangle \langle a| + \hbar\omega_b |b\rangle \langle b| + \hbar\omega_c |c\rangle \langle c| \\ \hat{V} &= -\frac{\hbar}{2} (\Omega_p |a\rangle \langle b| e^{-i\omega_1 t} + \Omega_p^* |b\rangle \langle a| e^{i\omega_1 t}) \\ &\quad -\frac{\hbar}{2} (\Omega_c |a\rangle \langle c| e^{-i\omega_2 t} + \Omega_c^* |c\rangle \langle a| e^{i\omega_2 t}) \end{aligned}$$

Since the transition between  $|b\rangle$  and  $|c\rangle$  are not dipole allowed, the  $\Omega_p$  and  $\Omega_c$  are Rabi frequencies associated with the coupling between atomic transition  $|a\rangle \rightarrow |b\rangle$  and  $|a\rangle \rightarrow |c\rangle$  with field frequencies of  $\omega_1$  and  $\omega_2$  respectively. The wave function represents the system can be written as

$$|\psi(t)\rangle = C_a(t)|a\rangle + C_b(t)|b\rangle + C_c(t)|c\rangle$$

Substituting  $\hat{H}$  and  $|\psi(t)\rangle$  into the Schrodinger equation Eq.2.2 produces

$$i\hbar \frac{d}{dt} |\psi(t)\rangle = (\hat{H}_0 + \hat{V}) |\psi(t)\rangle \quad (2.30)$$

Solving the right hand side for Schrodinger equation by substituting the wave equation and Hamiltonian of the system gives

$$\begin{aligned} H(t)|\psi(t)\rangle &= \hat{H}_0 [C_a(t)|a\rangle + C_b(t)|b\rangle + C_c(t)|c\rangle] \\ &+ V [C_a(t)|a\rangle + C_b(t)|b\rangle + C_c(t)|c\rangle] \\ &= \hbar\omega_a |a\rangle C_a(t) + \hbar\omega_b |b\rangle C_b(t) + \hbar\omega_c |c\rangle C_c(t) \\ &- \frac{\hbar}{2} \Omega_p^* |b\rangle e^{i\omega_1 t} C_a(t) - \frac{\hbar}{2} \Omega_p |a\rangle e^{-i\omega_1 t} C_b(t) \\ &- \frac{\hbar}{2} \Omega_c |a\rangle e^{-i\omega_2 t} C_c(t) - \frac{\hbar}{2} \Omega_c^* |c\rangle e^{i\omega_2 t} C_a(t) \end{aligned} \quad (2.31)$$

By projecting the whole equation with  $\langle a|$ ,  $\langle b|$  and  $\langle c|$ , we obtain the following equations of motion for amplitude

$$\frac{d}{dt} C_a(t) = -i\omega_a C_a(t) + \frac{i\Omega_p}{2} e^{-i\omega_1 t} C_b(t) + \frac{i\Omega_c}{2} e^{-i\omega_2 t} C_c(t) \quad (2.32)$$

$$\frac{d}{dt} C_b(t) = -i\omega_b C_b(t) + \frac{i\Omega_p^*}{2} e^{i\omega_1 t} C_a(t) \quad (2.33)$$

$$\frac{d}{dt} C_c(t) = -i\omega_c C_c(t) + \frac{i\Omega_c^*}{2} e^{i\omega_2 t} C_a(t) \quad (2.34)$$

Let us denote the density matrix element as  $\rho_{nm} = C_n C_m^*$ . Thus, we obtain

$$\begin{aligned} \frac{d}{dt} \rho_{aa} &= -\frac{i\Omega_p}{2} [\rho_{ab}(t) e^{i\omega_1 t} - \rho_{ba}(t) e^{-i\omega_1 t}] \\ &- \frac{i\Omega_c}{2} [\rho_{ac}(t) e^{i\omega_2 t} - \rho_{ca}(t) e^{-i\omega_2 t}] \end{aligned} \quad (2.35)$$

$$\frac{d}{dt} \rho_{bb} = \frac{i\Omega_p}{2} [\rho_{ab}(t) e^{i\omega_1 t} - \rho_{ba}(t) e^{-i\omega_1 t}]$$

$$\frac{d}{dt} \rho_{cc} = \frac{i\Omega_c}{2} [\rho_{ac}(t) e^{i\omega_2 t} - \rho_{ca}(t) e^{-i\omega_2 t}]$$

$$\frac{d}{dt} \rho_{ab} = -i\Delta_p \rho_{ab}(t) + \frac{i\Omega_p}{2} [\rho_{bb}(t) - \rho_{aa}(t)] e^{-i\omega_1 t}$$



$$\begin{aligned}
& + \frac{i\Omega_c}{2} e^{-i\omega_2 t} \rho_{cb}(t) \\
\frac{d}{dt} \rho_{ac} &= \frac{d}{dt} c_a(t) c_c^*(t) + c_a(t) \frac{d}{dt} c_c^*(t) \\
&= -i\Delta_c \rho_{ac}(t) + \frac{i\Omega_c}{2} [\rho_{cc}(t) - \rho_{aa}(t)] e^{-i\omega_2 t} \\
& + \frac{i\Omega_p}{2} e^{-i\omega_1 t} \rho_{bc}(t) \\
\frac{d}{dt} \rho_{ba} &= \frac{d}{dt} \rho_{ab}^* \\
\frac{d}{dt} \rho_{ca} &= \frac{d}{dt} \rho_{ac}^*
\end{aligned}$$

where

$$\Delta_p = \omega_a - \omega_b$$

$$\Delta_c = \omega_a - \omega_c$$

$\Lambda$ -type and  $\Xi$ -type three-level atom have two ground levels  $|b\rangle$  and  $|c\rangle$ , the inversion is stated by

$$n_{abc}(t) = |c_a(t)|^2 - |c_b(t)|^2 - |c_c(t)|^2 \quad (2.36)$$

while for  $V$ -type has one ground level  $|c\rangle$ , the inversion become

$$n_{abc}(t) = |c_a(t)|^2 + |c_b(t)|^2 - |c_c(t)|^2 \quad (2.37)$$

## 2.3 Full Quantum Treatment

Fully quantum treatment is applied to the system when both, atom and field are treated quantum mechanically. Both subsystems are represented by operators  $\hat{\sigma}_+$  and  $\hat{\sigma}_-$  for atom show the atomic excitation and de-excitation(emmission), while  $\hat{a}$  and  $\hat{a}^\dagger$  denote the annihilation and creation of photons. The analytical solutions are not much different than the semiclassical derivation. It contains some modification in the Hamiltonian which will be discussed in the next sub-section.

### 2.3.1 The Jaynes-Cumming Model

An interaction between two-level atom with a quantized single mode field can be described theoretically by the Jaynes-Cumming Model(JCM) (Jaynes & Cummings, 1963). It is the simplest case to study light-matter interaction in a fully quantum treatment as illustrated in Fig.2.1.

The interaction can be represented by the Hamiltonian (Milburn & Walls, 2008):

$$\hat{H}_{AF} = \hat{H}_A + \hat{H}_F + \hat{V} \quad (2.38)$$

where

$$\begin{aligned} \hat{H}_o &= \hat{H}_A + \hat{H}_F \\ &= \frac{\hbar\omega}{2} \hat{\sigma}_z + \hbar\nu \hat{a}^\dagger \hat{a} \end{aligned} \quad (2.39)$$

$$\begin{aligned} \hat{V} &= \frac{\hbar\omega}{2} \hat{F} \cdot \hat{S} \\ &= \frac{\hbar\omega}{2} (\hat{a} + \hat{a}^\dagger) (\hat{\sigma}_+ + \hat{\sigma}_-) \\ &= \frac{\hbar\omega}{2} (\hat{a}\hat{\sigma}_+ + \hat{a}^\dagger\hat{\sigma}_+ + \hat{a}\hat{\sigma}_- + \hat{a}^\dagger\hat{\sigma}_-) \end{aligned} \quad (2.40)$$

with  $\hat{F}$  is the field operator, and  $\hat{S}$  is the atom operator. The term  $\hat{a}\hat{\sigma}_+$  tells that the electron goes from the ground state  $|b\rangle$  to the excited state  $|a\rangle$ , and in the process one photon of energy  $\hbar\omega$  is annihilated. The energy is conserved during this process (Yamamoto & Imamoglu, 1999). The energy is also conserved if an atom having a transition from the excited to the ground state with one photon is created during the process by  $\hat{a}^\dagger\hat{\sigma}_-$ . The terms  $\hat{a}^\dagger\hat{\sigma}_+$  and  $\hat{a}\hat{\sigma}_-$  are energy nonconservative process and can be ignored. This is referred to as the rotating wave approximation. By eliminating the nonconserving terms, we obtain

$$\hat{V} = \frac{\hbar\omega}{2} (\hat{a}\hat{\sigma}_+ + \hat{a}^\dagger\hat{\sigma}_-) \quad (2.41)$$

So the JCM in rotating wave approximation gives

$$\begin{aligned} \hat{H}_{af} &= \hat{H}_a + \hat{H}_f + \hat{V} \\ &= \frac{\hbar\omega}{2} \hat{\sigma}_z + \hbar\nu \hat{a}^\dagger \hat{a} + \hbar g (\hat{a}\hat{\sigma}_+ + \hat{a}^\dagger\hat{\sigma}_-) \end{aligned} \quad (2.42)$$

The free Hamiltonian for atom  $\hat{H}_A$ , and field  $\hat{H}_F$  in Eq.2.39 describes the unperturbed system which define the energies of atom and radiation field.  $\hat{V}$  in Eq.2.41 describes the interaction between the single atom and the quantized field.  $\omega$  and  $\nu$  are atomic transition frequency and field frequency respectively while the coupling constant  $g$  determines the strength of interaction between the atom and the field.

Eq.2.42 can be simplified by transforming the Hamiltonian into the interaction picture. It can be done by introducing

$$\hat{V}_{AF}(t) = e^{i\frac{H_0 t}{\hbar}} \hat{V} e^{-i\frac{H_0 t}{\hbar}} \quad (2.43)$$

where  $\hat{V}_{AF}(t)$  denote the atom-field Hamiltonian in interaction picture. Using (Scully & Zubairy, 1997)

$$\begin{aligned} e^{i\omega\hat{\sigma}_z t/2} \hat{\sigma}_+ e^{-i\omega\hat{\sigma}_z t/2} &= \hat{\sigma}_+ e^{i\omega t} \\ e^{i\omega\hat{\sigma}_z t/2} \hat{\sigma}_- e^{-i\omega\hat{\sigma}_z t/2} &= \hat{\sigma}_- e^{-i\omega t} \\ e^{i\nu\hat{a}^\dagger \hat{a} t} \hat{a} e^{-i\nu\hat{a}^\dagger \hat{a} t} &= \hat{a} e^{-i\nu t} \\ e^{i\nu\hat{a}^\dagger \hat{a} t} \hat{a}^\dagger e^{-i\nu\hat{a}^\dagger \hat{a} t} &= \hat{a}^\dagger e^{i\nu t} \end{aligned}$$

the Hamiltonian becomes

$$\begin{aligned} \hat{V}_{AF}(t) &= e^{iH_0 t/\hbar} \hat{V} e^{-iH_0 t/\hbar} \\ &= \hbar g \left( \hat{\sigma}_+ \hat{a} e^{i(\omega-\nu)t} + \hat{a}^\dagger \hat{\sigma}_- e^{-i(\omega-\nu)t} \right) \\ &= \hbar g \left( \hat{\sigma}_+ \hat{a} e^{i\Delta t} + \hat{a}^\dagger \hat{\sigma}_- e^{-i\Delta t} \right) \end{aligned} \quad (2.44)$$

where the difference between atomic transition frequency and field frequency defined as the detuning:

$$\Delta = \omega - \nu$$

Several methods can be applied to the Hamiltonian to derive the evolution of atom-field system described above such as probability amplitude method, unitary time evolution method and Heisenberg method (Barnett & Radmore, 1997). The first two methods will be discussed in the following section since they will be used in the preceediing chapters.

### 2.3.1 (a) Probability Amplitude Method

Due to superposition of states of an atom which is between the excited and ground state, the evolution of the atom-field system can be described by the state vector at any time,  $t$  as

$$|\psi(t)\rangle = \sum_n [C_{a,n}(t)|a,n\rangle + C_{b,n}(t)|b,n\rangle] \quad (2.45)$$

with the time dependent atom-field coefficients  $C_{i,n}$  for level ( $i = a, b$ ) with  $n$  photons.  $|a, n\rangle$  ( $|b, n\rangle$ ) is the state in which the atom is in the excited state  $|a\rangle$  (ground state  $|b\rangle$ ) with the field contains  $n$  photons. By substituting Eq.2.45 and Eq.2.44 in Eq.2.2, we obtain

$$\begin{aligned} i\hbar \frac{d}{dt} |\psi(t)\rangle &= i\hbar \frac{d}{dt} [C_{a,n}(t)|a, n\rangle + C_{b,n}(t)|b, n\rangle] \\ &= \hbar g \left( \hat{\sigma}_+ \hat{a} e^{i\Delta t} + \hat{a}^\dagger \hat{\sigma}_- e^{-i\Delta t} \right) [C_{a,n}(t)|a, n\rangle + C_{b,n}(t)|b, n\rangle] \end{aligned} \quad (2.46)$$

It is known that interaction energy can only cause transition between  $|a, n\rangle$  and  $|b, n+1\rangle$  since one photon is created during transition process from the excited to the ground state. By denoting  $\hat{\sigma}_+ = |a\rangle \langle b|$  and  $\hat{\sigma}_- = |b\rangle \langle a|$  and using the field operations base on the (Eq.1.15), we get

$$\begin{aligned} &\frac{d}{dt} [C_{a,n}(t)|a, n\rangle + C_{b,n+1}(t)|b, n+1\rangle] \\ &= -ig(\hat{\sigma}_+ \hat{a} e^{i\Delta t} + \hat{\sigma}_- \hat{a}^\dagger e^{-i\Delta t}) C_{a,n}(t)|a, n\rangle \\ &\quad -ig(\hat{\sigma}_+ \hat{a} e^{i\Delta t} + \hat{\sigma}_- \hat{a}^\dagger e^{-i\Delta t}) C_{b,n+1}(t)|b, n+1\rangle \\ &= -ig|a\rangle \langle b| \hat{a} e^{i\Delta t} C_{a,n}(t)|a\rangle |n\rangle - ig|b\rangle \langle a| \hat{a}^\dagger e^{-i\Delta t} C_{a,n}(t)|a\rangle |n\rangle \\ &\quad -ig|a\rangle \langle b| \hat{a} e^{i\Delta t} C_{b,n+1}(t)|b\rangle |n+1\rangle - ig|b\rangle \langle a| \hat{a}^\dagger e^{-i\Delta t} C_{b,n+1}(t)|b\rangle |n+1\rangle \\ &= -ig\sqrt{n+1} e^{-i\Delta t} C_{a,n}(t)|b\rangle |n+1\rangle - ig\sqrt{n+1} e^{i\Delta t} C_{b,n+1}(t)|a\rangle |n\rangle \end{aligned} \quad (2.47)$$

Now by projecting the resulting equation with  $\langle a, n|$  and  $\langle b, n+1|$  we get coupled equations

$$\frac{d}{dt} C_{a,n}(t) = -ig\sqrt{n+1} e^{i\Delta t} C_{b,n+1}(t) \quad (2.48)$$

$$\frac{d}{dt} C_{b,n+1}(t) = -ig\sqrt{n+1} e^{-i\Delta t} C_{a,n}(t) \quad (2.49)$$

where  $g$  is the atom-field coupling constant and  $|C_{i,n}|^2$  is the probability of atom in state  $|i\rangle$  with  $n$  photons. Using the Laplace transform, we obtain the general solution that is given by:

$$C_{a,n}(t) = e^{i\Delta t/2} [C_{a,n}(0)r_n(t) - iC_{b,n+1}(0)q_n(t)] \quad (2.50)$$

$$\begin{aligned}
C_{b,n+1}(t) &= e^{-i\Delta t/2} [C_{b,n+1}(0)r_n^*(t) - iC_{a,n}(0)q_n(t)] \\
C_{b,n}(t) &= e^{-i\Delta t/2} [C_{b,n}(0)r_{n-1}^*(t) - iC_{a,n-1}(0)q_{n-1}(t)]
\end{aligned}$$

where  $r_n(t) = \cos(\frac{\Omega_n t}{2}) - i\frac{\Delta}{\Omega_n} \sin(\frac{\Omega_n t}{2})$ ,  $q_n(t) = \frac{2g\sqrt{n+1}}{\Omega_n} \sin(\frac{\Omega_n t}{2})$ , and  $\Omega_n^2 = \Delta^2 + 4g^2(n+1)$ .

$\Omega_n$  is defined as Rabi frequency. A vacuum Rabi oscillation occurs when the atom alternately emits photons into a single-mode cavity and reabsorbs them. This behaviour is due to spontaneous emission as a consequence of coupling between the atom and the vacuum fluctuations of the cavity field.

The probabilities of finding the system in the excited or ground state with the field has  $n$  photons, at time  $t$ , are given by  $|c_{a,n}(t)|^2$  and  $|c_{b,n}(t)|^2$ , respectively. By taking the trace over the atomic states, the probability  $p(n)$  that there are  $n$  photons in the field at time  $t$  is given by:

$$p(n) = |c_{a,n}(t)|^2 + |c_{b,n}(t)|^2 \quad (2.51)$$

$$\begin{aligned}
&= \rho_{nn}(0) \left[ \cos^2\left(\frac{\Omega_n t}{2}\right) + \left(\frac{\Delta}{\Omega_n}\right)^2 \sin^2\left(\frac{\Omega_n t}{2}\right) \right] \\
&\quad + \rho_{n-1,n-1}(0) \left(\frac{4g^2 n}{\Omega_{n-1}^2}\right) \sin^2\left(\frac{\Omega_{n-1} t}{2}\right)
\end{aligned} \quad (2.52)$$

where  $\rho_{nn}(0) = |c_n(0)|^2$  is the probability that there are  $n$  photons present in the field at time  $t = 0$ . The initial coherent state is given by

$$\rho_{nn}(0) = \frac{\langle n \rangle^n e^{-\langle n \rangle}}{n!} \quad (2.53)$$

One of the most important parameter in understanding the dynamics of atom is the population inversion, denoted as  $n_{ab}(t)$ . The inversion (Lambropoulos & Petrosyan, 2007) can be defined as the probability of finding a particle in its excited state.  $n_{ab}(t)$  is related to the probability amplitude by the expression:

$$n_{ab}(t) = \sum_n \left[ |c_{a,n}(t)|^2 - |c_{b,n}(t)|^2 \right] \quad (2.54)$$

By substituting  $c_{a,n}(t)$  and  $c_{b,n}(t)$  and making some arrangements, we obtain the analytical solution for  $n_{ab}(t)$ :

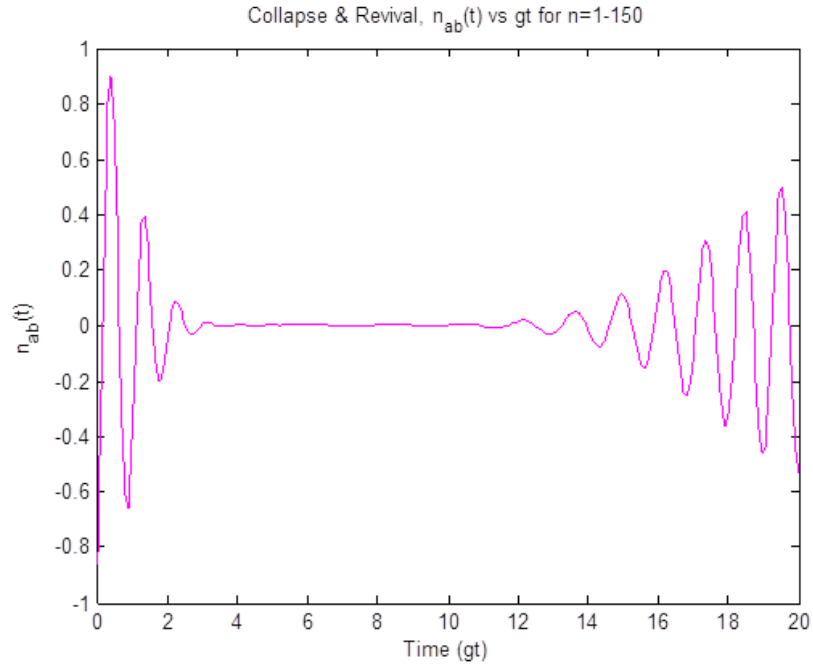


Figure 2.4: Collapse and Revival pattern for an inversion of the JCM for photon number  $n=150$

$$n_{ab}(t) = \sum_{n=0}^{\infty} \rho_{nn}(0) \left[ \frac{\Delta^2}{\Omega_n^2} + \frac{4g^2(n+1)}{\Omega_n^2} \cos(\Omega_n t) \right] \quad (2.55)$$

For an initial vacuum field ( $\rho_{nn}(0) = \delta_{n0}$ ), the inversion takes

$$n_{ab}(t) = \frac{1}{\Delta^2 + 4g^2} \left\{ \Delta^2 + 4g^2 \cos \left[ (\Delta^2 + 4g^2)^{1/2} t \right] \right\} \quad (2.56)$$

This result shows that there is a possibility of an atom to make a transition from an upper to a lower level in the absence of driving field. This is different from what has been expected in the prediction of the semiclassical theory. In the fully quantum mechanical treatment, the transition in vacuum becomes possible due to spontaneous emission. Eq.2.56 is the simplest example of spontaneous emission in which the spontaneously emitted photons contributes to the single mode of the field considered.

Fig.2.4 shows a plot of  $n_{ab}(t)$  versus normalized times  $\tau = gt$ . As the time increases, the oscillations appear to collapse and after some time, it will revive again. This process of collapse-revival is repeated as the time is increased with the Rabi oscillation damped and the time duration in which revival takes place is also increasing. The time period of the Rabi oscillation and the collapse time, are given by  $t_R$  and  $t_c$  are

$$t_R \sim \frac{1}{\Omega_n} = \frac{1}{(\Delta^2 + 4g^2 \langle n \rangle)^{1/2}} \quad (2.57)$$

$$\left(\Omega_{\langle n \rangle + \sqrt{\langle n \rangle}} - \Omega_{\langle n \rangle - \sqrt{\langle n \rangle}}\right) t_c \sim 1 \quad (2.58)$$

Since  $\langle n \rangle \gg \sqrt{\langle n \rangle}$  in the limit  $\langle n \rangle \gg 1$ , then we can assume

$$\begin{aligned} t_c &\sim \frac{1}{\Omega_{\langle n \rangle + \sqrt{\langle n \rangle}} - \Omega_{\langle n \rangle - \sqrt{\langle n \rangle}}} \\ &\simeq \frac{1}{\left[\Delta^2 + 4g^2 \left(\langle n \rangle + \sqrt{\langle n \rangle}\right)\right]^{1/2} - \left[\Delta^2 + 4g^2 \left(\langle n \rangle - \sqrt{\langle n \rangle}\right)\right]^{1/2}} \\ &\simeq \frac{1}{2g} \left(1 + \frac{\Delta^2}{4g^2 \langle n \rangle}\right)^{1/2} \end{aligned} \quad (2.59)$$

From the condition

$$\left(\Omega_{\langle n \rangle} - \Omega_{\langle n \rangle - 1}\right) t_r = 2\pi m, (m = 1, 2, \dots) \quad (2.60)$$

The interval between revival,  $t_r$  is

$$t_r = \frac{2\pi m}{\Omega_{\langle n \rangle} - \Omega_{\langle n \rangle - 1}} \quad (2.61)$$

$$\simeq \frac{2\pi m \sqrt{\langle n \rangle}}{g} \left(1 + \frac{\Delta^2}{4g^2 \langle n \rangle}\right)^{1/2} \quad (2.62)$$

### 2.3.1 (b) Unitary Time Evolution Method

Unitary time evolution method is one of the common solution used to deal with atom-field interaction. This method, however, valid for a system with no dissipation involved by taking the evolution of the system as unitary

$$U(t) = \exp\left(-\frac{i}{\hbar} \int_0^t \hat{V}_{AF}(t) dt\right) \quad (2.63)$$

By substituting Eq.2.44 and considering the system in an exact resonance where  $\Delta = 0$ , Eq.2.63 turns to

$$\begin{aligned} U(t) &= \exp\left(-\frac{i}{\hbar} \int_0^t \hat{V}_{AF}(t) dt\right) \\ &= \exp\left(-ig \int_0^t \left(\hat{\sigma}_+ \hat{a} + \hat{a}^\dagger \hat{\sigma}_-\right) dt\right) \end{aligned} \quad (2.64)$$

Using (Scully & Zubairy, 1997)

$$\begin{aligned} \left( \hat{\sigma}_+ \hat{a} + \hat{a}^\dagger \hat{\sigma}_- \right)^{2l} &= \left( \hat{a} \hat{a}^\dagger \right)^l |a\rangle \langle a| + \left( \hat{a}^\dagger \hat{a} \right)^l |b\rangle \langle b| \\ \left( \hat{\sigma}_+ \hat{a} + \hat{a}^\dagger \hat{\sigma}_- \right)^{2l+1} &= \left( \hat{a} \hat{a}^\dagger \right)^l \hat{a} |a\rangle \langle b| + \hat{a}^\dagger \left( \hat{a} \hat{a}^\dagger \right)^l |b\rangle \langle a| \end{aligned}$$

Eq.2.64 become

$$\begin{aligned} U(t) &= \cos \left( gt \sqrt{\hat{a}^\dagger \hat{a} + 1} |a\rangle \langle a| \right) + \cos \left( gt \sqrt{\hat{a}^\dagger \hat{a} + 1} |b\rangle \langle b| \right) \\ &\quad - i \frac{\sin \left( gt \sqrt{\hat{a}^\dagger \hat{a} + 1} \right)}{\sqrt{\hat{a}^\dagger \hat{a} + 1}} \hat{a} |a\rangle \langle b| - i \hat{a}^\dagger \frac{\sin \left( gt \sqrt{\hat{a}^\dagger \hat{a} + 1} \right)}{\sqrt{\hat{a}^\dagger \hat{a} + 1}} |b\rangle \langle a| \end{aligned} \quad (2.65)$$

A vector state is given as

$$|\psi(t)\rangle = U(t) |\psi(0)\rangle \quad (2.66)$$

with  $U(t)$  is considered as in the previous method where the interaction energy is between  $|a\rangle$  and  $|b+1\rangle$ , initial condition of the atom is in the excited state, while initial field at time  $t = 0$  is given by  $|\psi(0)\rangle = \sum_{n=0}^{\infty} c_n(0) |a, n\rangle$ . putting eq.2.65 and  $|\psi(0)\rangle$  into eq.2.66, we obtain

$$\begin{aligned} |\psi(t)\rangle &= \sum_{n=0}^{\infty} c_n(0) [\cos \left( gt \sqrt{n+1} \right) |a, n\rangle \\ &\quad - i \sin \left( gt \sqrt{n+1} \right) |b, n+1\rangle] \end{aligned} \quad (2.67)$$

similar to the previous derivation in probability amplitude method.

### 2.3.2 Three-Level Atom

In previous section, two-level atom interact with a single mode quantized field has been considered. Another system of interest that has been studied extensively in quantum electrodynamics is a system of a three-level atom. We consider a  $\Lambda$ -type three-level atom interacting with two-mode quantized fields of frequencies  $\omega_1$  and  $\omega_2$  as shown in Fig.2.3. We denote  $|a\rangle$  as a single upper level while  $|b\rangle$  and  $|c\rangle$  are lower levels with  $E_b < E_c$  and  $\omega_a$ ,  $\omega_b$ , and  $\omega_c$  are frequencies for each level. The Hamiltonian for the system in the rotating wave approximation can be expressed as

$$\hat{H} = \hat{H}_o + \hat{V} \quad (2.68)$$

$$\begin{aligned} \hat{H}_o &= \hbar \omega_a |a\rangle \langle a| + \hbar \omega_b |b\rangle \langle b| + \hbar \omega_c |c\rangle \langle c| + \hbar \omega_1 \hat{a}_1^\dagger \hat{a}_1 + \hbar \omega_2 \hat{a}_2^\dagger \hat{a}_2 \\ \hat{V} &= -\frac{\hbar}{2} \Omega_p \left( |a\rangle \langle b| \hat{a}_1 + \hat{a}_1^\dagger |b\rangle \langle a| \right) - \frac{\hbar}{2} \Omega_c \left( |a\rangle \langle c| \hat{a}_2 + \hat{a}_2^\dagger |c\rangle \langle a| \right) \end{aligned}$$



Here  $\Omega_p$  and  $\Omega_c$  are the complex Rabi frequencies due to the coupling between the atomic transition  $|a\rangle \rightarrow |b\rangle$  and  $|a\rangle \rightarrow |c\rangle$  with the field frequencies of  $\omega_1$  and  $\omega_2$  respectively. The transition between  $|b\rangle \rightarrow |c\rangle$  is forbidden as it is not dipole allowed. The determination whether the transition is allowed under the electric dipole interaction is associated with the selection rule.

The Hamiltonian above can be represented in interaction picture as shown in calculation below.

$$\begin{aligned}
\hat{V}_I(t) &= e^{iH_0 t/\hbar} \hat{V} e^{-iH_0 t/\hbar} \\
&= e^{i(\omega_a|a\rangle\langle a|)t} e^{i(\omega_b|b\rangle\langle b|)t} e^{i(\omega_c|c\rangle\langle c|)t} \\
&\quad e^{i(\omega_1 \hat{a}_1^\dagger \hat{a}_1)t} e^{i(\omega_2 \hat{a}_2^\dagger \hat{a}_2)t} \\
&\quad \left[ -\frac{\hbar}{2} \Omega_p \left( |a\rangle\langle b| \hat{a}_1 + \hat{a}_1^\dagger |b\rangle\langle a| \right) \right. \\
&\quad \left. -\frac{\hbar}{2} \Omega_c \left( |a\rangle\langle c| \hat{a}_2 + \hat{a}_2^\dagger |c\rangle\langle a| \right) \right] \\
&\quad e^{-i(\omega_a|a\rangle\langle a|)t} e^{-i(\omega_b|b\rangle\langle b|)t} e^{-i(\omega_c|c\rangle\langle c|)t} \\
&\quad e^{-i(\omega_1 \hat{a}_1^\dagger \hat{a}_1)t} e^{-i(\omega_2 \hat{a}_2^\dagger \hat{a}_2)t} \\
&= -\frac{\hbar}{2} \Omega_p \left( |a\rangle\langle b| \hat{a}_1 e^{i\Delta_1 t} + \hat{a}_1^\dagger |b\rangle\langle a| e^{-i\Delta_1 t} \right) \\
&\quad -\frac{\hbar}{2} \Omega_c \left( |a\rangle\langle c| \hat{a}_2 e^{i\Delta_2 t} + \hat{a}_2^\dagger |c\rangle\langle a| e^{-i\Delta_2 t} \right)
\end{aligned} \tag{2.69}$$

where

$$\Delta_1 = \omega_a - \omega_b - \omega_1$$

$$\Delta_2 = \omega_a - \omega_b - \omega_2$$

From the above equation, the total density matrix can be derived by equation

$$\frac{d\hat{\rho}}{dt} = \frac{1}{i\hbar} [\hat{V}_I(t), \hat{\rho}]$$

that gives

$$\begin{aligned}
\dot{\hat{\rho}}(t) &= \frac{i}{2} \Omega_p \left( |a\rangle\langle b| \hat{a}_1 e^{i\Delta_1 t} \hat{\rho} + \hat{a}_1^\dagger |b\rangle\langle a| e^{-i\Delta_1 t} \hat{\rho} \right) \\
&\quad + \frac{i}{2} \Omega_c \left( |a\rangle\langle c| \hat{a}_2 e^{i\Delta_2 t} \hat{\rho} + \hat{a}_2^\dagger |c\rangle\langle a| e^{-i\Delta_2 t} \hat{\rho} \right) \\
&\quad - \left( \frac{i}{2} \Omega_p \left( \hat{\rho} |a\rangle\langle b| \hat{a}_1 e^{i\Delta_1 t} + \hat{\rho} \hat{a}_1^\dagger |b\rangle\langle a| e^{-i\Delta_1 t} \right) \right. \\
&\quad \left. - \hat{\rho} \left( \frac{i}{2} \Omega_c \left( \hat{\rho} |a\rangle\langle c| \hat{a}_2 e^{i\Delta_2 t} + \hat{\rho} \hat{a}_2^\dagger |c\rangle\langle a| e^{-i\Delta_2 t} \right) \right) \right)
\end{aligned} \tag{2.70}$$

The matrix element can be obtained by projecting the basis  $|a\rangle$  and  $|b\rangle$  for atomic element while  $|n\rangle$  and  $|m\rangle$  for field element. By applying the Kronecker delta function as stated in Eq.2.11 we obtain

$$\begin{aligned}
\dot{\rho}_{aa}(t) &= \frac{i}{2}\Omega_p \left( \langle a|a\rangle \langle b|\hat{a}_1 e^{i\Delta_1 t} \rho|a\rangle + \hat{a}_1^\dagger \langle a|b\rangle \langle a|e^{-i\Delta_1 t} \rho|a\rangle \right) \\
&\quad + \frac{i}{2}\Omega_c \left( \langle a|a\rangle \langle c|\hat{a}_2 e^{i\Delta_2 t} \rho|a\rangle + \hat{a}_2^\dagger \langle a|c\rangle \langle a|e^{-i\Delta_2 t} \rho|a\rangle \right) \\
&\quad - \frac{i}{2}\Omega_p \left( \langle a|\rho|a\rangle \langle b|a\rangle \hat{a}_1 e^{i\Delta_1 t} + \langle a|\rho \hat{a}_1^\dagger|b\rangle \langle a|a\rangle e^{-i\Delta_1 t} \right) \\
&\quad - \frac{i}{2}\Omega_c \left( \langle a|\rho|a\rangle \langle c|a\rangle \hat{a}_2 e^{i\Delta_2 t} + \langle a|\rho \hat{a}_2^\dagger|c\rangle \langle a|a\rangle e^{-i\Delta_2 t} \right) \\
&= \frac{i}{2}\Omega_p \langle b|\hat{a}_1 e^{i\Delta_1 t} \rho|a\rangle + \frac{i}{2}\Omega_c \langle c|\hat{a}_2 e^{i\Delta_2 t} \rho|a\rangle \\
&\quad - \frac{i}{2}\Omega_p \left( \langle a|\rho \hat{a}_1^\dagger|b\rangle e^{-i\Delta_1 t} \right) - \frac{i}{2}\Omega_c \langle a|\rho \hat{a}_2^\dagger|c\rangle e^{-i\Delta_2 t} \\
&= \frac{i}{2}\Omega_p \left( \hat{a}_1 e^{i\Delta_1 t} \rho_{ba} - \rho_{ab} \hat{a}_1^\dagger e^{-i\Delta_1 t} \right) \\
&\quad + \frac{i}{2}\Omega_c \left( \hat{a}_2 e^{i\Delta_2 t} \rho_{ca} - \rho_{ac} \hat{a}_2^\dagger e^{-i\Delta_2 t} \right)
\end{aligned}$$

$$\begin{aligned}
\dot{\rho}_{aa}(n,m) &= \frac{i}{2}\Omega_p \left( \langle n|\hat{a}_1 e^{i\Delta_1 t} \rho_{ba}|m\rangle - \langle n|\rho_{ab} \hat{a}_1^\dagger e^{-i\Delta_1 t}|m\rangle \right) \\
&\quad + \frac{i}{2}\Omega_c \left( \langle n|\hat{a}_2 e^{i\Delta_2 t} \rho_{ca}|m\rangle - \langle n|\rho_{ac} \hat{a}_2^\dagger e^{-i\Delta_2 t}|m\rangle \right) \\
&= \frac{i}{2}\Omega_p \sqrt{n_1+1} \rho_{ba}(n_1+1, m_1) e^{i\Delta_1 t} \\
&\quad - \frac{i}{2}\Omega_p \sqrt{m_1+1} \rho_{ab}(n_1, m_1+1) e^{-i\Delta_1 t} \\
&\quad + \frac{i}{2}\Omega_c \sqrt{n_2+1} \rho_{ca}(n_2+1, m_2) e^{i\Delta_2 t} \\
&\quad - \frac{i}{2}\Omega_c \sqrt{m_2+1} \rho_{ac}(n_2, m_2+1) e^{-i\Delta_2 t}
\end{aligned}$$

The same step by step calculation applied to  $\dot{\rho}_{bb}(n,m)$ ,  $\dot{\rho}_{cc}(n,m)$ ,  $\dot{\rho}_{ab}(n,m)$ ,  $\dot{\rho}_{ba}(n,m)$ ,  $\dot{\rho}_{ac}(n,m)$ ,  $\dot{\rho}_{ca}(n,m)$ ,  $\dot{\rho}_{bc}(n,m)$  and  $\dot{\rho}_{cb}(n,m)$  so it become

$$\begin{aligned}
\dot{\rho}_{bb}(t) &= \frac{i}{2}\Omega_p \sqrt{n_1} \rho_{ab}(n_1-1, m_1) e^{-i\Delta_1 t} \\
&\quad - \frac{i}{2}\Omega_p \sqrt{m_1} \rho_{ba}(n, m_1-1) e^{i\Delta_1 t} \\
\dot{\rho}_{cc}(t) &= + \frac{i}{2}\Omega_c \sqrt{n_2} \rho_{ac}(n_2-1, m_2) e^{-i\Delta_2 t} \\
&\quad - \frac{i}{2}\Omega_c \sqrt{m_2} \rho_{ca}(n_2, m_2-1) e^{i\Delta_2 t} \\
\dot{\rho}_{ac}(t) &= \frac{i}{2}\Omega_p \sqrt{n_1+1} \rho_{bc}(n_1+1, m_1) e^{i\Delta_1 t} \\
&\quad + \frac{i}{2}\Omega_c \sqrt{n_2+1} \rho_{cc}(n_2+1, m_2) e^{i\Delta_2 t}
\end{aligned} \tag{2.71}$$

$$\begin{aligned}
\dot{\rho}_{ca}(t) &= -\frac{i}{2}\Omega_c\sqrt{m_2}\rho_{aa}(n_2, m_2 - 1)e^{i\Delta_2 t} \\
&\quad -\frac{i}{2}\Omega_p\sqrt{m_1 + 1}\rho_{cb}(n_1, m_1 + 1)e^{-i\Delta_1 t} \\
&\quad -\frac{i}{2}\Omega_c\sqrt{m_2 + 1}\rho_{cc}(n_2, m_2 + 1)e^{-i\Delta_2 t} \\
&\quad +\frac{i}{2}\Omega_c\sqrt{n_2}\rho_{aa}(n_2 - 1, m_2)e^{-i\Delta_2 t} \\
\dot{\rho}_{ab}(t) &= \frac{i}{2}\Omega_p\sqrt{n_1 + 1}\rho_{bb}(n_1 + 1, m_1)e^{i\Delta_1 t} \\
&\quad +\frac{i}{2}\Omega_c\sqrt{n_2 + 1}\rho_{cb}(n_2 + 1, m_2)e^{i\Delta_2 t} \\
&\quad -\frac{i}{2}\Omega_p\sqrt{m_1}\rho_{aa}(n_1, m_1 - 1)e^{i\Delta_1 t} \\
\dot{\rho}_{ba}(t) &= -\frac{i}{2}\Omega_p\sqrt{m_1 + 1}\rho_{bb}(n_1, m_1 + 1)e^{-i\Delta_1 t} \\
&\quad -\frac{i}{2}\Omega_c\sqrt{m_2 + 1}\rho_{bc}(n_2, m_2 + 1)e^{-i\Delta_2 t} \\
&\quad +\frac{i}{2}\Omega_p\sqrt{n_1}\rho_{aa}(n_1 - 1, m_1)e^{-i\Delta_1 t} \\
\dot{\rho}_{cb}(t) &= \frac{i}{2}\Omega_c\sqrt{n_2}\rho_{ab}(n_2 - 1, m_2)e^{-i\Delta_2 t} \\
&\quad -\frac{i}{2}\Omega_p\sqrt{m_1}\rho_{ca}(n_1, m_1 - 1)e^{i\Delta_1 t} \\
\dot{\rho}_{bc}(t) &= -\frac{i}{2}\Omega_c\sqrt{m_2}\rho_{ba}(n_2, m_2 - 1)e^{i\Delta_2 t} \\
&\quad +\frac{i}{2}\Omega_p\sqrt{n_1}\rho_{ac}(n_1 - 1, m_1)e^{-i\Delta_1 t}
\end{aligned}$$

## 2.4 Conclusion

There are several ways to solve the Hamiltonian of the system such as the probability amplitude method, Heissenberg operator method, master equation method and unitary time evolution method. The most essential part in the light-matter interaction scheme is its Hamiltonian which describes the whole system. It consists of all of the information needed to understand the scheme including the total system's levels, light treatment whether classically or quantum mechanically, the mode of the fields, and many more. Once the Hamiltonian is derived correctly, the properties of the system can be investigated so the interesting features can be studied extensively.

## CHAPTER 3

### NONCLASSICAL PROPERTIES OF LIGHT

#### 3.1 Introduction

The basics of quantum theory is wave-particle duality which explains the wave behaviour of particle in Young's double slit experiment and likewise, explains the particle-like phenomenon of light for example in Compton scattering. Nonclassical light is the properties of light that cannot be described by classical interpretation of electromagnetic waves. It can only be explained by quantum mechanics. For example, in photon antibunching, the experiment show that the photon detector will detect one photon at a time which is the sign of quantum behaviour. In squeezed light, we can squeezed the uncertainty region in one quadrature (Milburn & Walls, 2008). Let us say the amplitude noise by reducing the width of the amplitude direction but at the same time, as the consequence, the phase uncertainty is increased. As an analogy to squeeze the toothpaste, when we squeeze one part, the other part anywhere in the toothpaste will increase in volume.

Various physical parameters have been defined to determine the nonclassical states of light as well as the degree of nonclassicality (Lee, 1991). The typical ones are the squeezing parameter  $S = \langle \hat{p}^2 \rangle - \langle \hat{p} \rangle^2$  with  $\hat{p} = \hat{a}e^{i\theta} + \hat{a}^\dagger e^{-i\theta}$ , antibunching in  $G^{(2)}$ , entanglement criteria, Mandel's  $Q = (\langle \hat{n}^2 \rangle - \langle \hat{n} \rangle^2) / \langle \hat{n} \rangle$ ,  $\hat{n} = \hat{a}^\dagger \hat{a}$  and the Wigner function  $W$ . Each quantity displays nonclassicality from certain aspects. There are states which do not meet all the nonclassical criteria. For example, Schrödinger cat is not squeezed and has  $Q > 0$  (super-Poissonian statistics) for certain values of phase  $\theta$ , but it shows nonclassicality through negativity in  $W$  and Agarwal's parameter (Agarwal & Tara, 1992).

These states of the nonclassical light provide the fundamental differences between quantum and classical physics. Many experiments conducted by scientists showed that the laws of classical mechanics are inapplicable thus enable to test the validity of quantum mechanics. Nonclassical states of light and atoms play an essential role in quantum communication between distant parties, as well as processing of quantum information (Bouwmeester, Ekert, & Zeilinger, 2000). Several properties of nonclassical light will be

discussed in this chapter to provide useful knowledge on the phenomenon and behaviour of a particular system that cannot be explained in a common laws of classical mechanics. The nonclassical phenomenon can be used to detect the entanglement between two quantum parties. This chapter is basically from the discussion on entanglement criteria that has been carried out thoroughly in the review paper published to Journal of Modern Optics (Sumairi, Hazmin, & Ooi, 2013).

### **3.2 Literature Review**

One of the nonclassical quantity of interest is the Glauber's two-photon correlation  $g^{(2)}$  which can show the violation of Cauchy-Schwarz inequality (Glauber, 1963). In this study, the concept of coherence is used to fields of arbitrary time dependence and a succession of correlation functions for the complex field strengths is defined. Glauber suggested that coherence does not require monochromaticity. Coherent fields can be generated with arbitrary spectra.

The quantum correlation of photon pairs from a  $\Lambda$ -type particle driven by laser fields in a modified photon density of states such as a cavity or a defect in a photonic crystal has been studied (Ooi & Gong, 2012). An exact semianalytical expression for the photon correlation, which is characterized by two complex decay functions were obtained associated with the levels splitting that depend on the control laser field. They have reported that the position and width of the cavity density of state with respect to the anti-Stokes transition can determine the features in the two-photon correlation profile.

In the related studies, the quantum statistical properties of light emitted by a similar two-photon double Raman laser is investigated in the context of squeezing and entanglement properties of the cavity. They found that the cavity radiation exhibits two-mode squeezing and entanglement in the transient as well as steady state regime for realizable parameters, and then established a connection between these two quantum features (Sete & Ooi, 2012).

The limit of resolution is related to the wavelength of light used to illuminate the sample in classical microscopy. However, by using the correlated photon pairs produced in Raman quantum erasure, the resolution of two-photon quantum microscopy is substantially improved (Scully & Ooi, 2004). In this study, the strongly correlated two-photon

quantum state generated by Raman quantum erasure scheme (Scully & Drühl, 1982) has been analyzed to see the possibility to exceed the Rayleigh resolution limit of classical microscopy. The photon-photon correlation function for Raman pairs is of interest in itself and has features in common with photon antibunching.

A diffraction of classical optical lithography is limited to writing features of an optical wavelength size  $\frac{\lambda}{2}$  or greater. Boto has reported that nonclassical photon-number states, entangled  $N$  at a time, is possible to use to write features of minimum size  $\frac{\lambda}{2N}$  in an  $N$ -photon absorbing substrate. Optical parametric down-conversion technique is used to generate entangled photon pairs to provide subwavelength resolution and they have shown how to write arbitrary 2D patterns by using this method (Boto et al., 2000). An experimental demonstration of quantum lithography has been carried out by Angelo's team by utilizing the entangled nature of a two-photon state without violating the uncertainty principle. They successfully suggested the improvement of the resolution of optical microscopy and lithography by using photon correlation interferometry and showed that the experimental results have beaten the classical diffraction limit by a factor of 2 (D'Angelo, Chekhova, & Shih, 2001).

Several related studies have been conducted and make use of the nature of nonclassical photons such as, to enhanced spectral resolution (Scully, Rathe, Su, & Agarwal, 1997), quantum imaging (Gatti, Brambilla, Bache, & Lugiato, 2004), subwavelength measurement of atomic separation using  $g^{(2)}$  and discussed on antibunching (Ooi, Kim, & Lee, 2007), and the new coherent effects due to dipole-dipole interaction (Ooi, 2007), and provide interesting effects on spatial propagation and quantum noise (Ooi, Sun, Zubairy, & Scully, 2007). This showed us that the nonclassical light is a popular field of research, and scientists are interested to discover more the underlying truth of quantum world. The nonclassical properties of light has opened a remarkable impact to physics particularly in microscopic scale.

### 3.3 Squeezed Light

We can have various type of light sources; each of them is described by certain statistic. In light squeezing, the quantum noise of light is actually been squeezed so it benefited optical communication and measurements, quantum teleportation and quantum

cryptography, and also can produce the entangled states of light (Lambropoulos & Petrosyan, 2007). There are uncertainties in quantum optics measurements leads to the idea of squeezing the noise for example amplitude and phase. When squeezing, let say the amplitude, its width is reduced but at the same time, the phase uncertainty is increased. Likewise, when phase squeezing of light takes part, the amplitude fluctuations is raised. Fig. 3.1 illustrates the squeezed vacuum where the center of the uncertainty region (the average amplitude) is at the origin of the coordinate system, and the fluctuations are reduced in some direction. There are two types of squeezed state: quadrature-squeezed and

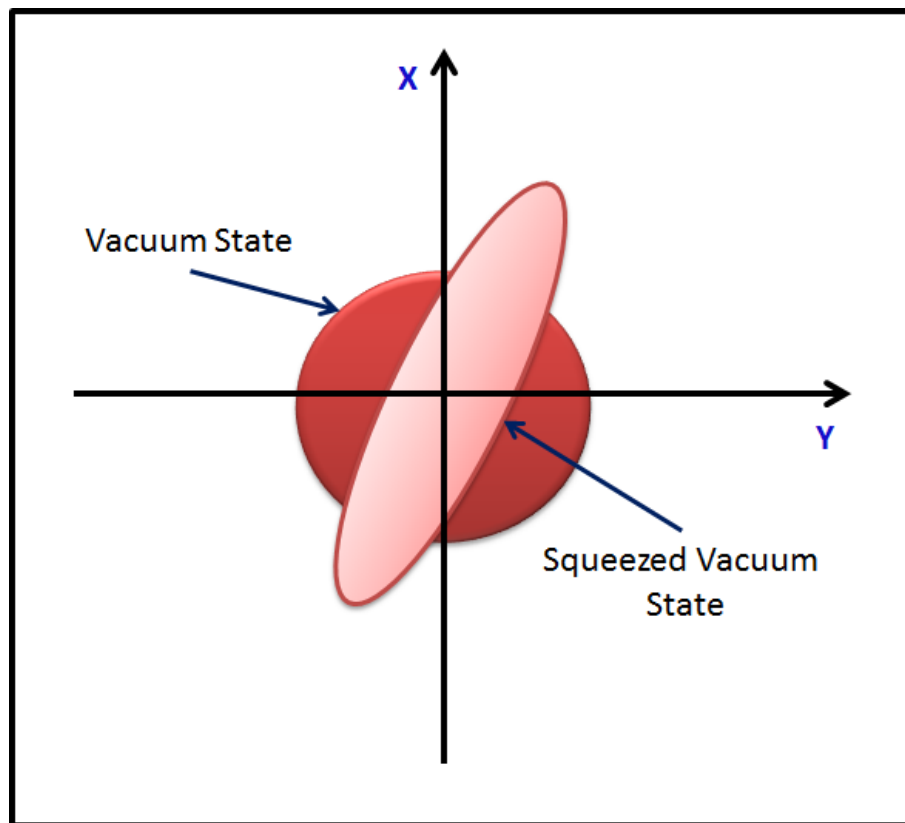


Figure 3.1: Quadrature-squeezed state compared with vacuum state

photon-number-squeezed. The former squeezed state is only can occurs when stretching the uncertainty in other quadrature which has a standard deviation that falls below the vacuum-state of value  $\frac{1}{2}$ . The latter squeezed state, defined as if its photon-number uncertainty falls below the value of  $\langle n \rangle^{1/2}$  of the coherent state. The uncertainty in photon number  $n$  may be squeezed when squeezing the phase uncertainty. Photon-number-squeezed light is often referred to as sub-Poissonian statistic because its standard deviation falls below (sub) that of the Poisson distribution that characterises the coherent state.

The correlation between two orthogonal quadratures,  $\hat{c}_+$  and  $\hat{c}_-$  formed by the anni-

hilation operator  $\hat{a}^\dagger$ , and creation operator  $\hat{a}$  are given by

$$\hat{c}_+ = \frac{1}{2} (\hat{a}^\dagger + \hat{a}) \quad (3.1)$$

$$\hat{c}_- = \frac{1}{2i} (\hat{a}^\dagger - \hat{a}) \quad (3.2)$$

which satisfy the commutation relation

$$[\hat{c}_+, \hat{c}_-] = \frac{i}{2} \quad (3.3)$$

The product of quadrature variance should satisfy

$$\langle (\Delta \hat{c}_+)^2 \rangle \langle (\Delta \hat{c}_-)^2 \rangle \geq \frac{1}{16} \quad (3.4)$$

### 3.4 Photon Anti-bunching

Physicists have attempted to discover more nonclassical phenomenon associated with light and found the anti-bunching behaviour of photons. The anti-bunching phenomena is first explained when the time delay is detected between two successive photons emitted from the atom. This phenomena which is of incredible interest in quantum theory of light has a very sharp contrast with the behaviour of photons in thermal light which are coming in a bunch. The experiment set up to demonstrate this anti-bunching behaviour of photon is prepared by Hanbury Brown-Twiss using the experiment scheme as shown in fig.

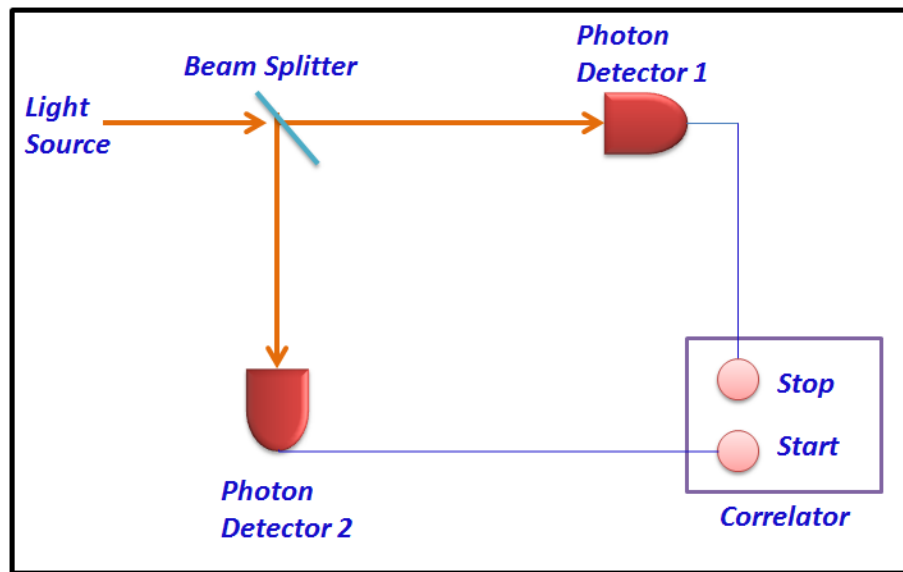


Figure 3.2: Hanbury Brown-Twiss experiment to demonstrate the phenomena of anti-bunching using photon detector



This experiment consist of a 50:50 beam splitter which divide the initial light beam in two equal portions that will be detected by two single photon detectors. The output signals of the detectors are sent to a timer-correlated single-photon counting which records the time elapsed between the pulse of each detector and count the number of pulses at each input. This is the starting point of the quantum correlation pioneered by Glauber which reported on photon counting. The phenomenon of photon anti-bunching shows behaviour of the second order correlation function  $g^{(2)}(\tau)$ .

An anti-bunched photon can be observed from a single particle through resonance fluorescence. The phenomenon of anti-bunching is related to the effect of sub-Poissonian statistics which is the probability of finding  $n$ -photons in a Poissonian distribution (Schleich, 2001). The correlation of scattered photons is studied using second order correlation function of photodetection with respect to time

$$g^{(2)}(\tau) = \frac{\langle \hat{a}^\dagger(t) \hat{a}^\dagger(t+\tau) \hat{a}(t+\tau) \hat{a}(t) \rangle}{\langle \hat{a}^\dagger \hat{a} \rangle^2} \quad (3.5)$$

### 3.5 Wigner Function

The properties of a quantum state in phase-space lies in the representation of Wigner function,  $W$ . Consider a one-dimensional motion described by the position and momentum operators  $\hat{x}$ , and  $\hat{p}$  which has the relation  $[\hat{x}, \hat{p}] = i\hbar$ . It is not possible to define a genuine phase space distribution. The most interesting feature in Wigner fuction is the negative parts in its distribution. Wigner phase space distribution can be described by

$$W(x, p) \equiv \frac{1}{2\pi\hbar} \int_{-\infty}^{\infty} d\xi \exp\left(-\frac{i}{\hbar} p\xi\right) \left\langle x + \frac{1}{2}\xi \left| \hat{\rho} \right| x - \frac{1}{2}\xi \right\rangle \quad (3.6)$$

The normalization factor is included to ensure the property of

$$\int_{-\infty}^{\infty} dx \int_{-\infty}^{\infty} dp W(x, p) = 1 \quad (3.7)$$

Using Fourier transform, the Wigner function now become

$$W(x, p) = \frac{1}{2\pi\hbar} \int_{-\infty}^{\infty} d\xi \exp\left(-\frac{i}{\hbar} p\xi\right) \hat{\rho}(x, \xi) \quad (3.8)$$

of the density operator  $\rho(x'', x') \equiv \langle x'' | \rho | x' \rangle$  in position representation expressed in the variables  $x \equiv (x' + x'')/2$  and  $\xi = x'' - x'$  where

$$\begin{aligned} x' &= x - \frac{1}{2}\xi \\ x'' &= x + \frac{1}{2}\xi \end{aligned}$$

It can be shown that

$$\begin{aligned}
\hat{\rho}(x, \xi) &= \rho(x'', x') \\
&= \rho\left(x + \frac{1}{2}\xi, x - \frac{1}{2}\xi\right) \\
&= \left\langle x + \frac{1}{2}\xi \left| \hat{\rho} \right| x - \frac{1}{2}\xi \right\rangle
\end{aligned} \tag{3.9}$$

For the case of pure states, the Wigner expression reduces to

$$W(x, p) = \frac{1}{2\pi\hbar} \int_{-\infty}^{\infty} d\xi \exp\left(-\frac{i}{\hbar} p\xi\right) \psi^*\left(x - \frac{1}{2}\xi\right) \psi\left(x + \frac{1}{2}\xi\right) \tag{3.10}$$

where  $\psi(x) \equiv \langle x | \psi \rangle$  is the position representation of the state  $|\psi\rangle$ .

In a harmonic oscillator, Schrodinger equation is solved to get the position representation of an energy eigenstate. Due to the quantization of energy, the Wigner function of the  $m$ th energy eigenstate reads

$$\begin{aligned}
W_m(x, p) &= \frac{(-1)^m}{\pi\hbar} \exp\left\{-\left[\left(\frac{p}{\hbar\kappa}\right)^2 + (\kappa x)^2\right]\right\} \\
&\quad L_m\left\{2\left[\left(\frac{p}{\hbar\kappa}\right)^2 + (\kappa x)^2\right]\right\}
\end{aligned}$$

consisting of the  $m$ th Laguerre polynomial represents a normalizable solution of the ordinary differential equation

### 3.6 Entropy

The entropy describes the lack of knowledge in the particular system. The entropy of the system,  $S$  is a measure of the uncertainty of a quantum state, where

$$S(\rho) = -Tr(\rho \ln \rho)$$

is the Von-Neumann quantum mechanical property associated with  $\rho$ . This property can determine the strength of entanglement where the higher the entropy, the stronger the degree of entanglement. The entropy measurement is used to measure the disorder in the quantum system, and of the purity of a quantum state. The relation among entropies can be expressed by entropy inequality (Araki & Lieb, 1970)

$$|S_A - S_F| \leq S \leq |S_A + S_F| \tag{3.11}$$

If the system is initially in a pure state, the entropy vanishes where  $S = 0$ . Then the component systems, which are atom and field have an equal entropies throughout the entire evolution of the system and independent to each other

$$S_A = S_F$$

For a statistical mixture, however, the entropy is non-zero,  $S \neq 0$ . The entropy of a total system remains constant whenever the time-dependent Schrodinger equation governs the entire time evolution (Shore & Knight, 1993). The most interested quantity are the partial entropies of the subsystem, let say atom alone or field. If we treated the component as a separate system, from the reduced density matrices, we find the entropy of atom(subscript  $A$ ) and field(subscript  $F$ ) are

$$S_A(t) = -Tr_F(\hat{\rho}_A(t) \ln \hat{\rho}_A(t)) \quad (3.12)$$

$$S_F(t) = -Tr_A(\hat{\rho}_F(t) \ln \hat{\rho}_F(t)) \quad (3.13)$$

where the reduced density operator for atom and field are  $\hat{\rho}_A = Tr_F(\hat{\rho})$  and  $\hat{\rho}_F = Tr_A(\hat{\rho})$  respectively. These partial entropy changes with time, unlike the total entropy, and this properties makes it an interesting feature to play with. The decrease of partial entropy shows that the particular subsystem is approaching its pure state, while the increasing in entropy tells that the two components tend to lose their individuality and become correlated or entangled. If we have a two-level system interact with a field in a high quality cavity is of interest, the plot of entropy of field for the system is shown in the Fig.3.3 while to get a broader view, Fig.3.4 show the time duration from  $gt = 0$  to  $gt = 100$

The plot of entropy for atom is shown as in Fig.3.5 From the derived Schrodinger equation, the equations of motion for amplitude  $C_a$ (excited state) and  $C_b$ (ground state) are obtained. The eigenvalues for  $\hat{\rho}_F(t)$  are the sum of diagonal element for atom given by

$$\hat{\rho}_F(t) = Tr_A(\hat{\rho}(t)) \quad (3.14)$$

$$\begin{aligned} &= \rho_{aa}(t) + \rho_{bb}(t) \\ &= C_a C_a^* + C_b C_b^* \end{aligned} \quad (3.15)$$

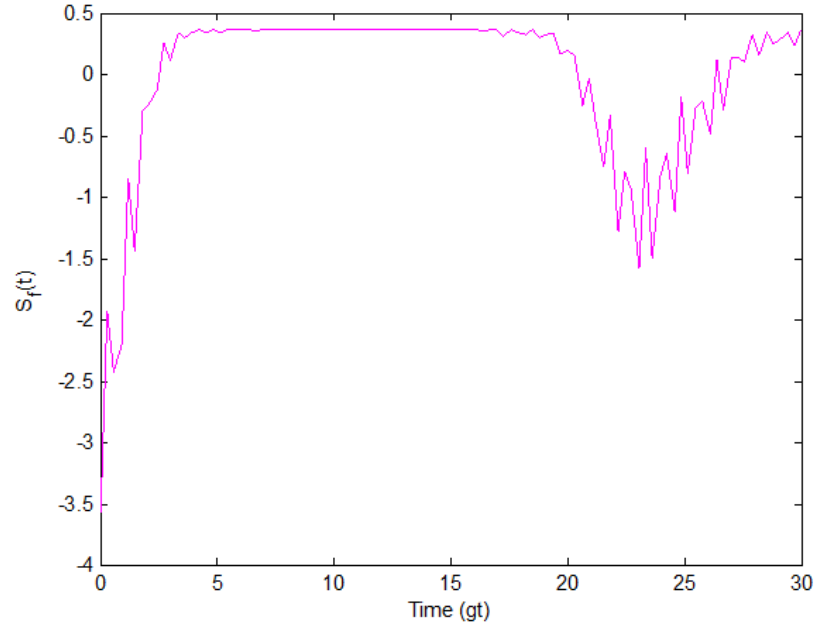


Figure 3.3: Field entropy for two level atom interact with a single mode field(without damping effect) in time duration  $gt = 0$  to  $gt = 30$ .

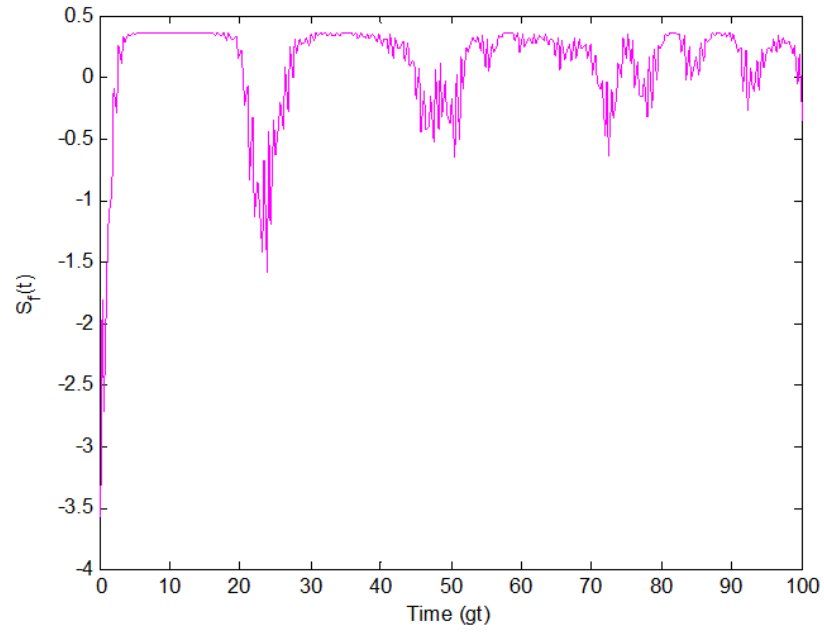


Figure 3.4: Field entropy for two level atom interact with a single mode field(without damping effect) in time duration  $gt = 0$  to  $gt = 100$ .

The total amount of correlation between the atom and field can be obtained by taking the negative entropy difference (Hessian, Mohammed, & Mohamed, 2009)

$$S_D = \frac{1}{4} (S - S_A - S_F) \quad (3.16)$$

The degree of entanglement is determined through the measure of negativity of this quan-

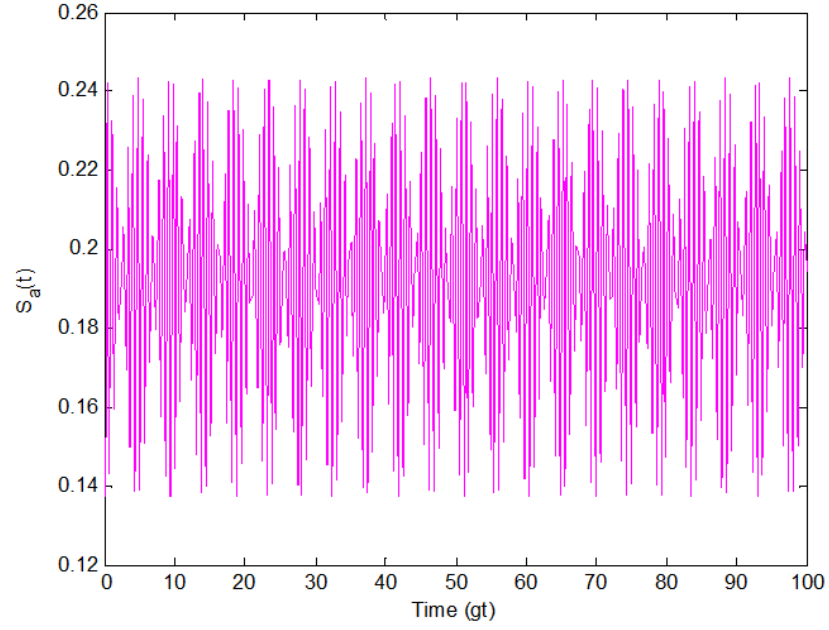


Figure 3.5: Atom entropy for two level atom interact with a single mode field(without damping effect) in time duration  $gt = 0$  to  $gt = 100$ .

tity.

### 3.7 Conclusion

There are so many nonclassical properties discovered when scientist first found that light can exhibit the particle-like behaviour. Several properties have been discussed in this chapter which will be used in the preceeding chapters. The nonclassicality of light provide useful information and application for advanced optics technology and physics in general.

## CHAPTER 4

### TIME- & INTENSITY-DEPENDENT TWO-LEVEL ATOM

#### 4.1 Introduction

Nonclassical light and collapse-revival dynamics are consequences of dynamical quantum interference in transient atom-photon interaction (Ooi et al., 2012). A system of two-level atom interacting with a quantized field in a high quality cavity is studied. The dissipation is neglected since the quality of the cavity is very high by assuming the system is confined in a cavity and neither interaction with the environment nor spontaneous effect occurs to the system. The time- and intensity-dependent atom-field coupling are applied to the system, with different initial field states and initial atomic states. Further investigation on the dynamics of the atom(matter) and photon(light) in the collapse-revival pattern of inversion and the Wigner function are investigated and the connection between these two has been conducted. Nonclassical effects are useful to gather more information and to get a better understanding of the system.

The general overview of step-by-step calculation in this study of two-level atom interact with a single mode field in a high quality cavity is as the flow chart of Fig.4.1 below.

The simulation of Wigner evolution and inversion plot is developed using MATLAB programming to observe the behaviour of light and atom theoretically. In this study, the atom-cavity scheme is described where a desired quantum state of light can be coherently extracted on demand. The density matrix elements  $\rho_{nm}$  for the atom-field dynamics, the inversion  $n_{ab}$  and the expressions relating  $W$  and  $\rho_{nm}$  are obtained. The  $\rho_{nm}$  are acquired for different initial states of the atom (pure and superposition) and different initial field states (coherent, Schrödinger cat). The main results will be discussed, particularly on the Wigner plot and anti-Zeno effect in the collapse-revival with a peculiar transient dynamics due to the transient couplings  $g(t)$ . We analyzed the system using three coupling function that are constant coupling, sinusoidal coupling function and hat pulse function which will be discussed in detail later.

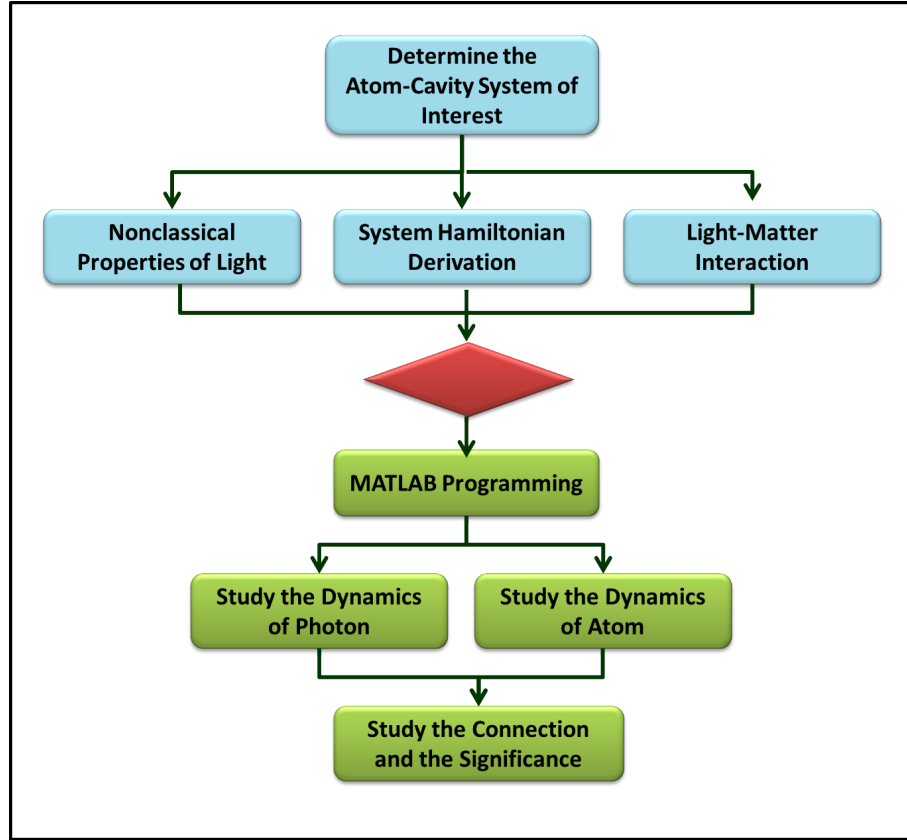


Figure 4.1: Research methodology for JCM with time- and intensity-dependent coupling

## 4.2 Related Studies

One of the challenges in developing quantum communication technology is to generate nonclassical state with large  $|\alpha|^2$ . Schrödinger cat state  $|\alpha\rangle \pm e^{i\phi} |-\alpha\rangle$ , a superposition of classical (coherent) states, is a nonclassical state. Six atomic qubits cat state has been created by Leibfried which each qubit's state space is defined by two hyperfine ground states of beryllium ion (Leibfried et al., 2005). The cat state for fields may be produced from squeezed sources, linear processes, simple photon counting scheme as suggested by Ralph group. They constructed a simple networks and showed the quantum computation circuits using coherent states as the logical qubits (Ralph, Gilchrist, & Milburn, 2003). The cat state of a single-mode optical field can be produced by conditional measurement (Dakna, Anhut, Opatrny, Knoll, & Welsch, 1997). The study showed by feeding a squeezed vacuum into a beam splitter and counting the photons in one of the output channels, the conditional states in the other output channel exhibit a Schrodinger cat-like states. They presented the Wigner and Husimi function numerically and analytically. All these three studies generated a cat state, while in the study conducted, a

Schrodinger cat state is used as an initial state to study the interaction between light and matter.

Single two-level atom interacting with quantized field in a cavity is convenient for studying the connection between collapse-revival and the nonclassicality of light. It is simpler than more complex systems, such as two atoms and multiphoton cases. Although the single atom-field system was studied by Jones et al. (Jones, Haight, & Lee, 1997), it was confined only to photon addition process on single mode thermal field in weak coupling (short time) regime  $\int_0^t g(t')dt' \ll 1$ , where  $g(t)$  is the time-dependent atom-field coupling. The connection between nonclassical light and collapse-revival dynamics in two-level system has been studied extensively, mainly by Banacloche. Spatial dependent coupling and atomic center of mass motion give rise to novel collapse-revival. However, the situation of time-dependent coupling  $g(t)$  with intensity dependent has not been explored in the context of Wigner function. The closest is the work by Kurizki's group (Sherman, Kurizki, & Kadyshevitch, 1992) who studied the effect of time dependent field coupling on enhancing nonclassicality of light for atom moving through a photonic crystal with defect.

In this work, the atom and photon dynamics, particularly the dynamical quantum interference in collapse-revival and the Wigner function, are studied via exact nonperturbative approach, generalized to time- and Intensity-dependent atom-field coupling  $g(t)$  and with any initial field state. Nonclassical light in the cavity is only useful if the state can be frozen instantaneously and coupled out from the cavity. A setup which allows the possibility of extracting desirable state of field is proposed based on the knowledge of transient atomic dynamics and the evolutions of  $W(t)$  for any time dependent  $g(t)$ . The motivation of the present work is field-state control through time-dependent and intensity-dependent coupling. Despite many existing works on intensity-dependent coupling, the physical motivation remains unclear. Actually, such laser control may be realized by a dispersive cavity with coupling strength that is proportional to the square root of dielectric function (Glauber & Lewenstein, 1991) and the field intensity (optical Kerr effect). It may also employ preselection and/ or postselection of the atomic state, as discussed by G.Harel et al. (Harel, Kurizk, McIver, & Coutias, 1996) The motivation of the present-work is field-state control through time-dependent and intensity-dependent coupling.



### 4.3 Dynamics of the JCM with time- and intensity-dependent coupling

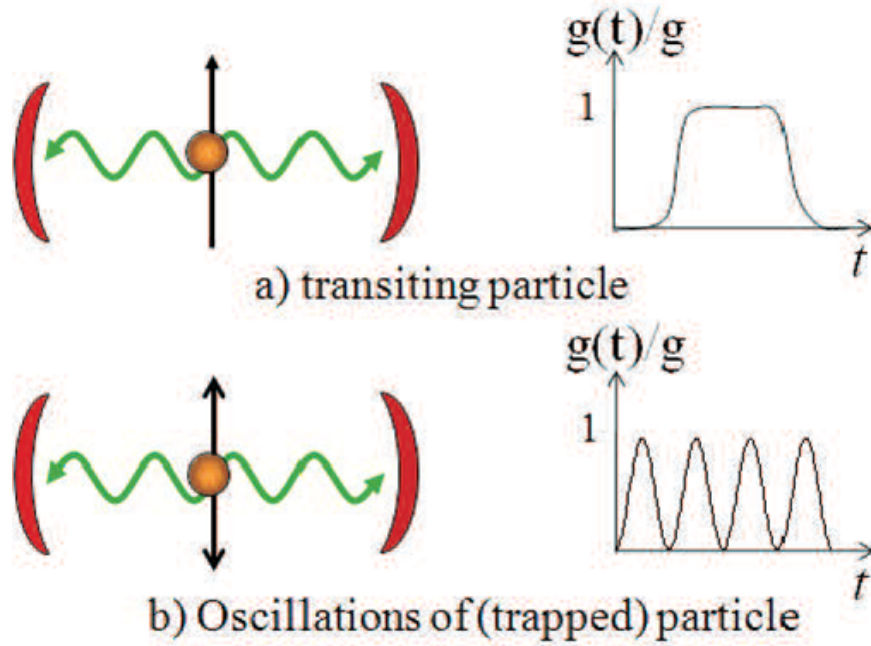


Figure 4.2: A two-level atom coupled to a quantized cavity field in arbitrary state. The cavity has negligible loss within the timescale of the atomic dynamics. Transient couplings realized by: a) transiting atom modelled by a "hat" function, and b) atom oscillating back and forth through the cavity modelled by sinusoidal function.

Single mode field resonantly interacting with single two-level atom which is known as Jaynes-Cumming Model(JCM) as shown in Fig.4.2 has the usual Hamiltonian

$$\hat{H} = \frac{\hbar}{2}\omega\hat{\sigma}_z + \hbar\nu\hat{a}^\dagger\hat{a} - \hbar g(t) \left( \hat{\sigma}_+\hat{a} + \hat{a}^\dagger\hat{\sigma}_- \right)$$

where  $\omega$ =atomic transition frequency,  $\nu$ =field frequency,  $\hat{\sigma}_+ = |a\rangle\langle b|$ (atomic raising operator),  $\hat{\sigma}_- = |b\rangle\langle a|$ (atomic lowering operator),  $\hat{\sigma}_z = |a\rangle\langle a| - |b\rangle\langle b|$ ,  $\hat{a}^\dagger$ =creation operator for field and  $\hat{a}$ =annihilation operator. Using the same derivation as discussed in Eq.2.44 of chapter 2, the interaction picture for the JCM system now becomes

$$\hat{V}(t) = \hbar g(t) \left( \hat{\sigma}_+\hat{a}e^{-i\Delta t} + \hat{a}^\dagger\hat{\sigma}_-e^{-i\Delta t} \right) \quad (4.1)$$

where  $g(t)$  is the atom-field coupling factor and the difference between atomic transition frequency and field frequency defined by the detuning:

$$\Delta = \omega - \nu$$

Spontaneous emission and dissipation can be neglected for interaction time smaller than the spontaneous lifetime. This means neglecting the coupling between the vacuum radiation and the atom which is possible for typical transition frequency below the infrared or photonic crystal cavity.

It is useful to note that since photon absorption(PhA) (photon emission(PhS)) corresponds to downward (upward) transition of an atom, the atom and the field dynamics are correlated. The PhA and PhS processes are respectively described by  $\hat{\sigma}_- \hat{a}^\dagger |a, f\rangle = \sqrt{f+1} |b, f+1\rangle$  and  $\hat{\sigma}_+ \hat{a} |b, f\rangle = \sqrt{f} |a, f-1\rangle$  as the first order perturbative expansion of the evolution operator  $\hat{U} = \exp[i(\lambda(t)(\hat{\sigma}_+ \hat{a} + \hat{\sigma}_- \hat{a}^\dagger)]$  with  $\hat{\sigma}_+ = |a\rangle\langle b|$ ,  $\hat{\sigma}_- = |b\rangle\langle a|$ ,  $\lambda(t) = \int_0^t g(t') dt'$ . The second order terms  $(\lambda(t))^2(|a\rangle\langle a| \hat{a} \hat{a}^\dagger |a, f\rangle$  and  $(\lambda(t))^2 |b\rangle\langle b| \hat{a}^\dagger \hat{a} |b, f\rangle$  describe PhS-PhA and PhA-PhS respectively but do not correspond to a transition. Higher order odd and even terms contribute similarly, such that the sum gives the nonlinear dependence on  $\lambda(t)$  and  $\hat{a}^\dagger \hat{a}$  contained in the nonperturbative solutions.

The details of atomic dynamics evolution in the atom-field system can be studied non-perturbatively by using the Schrodinger approach with the state vector

$$|\psi(t)\rangle = \sum_n [C_{a,n}(t)|a, n\rangle + C_{b,n}(t)|b, n\rangle] \quad (4.2)$$

with the time dependent atom-field coefficients  $C_{x,n}$  for level  $x$  ( $= a, b$ ) with  $n$  photons. The equation of motion for  $|\psi(t)\rangle$

$$i\hbar \frac{d}{dt} |\psi(t)\rangle = \hat{V}(t) |\psi(t)\rangle \quad (4.3)$$

For intensity dependent coupling which will be discussed in the next section, field operator,  $\hat{a}$  and  $\hat{a}^\dagger$  are replaced by  $\hat{R} = \hat{a} \sqrt{\hat{a}^\dagger \hat{a}}$  and  $\hat{R}^\dagger = \sqrt{\hat{a}^\dagger \hat{a}} \hat{a}^\dagger$ ,  $\hat{V}(t) = \hbar g(t)(\hat{\sigma}_+ \hat{a} \sqrt{\hat{a}^\dagger \hat{a}} e^{-i\Delta t} + \sqrt{\hat{a}^\dagger \hat{a}} \hat{a} \hat{\sigma}_- e^{-i\Delta t})$  and the interaction energy can only cause transition between  $|a, n\rangle$  and  $|b, n+1\rangle$  so the coupled equation (See Appendix B for complete calculation) are written by

$$\frac{d}{dt} C_{a,n}(t) = -ig(t)(n+1)e^{i\Delta t} C_{b,n+1}(t) \quad (4.4)$$

$$\frac{d}{dt} C_{b,n+1}(t) = -ig(t)(n+1)e^{-i\Delta t} C_{a,n}(t) \quad (4.5)$$

where  $g(t)$  is the atom-field coupling factor and  $|C_{x,n}|^2$  being the probability with  $n$  photons and atom in state  $|a\rangle$ . Equations 4.4-4.5 can be solved numerically for finite detuning and any time-dependence  $g(t)$  but it is not possible to obtain general analytical solutions. For time independent coupling and finite detuning the analytical solutions (see Appendix C) are known (Scully & Zubairy, 1997)

$$\begin{aligned} C_{a,n}(t) &= e^{i\Delta t/2} [C_{a,n}(0)r_n(t) - iC_{b,n+1}(0)q_n(t)] \\ C_{b,n+1}(t) &= e^{-i\Delta t/2} [C_{b,n}(0)r_n^*(t) - iC_{a,n}(0)q_n(t)] \end{aligned} \quad (4.6)$$

where

$$\begin{aligned} r_n(t) &= \cos(\phi_n(t)) - i \frac{\Delta}{\Omega_n} \sin(\phi_n(t)) \\ q_n(t) &= \frac{2g(t)(n+1)}{\Omega_n} \sin(\phi_n(t)) \\ \phi_n(t) &= \frac{1}{2}\Omega_n t \\ \Omega_n^2 &= \Delta^2 + (2g(n+1))^2 \end{aligned}$$

On the other hand, for zero detuning ( $\Delta = 0$ ) with arbitrary time dependence the solutions are

$$\begin{aligned} C_{a,n}(t) &= C_{a,n}(0)r_n(t) - iC_{b,n+1}(0)q_n(t) \\ C_{b,n}(t) &= C_{b,n}(0)r_{n-1}^*(t) - iC_{a,n-1}(0)q_{n-1}(t) \end{aligned} \quad (4.7)$$

where

$$\begin{aligned} r_n(t) &= \cos(\phi_n(t)) \\ q_n(t) &= \sin(\phi_n(t)) \\ \phi_n(t) &= \frac{1}{2} \int_0^t \Omega_n(t') dt' \\ \Omega_n &= 2g(n+1) \end{aligned}$$

In general, the density matrix elements of the field  $\rho_{nm}$  are obtained by tracing out the atomic system (subscript "s"),  $\rho_{nm} = \langle n|\hat{\rho}_f|m\rangle = \sum_x \langle n|\hat{\rho}_{xx}|m\rangle$  where  $\hat{\rho}_f = Tr_s\{\hat{\rho}(t)\} = \sum_{x=a,b} \hat{\rho}_{xx}$  is the reduced density matrix of the field (subscript "f"),  $\hat{\rho}_{xx} = \langle x|\hat{\rho}|x\rangle$  ( $x = a, b$ )

and  $\langle n|\hat{\rho}_{xx}|m\rangle = C_{x,n}(t)C_{x,m}^*(t)$  ( $x = a, b$ ). The transient state of the field is governed by the matrix element of the field  $\rho_{nm}(t)$ . For the two-level atom,

$$\begin{aligned}\rho_{nm}(t) &= \langle n|\{\hat{\rho}_{aa}(t) + \hat{\rho}_{bb}(t)\}|m\rangle \\ &= C_{a,n}(t)C_{a,m}^*(t) + C_{b,n}(t)C_{b,m}^*(t)\end{aligned}\quad (4.8)$$

where  $C_{x,n}(t)$  is obtained from the solutions of the standard coupled equations 4.4 and 4.5 for a two-level atom.

Initially, the atomic system  $\hat{\rho}_s(0)$  is uncorrelated to the field state  $\hat{\rho}_f(0)$ , i.e.  $\hat{\rho}(0) = \hat{\rho}_f(0) \otimes \hat{\rho}_s(0)$  since both are not coupled. Thus, the initial coefficients can be decomposed into products of the atomic (subscript ' $x = a, b$ ') and photonic coefficients (subscript ' $n$ '),

$$C_{x,n}(0) = C_x(0)C_n(0) \quad (4.9)$$

satisfying  $|C_a(0)|^2 + |C_b(0)|^2 = \rho_{aa}(0) + \rho_{bb}(0) = 1$  with  $\rho_{xx}(0) = \langle x|\hat{\rho}_s(0)|x\rangle = C_x(0)C_x^*(0)$ . Thus  $C_{x,n}(0)C_{y,m}^*(0) = C_x(0)C_y^*(0)\rho_{nm}(0)$ . The initial coherence between photon numbers is

$$\rho_{nm}(0) = \langle n|\hat{\rho}_f(0)|m\rangle = C_n(0)C_m^*(0) \quad (4.10)$$

where Eqs.4.8 and Eq.4.9 are used(see Appendix D). As expected, the initial matrix element of the field  $\rho_{nm}(0)$  does not depend on the atomic initial conditions.

#### 4.3.1 Atomic inversion and coherence

One quantity that characterizes the atomic dynamics is the atomic inversion  $n_{ab} = \sum_{n=0}^{\infty}(|C_{a,n}(t)|^2 - |C_{b,n}(t)|^2)$  which is obtained by tracing over the photon number states. The atomic inversion can be written as  $n_{ab}(t) = \sum_{n=0}^{\infty}(|C_{a,n}(t)|^2 - |C_{b,n+1}(t)|^2) - |C_{b,0}(t)|^2$  which is used to obtain an analytical expression(see Appendix E),

$$\begin{aligned}n_{ab}(t) &= \sum_{n=1}^{\infty} \{\rho_{aa}(0)p_n(0) - \rho_{bb}(0)p_{n+1}(0)\} (|r_n(t)|^2 - q_n^2(t)) \\ &\quad - \rho_{bb}(0)p_1(0)|r_0(t)|^2 - \rho_{aa}(0)p_0(0)q_0^2(t) \\ &\quad + i\rho_{ab}(0)[2 \sum_{n=1}^{\infty} \rho_{n,n+1}(0)q_n^*(t)r_n(t) + \rho_{0,1}(0)q_0^*(t)r_0(t)]\end{aligned}\quad (4.11)$$

$$- i\rho_{ba}(0)[2 \sum_{n=1}^{\infty} \rho_{n+1,n}(0)q_n(t)r_n^*(t) + \rho_{1,0}(0)q_0(t)r_0^*(t)] \quad (4.12)$$

where  $\rho_{mn}(0)$  is the initial field coherence and  $\rho_{xy}(0)$  is the initial atomic coherence or population (See Appendix 2 for full calculation).

Note that if one of the states is initially empty, i.e. either  $C_a(0)$  or  $C_b(0)$  being zero,  $n_{ab}(t)$  in Eq.4.11 depends only on  $p_n = \rho_{nn}$  the population in number state  $|n\rangle$  and not on the coherences  $\rho_{nm}$ . Similarly,  $n_{ab}(t)$  does not depend on the initial coherence  $\rho_{ab}(0)$  if the field has zero initial coherences, namely  $\rho_{n,n-1}(0)$  and  $\rho_{n+1,n}(0) = 0$ .

Using  $\langle a, n | \hat{\rho} | b, n \rangle = \langle n | \hat{\rho}_{ab} | n \rangle = \langle a | \hat{\rho}_{nn} | b \rangle = C_{a,n}(t) C_{b,n}^*(t)$ , the transient atomic coherence is given by

$$\rho_{ab}(t) = \sum_{n=0}^{\infty} \langle a, n | \hat{\rho} | b, n \rangle = \sum_{n=0}^{\infty} C_{a,n}(t) C_{b,n}^*(t) \quad (4.13)$$

which is used for the plots of inversions in Fig.4.3 -Fig.4.10.

#### 4.3.2 Wigner function

The Wigner function,  $W$  is a reliable quantity for studying PhA and PhS processes for producing nonclassical states. The relationship between  $W$  and the matrix elements for the field  $\rho_{nm}$  can be obtained using (Cahill & Glauber, 1969),

$$W(\alpha, t) = \frac{2e^{2|\alpha|^2}}{\pi^2} \sum_{m,n=0}^{\infty} \rho_{nm}(t) \int \langle -\beta | n \rangle \langle m | \beta \rangle e^{2(\beta^* \alpha - \beta \alpha^*)} d^2 \beta \quad (4.14)$$

where  $\hat{\rho}_f(t) = \sum_{m,n}^{\infty} |n\rangle \rho_{nm}(t) \langle m|$  is the field state in photon number basis  $\{|n\rangle\}$  and the field matrix element  $\rho_{nm}(t)$  is given by Eq.4.8. The complex coherent state variable  $\alpha = re^{i\theta}$  can be mapped into polar coordinates,  $r$  and  $\theta$ . The  $|r|^2$  corresponds to the number of photons while  $\theta$  is the coherent state phase. Similarly for  $\beta$ . Inserting  $\langle n | \alpha \rangle = e^{-|\alpha|^2/2} \frac{\alpha^n}{\sqrt{n!}}$  and  $\int \int \beta^m \beta^{*n} e^{-|\beta|^2} e^{(\beta^* 2\alpha - \beta 2\alpha^*)} d^2 \beta = \pi L_n^{m-n} (|2\alpha|^2) n! e^{-|2\alpha|^2} (2\alpha)^{m-n}$ , the Wigner function in the general analytical expression is obtained

$$\begin{aligned} \frac{W(\alpha, t)}{K(\alpha)} &= \sum_{m=0}^{\infty} (-1)^m L_m^0(x) \rho_{mm}(t) + \\ &\sum_{m=1}^{\infty} \sum_{n=0}^{m-1} (-1)^n \sqrt{\frac{n!}{m!}} L_n^k(x) 2 \text{Re} \{ z^k \rho_{nm}(t) \} \end{aligned} \quad (4.15)$$

with the coherence of the field

$$\rho_{nm}(t) = C_{a,n}(t) C_{a,m}^*(t) + C_{b,n}(t) C_{b,m}^*(t) \quad (4.16)$$

where  $K(\alpha) = \frac{2e^{-2|\alpha|^2}}{\pi}$ ,  $x = |z|^2$ ,  $z = 2\alpha$ ,  $k = m - n > 0$  and  $Re$  is the real part. Note that the field density matrix elements serve as time-dependent coefficients to the Laguerre polynomials. The first term in Eq.4.15 gives the dependency on  $|\alpha|^2$ , contains the Laguerre polynomial  $L_m^0$  and the field population. The second term depends on the associated Laguerre polynomial  $L_n^k$  which falls off for large  $|\alpha|^2$ , the coherences between photon numbers  $\rho_{nm}(t)$  ( $m \neq n$ ), and  $\alpha^k$  carries the phase of  $\alpha$ . In view of  $C_{b,0}(t) = 0$ , straightforward calculation from Eq. 4.15 gives (Schleich, 2001)

$$\begin{aligned} \frac{W(\alpha, t)}{K(\alpha)} = & \sum_{m=0}^{\infty} (-1)^m \{ L_m^0(x) |C_{a,m}(t)|^2 \\ & - L_{m+1}^0(x) |C_{b,m+1}(t)|^2 \} + \\ & \sum_{m=1}^{\infty} \sum_{n=0}^{m-1} (-1)^n \left[ \sqrt{\frac{n!}{m!}} L_n^k(x) 2Re\{z^k C_{a,n}(t) C_{a,m}^*(t)\} \right. \\ & \left. - \sqrt{\frac{n+1!}{m+1!}} L_{n+1}^k(x) 2Re\{z^k C_{b,n+1}(t) C_{b,m+1}^*(t)\} \right] \end{aligned} \quad (4.17)$$

The inversion  $n_{ab}(t)$  is obtained by tracing over the radiation states whereas the Wigner function is computed from  $\rho_{nm}(t)$  after tracing over the atomic states. Both quantities are related as they are computed from the same density matrix. This suggests that the nonclassicality of the radiation field can be noticed through the behavior of inversion. It has been shown (Dung, Tanas, & Shumovsky, 1990) that under certain conditions there is a direct relation between atomic inversion and the corresponding Wigner function at the phase space origin. This relationship is supported by the recent developments in photon counting experiment (Banaszek & Wodkiewicz, 1996)(Wallentowitz & Vogel, 1996) and trapped ion technique (Lutterbach & Davidovich, 1997)(Nogues et al., 2000) where the measurements have been focused on the phase space origin. As shown in the subsection below, expressions for the Wigner function and the inversion are very similar at  $\alpha = 0$  for initially excited atom.

### 4.3.3 Coupling Function Properties

#### 4.3.3 (a) Time Dependent $g(t)$

The interesting aspect of the time dependent coupling is that the arguments  $\phi_n(t)$  in the sine and cosine functions now can have nonlinear dependency on time, in contrast to the constant coupling case where the argument depends linearly on time, i.e.  $\phi_n(t) =$

$g(t)\sqrt{n+1}$  and  $\phi_n(t) = g(t)(n+1)$  for intensity independent and dependent couplings, respectively. Thus, the transient regime where the coupling varies rapidly with time is of interest. The generalization from the constant coupling  $g$  to arbitrary time dependent coupling  $g(t)$  enables us to model several new physical situations not studied before. We will focus on several examples. Deterministic profiles of  $g(t)$  may be realized by time-dependent alignment or orientation of the atomic/molecular dipole moment using laser pulse (Friedrich & Herschbach, 1995) and motion of the atom through the cavity. We consider the forms for  $g(t) = g \sin^2(xgt)$ ,  $\frac{g}{\cosh((t-t_0)/t_m)}$  and  $\frac{g}{\cosh((t-t_0)/t_m)^4}$ ,  $x$  being a constant. The former two can be integrated, respectively as

$$\lambda(t)_{osc} = \frac{gt}{2} - \frac{1}{4x} \sin(2xgt) \quad (4.18)$$

$$\lambda(t)_{hat} = 2gt_m [\tan^{-1}(e^{\frac{t-t_0}{t_m}}) - \tan^{-1}(e^{-\frac{t_0}{t_m}})] \quad (4.19)$$

In practice, the fluctuations in  $g(t)$  can be due to the random orientations of the atom or molecule that change the coupling between the electric dipole moment and the cavity field. This will also be modelled.

Since the initial atomic state is not correlated to the field,

$$C_{x,n}(0)C_{y,n'}^*(0) = C_x(0)C_y^*(0)\rho_{nn'}(0)$$

we may expand the coherence between the number states of the field  $\rho_{nm}(t)$  from Eq.4.8 and write in a general form (valid even for mixed field states),

$$\begin{aligned} \rho_{nm}(t) = & \{ \rho_{aa}(0)r_n(t)r_m^*(t) + \rho_{bb}(0)r_{n-1}^*(t)r_{m-1}(t) \} \rho_{n,m}(0) \\ & + \rho_{bb}(0)q_n(t)q_m(t)\rho_{n+1,m+1}(0) \end{aligned} \quad (4.20)$$

$$+ \rho_{aa}(0)q_{n-1}(t)q_{m-1}(t)\rho_{n-1,m-1}(0) \quad (4.21)$$

$$\begin{aligned} & + i\rho_{ab}(0) \{ r_n(t)q_m(t)\rho_{n,m+1}(0) - q_{n-1}(t)r_{m-1}(t)\rho_{n-1,m}(0) \} \\ & + i\rho_{ba}(0) \{ r_{n-1}^*(t)q_{m-1}(t)\rho_{n,m-1}(0) - q_n(t)r_m^*(t)\rho_{n+1,m}(0) \} \end{aligned} \quad (4.22)$$

where  $\rho_{nm}(0) = \langle n | \hat{\rho}_f(0) | m \rangle$  with  $\hat{\rho}_f(0)$  being the initial state of the field (see Appendix D). This expression will be used to compute the Wigner function for the field.

#### 4.3.3 (b) Intensity Dependent $g(t)$

The strength of force between atom and field is basically be the subject of interest in understanding the interaction. Light-matter interaction with an intensity-dependent coupling was first suggested by Buck (Buck & Sukumar, 1981) and Sukumar (Sukumar & Buck, 1981). They describes the dependence of atom-field coupling on the electromagnetic field intensity. The intensity dependent coupling has great relevance in understanding the interaction since the coupling is proportional to the amplitude of the field. It describes a nonlinear interaction which is one of the popular research field nowadays. For example in recent work, Ooi & Khoo reported the Casimir force between two plates driven by an external high-intensity laser source (Ooi & Khoo, 2012). They introduced the optical Kerr effect on the plates which can be controlled using combinations of dispersive metamaterials and nonlinear materials. They have shown that the force can be significantly varied and switched between positive and negative values by changing the intensity of the laser.

The results of this model can also give insight into the behavior of other quantum systems such as squeezed light, entropy and many more. The study by (Singh, Ooi, & Amrita, 2012) on the dynamics of two atom interact with two-mode quantized cavity fields also considered the intensity dependent coupling function which is given by  $f(n) = \sqrt{\hat{a}^\dagger \hat{a}}$  defined as

$$\begin{aligned}\hat{R} &= \hat{a}f(n) = \hat{a}\sqrt{\hat{a}^\dagger \hat{a}} \\ \hat{R}^\dagger &= f(n)\hat{a}^\dagger = \sqrt{\hat{a}^\dagger \hat{a}}\hat{a}^\dagger\end{aligned}\tag{4.23}$$

This function is used to replace the field operators  $\hat{a}$  and  $\hat{a}^\dagger$  to include the intensity dependent to atom-field coupling.

#### 4.3.4 Initial State of Atom and Field

##### 4.3.4 (a) Initially excited atom

For atom initially in the excited state  $|a\rangle$  and the radiation field is in the pure state, the matrix element for the field reduces to

$$\rho_{nm}(t) = C_{a,n}(0)C_{a,m}^*(0)r_n(t)r_m^*(t)\tag{4.24}$$



$$+C_{a,n-1}(0)C_{a,m-1}^*(0)q_{m-1}(t)q_{n-1}(t) \quad (4.25)$$

Inserting Eq.4.25 into Eq.4.15 we obtain

$$\frac{W(\alpha, t)}{K(\alpha)} = \sum_{m=0}^{\infty} (-1)^m |C_{a,m}(0)|^2 (L_m^0(x)|r_m(t)|^2 + L_{m+1}^0(x)q_m^2(t)) \quad (4.26)$$

$$+ \sum_{m=1}^{\infty} \sum_{n=0}^{m-1} (-1)^n C_{a,n}(0)C_{a,m}^*(0) \quad (4.27)$$

$$\left\{ \sqrt{\frac{n!}{m!}} L_n^{m-n}(x) 2Re \left( z^k r_n(t) r_m^*(t) \right) \right. \quad (4.28)$$

$$\left. + \sqrt{\frac{n+1!}{m+1!}} L_{n+1}^{m-n}(x) 2Re \left( z^k q_m(t) q_n(t) \right) \right\} \quad (4.29)$$

where  $\sqrt{2}(x+ip) = z = 2\alpha, x = |z|^2$ .

By comparing the analytical expressions for  $n_{ab}$  and  $W(t)$ , it is found that  $n_{ab}$  does not contain the coherences of the field. Therefore,  $n_{ab}$  may not be entirely correlated to the Wigner function  $W$  which depends on both diagonal and off-diagonal elements  $\rho_{mn}$  in general, unless all  $\rho_{nm}(t)$  are negligibly small or zero for all times, as we find for the case of initial thermal state.

At the origin  $\alpha = 0$  only the first line contributes

$$W(0, t) = \frac{2}{\pi} \sum_{n=0}^{\infty} (-1)^n p_n(0) (|r_n(t)|^2 - q_n^2(t)) \quad (4.30)$$

since  $L_m(0) = 1$ . Here, the inversion is

$$n_{ab}(t) = \sum_{n=1}^{\infty} p_n(0) (|r_n(t)|^2 - q_n^2(t)) - p_0(0)q_0^2(t) \quad (4.31)$$

which looks similar to the Wigner function. Both would be identical if the even coefficients and  $p_0(0)$  are zero. Atom field coupling will be discussed deeply in the next section.

#### 4.3.4 (b) Coherent state(CS) field

For initial coherent state,  $|\alpha_0\rangle = \sum_{n=0}^{\infty} C_n(0)|n\rangle$  with  $C_n(0) = e^{-|\alpha_0|^2/2} \frac{\alpha_0^n}{\sqrt{n!}}$ . The initial density matrix  $\hat{\rho}_f = |\alpha_0\rangle\langle\alpha_0| = e^{-|\alpha_0|^2} \sum_{m,n=0}^{\infty} \frac{\alpha_0^m \alpha_0^{*n}}{\sqrt{m!n!}} |m\rangle\langle n| = \sum_{m,n=0}^{\infty} \rho_{mn}(0) |m\rangle\langle n|$  gives

$$\rho_{mn}(0) = C_m(0)C_n^*(0) = e^{-|\alpha_0|^2} \frac{\alpha_0^m \alpha_0^{*n}}{\sqrt{m!n!}} \quad (4.32)$$

which gives the initial analytical Wigner function that is independent of the atomic initial condition,

$$W(\alpha, 0) = K(\alpha) e^{-|\alpha_0|^2} \sum_{n=0}^{\infty} \frac{1}{n!} [(-1)^n L_n^0(|z|^2) |\alpha_0|^{2n} + \sum_{m=0}^{n-1} (-1)^m L_m^k(|z|^2) 2 \operatorname{Re}\{z^k \alpha_0^m \alpha_0^{*n}\}]. \quad (4.33)$$

When the atom is initially in coherent superposition of states and the field is in the coherent state, the inversion has a small magnitude. This effect will be discussed in the subsequent section by using the analytical expression (which agrees with numerical results), obtained from Eq.4.11, i.e.

$$n_{ab}(t) = \frac{e^{-|\alpha_0|^2}}{2} \left[ \sum_{n=1}^{\infty} \frac{|\alpha_0|^{2n}}{n!} \right] \quad (4.34)$$

$$\left\{ \left(1 - \frac{|\alpha_0|^2}{n+1}\right) \left[ 1 - \left( \frac{8(g(t)(n+1))^2}{\Omega_n^2} \right) \left( \sin\left(\frac{\lambda(t)}{2}\right) \right)^2 \right] \right\} \quad (4.35)$$

$$+ \frac{|\alpha_0|^{2n} 2 \operatorname{Im}(\alpha_0)}{\sqrt{n!(n+1)!}} (D_n^* - D_n) \} \quad (4.36)$$

$$- |\alpha_0|^2 \left[ \left( \cos\left(\frac{\lambda_0(t)}{2}\right) \right)^2 + \frac{\Delta^2}{\Omega_0^2} \right] - \frac{4g^2(t)}{\Omega_0^2} \left( \sin\left(\frac{\lambda_0(t)}{2}\right) \right)^2 - \operatorname{Im}(\alpha_0) (D_0 - D_0^*) \quad (4.37)$$

#### 4.3.4 (c) Schrödinger's cat(SS) state

We now find the matrix elements for the even(+)/odd(-) Schrödinger's cat state,  $|\psi\rangle_{cat}^{\pm} = \mathcal{N}(|\alpha_0\rangle \pm e^{i\varphi} |-\alpha_0\rangle)$ , a nonclassical state formed from even/odd superposition of coherent states with relative phase  $\varphi$ . In number state basis,  $|\psi\rangle_{cat}^{\pm} = \sum_{n=0} C_n(0) |n\rangle$  where  $C_n(0) = \mathcal{N} e^{-|\alpha_0|^2/2} \frac{\alpha_0^n \pm (-\alpha_0)^n}{\sqrt{n!}}$  with the normalization factor  $\mathcal{N} = \frac{1}{\sqrt{2(1+e^{-2|\alpha_0|^2} \cos \varphi)}}$ . The cat state can be produced by atomic inversion via atomic superposition (Monroe, Meekhof, King, & Wineland, 1996). It can also be produced by linear optics with conditional measurements of photon number states using homodyne detection, which generates arbitrarily large squeezed Schrödinger's cat state (Ourjoumtsev, Jeong, Tualle-Brouri, & Grangier, 2007). The initial density matrix element for the cat state

$$\rho_{nm}^{\pm}(0) = e^{-|\alpha_0|^2} \frac{\{\alpha_0^n \pm (-\alpha_0)^n\} \{\alpha_0^{*m} \pm (-\alpha_0^*)^m\}}{2(1+e^{-2|\alpha_0|^2} \cos \varphi) \sqrt{n!m!}} \quad (4.38)$$

which is used to compute the results. The Schrödinger's cat has been realized experimentally in the context of atom-field interaction in a cavity (Monroe et al., 1996).

#### 4.3.4 (d) Diagonal number state

For fields with diagonal number state, i.e.  $\hat{\rho}_f = \sum_{n=0} \rho_{nn} |n\rangle\langle n|$  only the diagonal matrix elements contribute. Here  $\rho_{nm}(0) = \langle n | \hat{\rho}_f(0) | m \rangle = \delta_{mn} p_n = \delta_{mn} C_n(0) C_m^*(0)$  and  $C_n(0) = \sqrt{p_n}$  is chosen to be real. A special case is the thermal state, with the probability

$$p_n(0) \doteq \frac{1}{1 + \bar{n}} \left( \frac{\bar{n}}{1 + \bar{n}} \right)^n \quad (4.39)$$

where  $\bar{n} = (e^{\hbar\nu/k_B T} - 1)^{-1}$  is the mean number of thermal photons and  $\sum_{n=0} p_n(0) = 1$ .

The transient matrix element for initial thermal field in Eq.4.22 reduces to

$$\begin{aligned} \rho_{nm}(t) = & \delta_{mn} [\{|C_a(0)r_n|^2 + |C_b(0)r_{n-1}|^2\} p_n(0) + \\ & |C_a(0)q_{n-1}|^2 p_{n-1}(0) + |C_b(0)q_n|^2 p_{n+1}(0)] + \\ & \delta_{n,m-1} i C_{ab}^*(0) \{r_{n-1}^* q_n p_n(0) - q_n r_{n+1}^* p_{n+1}(0)\} + \\ & \delta_{n,m+1} i C_{ab}(0) \{r_n q_{n-1} p_n(0) - q_{n-1} r_{n-2} p_{n-1}(0)\} \end{aligned} \quad (4.40)$$

where  $\delta_{mn}$  is the delta Kronecker where  $C_{ab}(0) = C_a(0) C_b^*(0)$ . Here, the initial Wigner function has a simple form  $W(\alpha, 0) = K(\alpha) \sum_{n=0}^{\infty} (-1)^n L_n^0(|2\alpha|^2) p_n(0)$ . However, for finite  $t$  the emission and absorption processes may develop coherences between photon numbers  $n$  and  $m \pm 1$  through the last two lines of Eq.4.40. Although the initial radiation state is diagonal, for finite  $t$  the emission and absorption processes may develop coherences between photon numbers. The atomic dynamics [through the inversion  $n_{ab}(t)$  and coherence  $\rho_{ab}(t)$ ] with the pattern of the Wigner function are compared to investigate the interesting features resulted.

## 4.4 Transient Effects in Cavity Coupling

The Wigner plot and the atomic inversion concerning the collapse and revival pattern with a peculiar transient dynamics due to the transient couplings  $g(t)$  are discussed. A setup which allows the possibility of extracting desirable state of the field is proposed based on the knowledge of transient atomic dynamics and the evolutions of  $W(t)$  for any time dependent  $g(t)$  since nonclassical light in the cavity is only useful if the state can be frozen instantaneously and coupled out from the cavity.

The comparison of the collapse duration is also discussed to show the anti Zeno-like effect as illustrated in Fig.4.6 and Fig.4.7 for initial state  $C_a(0) = 1$  and  $\alpha_0 = \sqrt{15}$ .

#### 4.4.1 Constant Coupling Case

The evolution of Wigner function for the case of constant coupling  $g(t) = g$  with intensity independent for initial CS and initial SS are shown in Fig.4.3.

The Wigner function for intensity independent coupling for initial CS shows a single peak at  $\text{Re}(\alpha) = 0$  and  $\text{Im}(\alpha) = +6$  in Fig.4.3a(ii). It corresponds to the revival phase appear at the same point of time in inversion plot  $n_{ab}(t)$  vs time  $gt$ . However in SS, for each revival phase, two peaks appear opposite to each other: at  $\text{Re}(\alpha) = 0, \text{Im}(\alpha) = +6$  and  $\text{Re}(\alpha) = 0, \text{Im}(\alpha) = -6$  as illustrated in Fig.4.3b(ii). As the  $\text{Im}(\alpha)$  decreases from 6 to  $-6$  for CS (Fig.4.3a(iii)), the peak splits into two with the same amplitude but opposite phases. The peaks move to the right and left along the edge of a circle in a plane of  $\text{Re}(\alpha)$  and  $\text{Im}(\alpha)$  axis towards point  $\text{Im}(\alpha) = 0, \text{Re}(\alpha) = +5$  and  $\text{Im}(\alpha) = 0, \text{Re}(\alpha) = -5$  and recombine to form a single peak again at the point as shown in Fig.4.3a(iv). Then the peaks move back to its initial position. Referring to Fig.4.3a(iii) at  $t = 1.5g^{-1}$  and Fig.4.3a(v) at  $t = 5g^{-1}$ , we conclude that the field states generated at these times are the Schrödinger-cat states corresponding to the collapse phase of the inversion. In the SS case, there are two peaks at the beginning, corresponding to the revival phase in inversion plot. The peaks then split to four peaks which refer to collapse phase and recombine back to its initial position when the second revival phase reappear. The revival arises at the point of time when the single peak appear as shown in Figs.4.3b(i)-(vi). The movement of  $W(t)$  is faster while the revival phases are seen appear more frequently for SS case than in CS case within the same time interval.

The case of intensity dependent demonstrate more rapid movement in Wigner function evolution for both case. The pattern of peaks movement is absolutely the same with the intensity independent case. The revivals appear the most frequent in SS case with intensity dependent coupling. This can be seen in Fig.4.5. The revival appear 2 times for intensity independent in both cases with time interval  $t = 50g^{-1}$  for initial CS(Fig.4.4(i)) but in shorter time of  $t = 20g^{-1}$  for initial SS(Fig.4.4(ii)). If compared with intensity dependent case, the collapse-revival pattern is generated more often with 4 revivals in the duration between  $t = 0g^{-1}$  and  $t = 10g^{-1}$  for initial CS while between  $t = 0g^{-1}$  and  $t = 5g^{-1}$  for initial SS as shown in Fig.4.5(i) and Fig.4.5(ii) respectively. We can conclude that the initial SS with intensity dependent generates more revivals compared to other

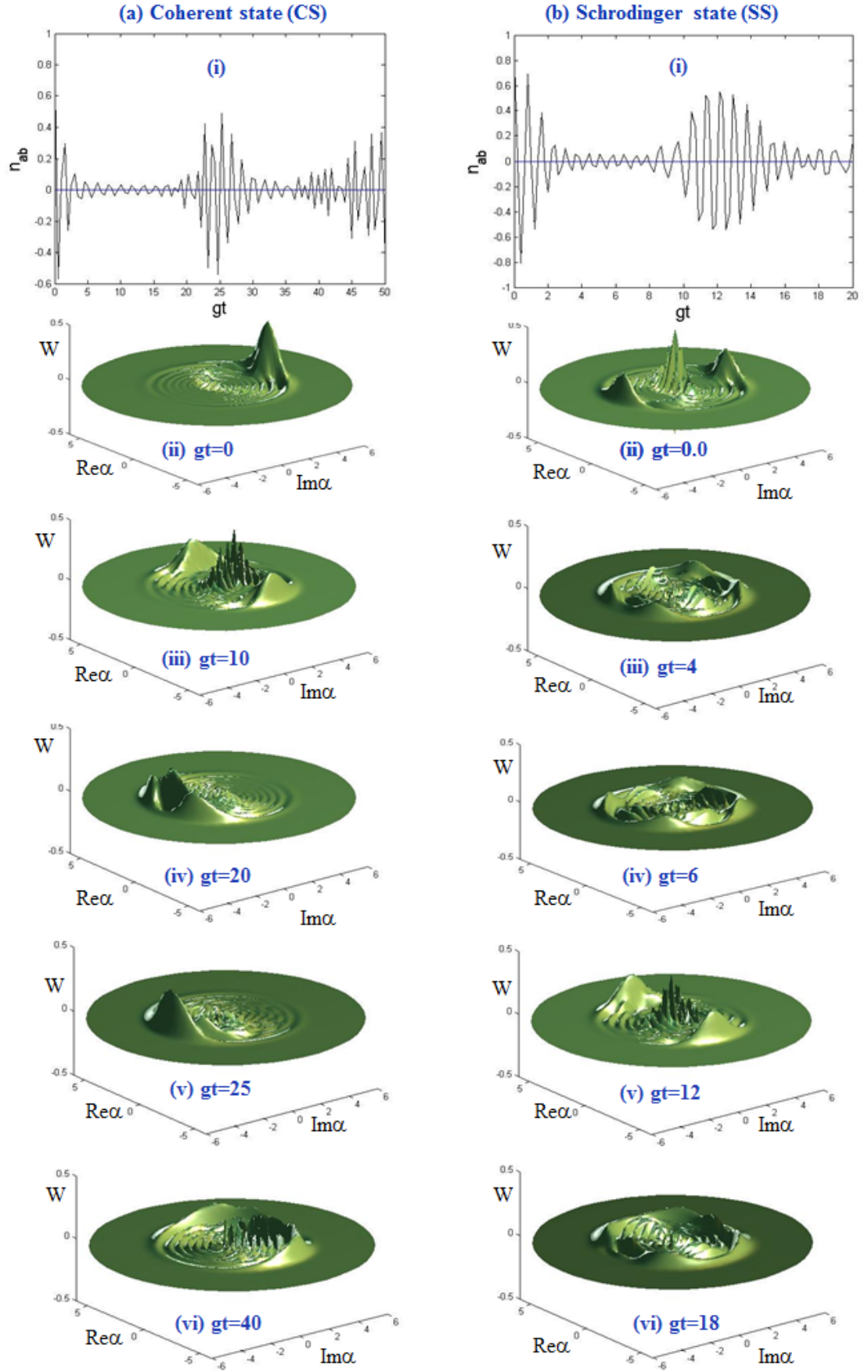


Figure 4.3: Wigner evolution and Inversion plot of  $g(t) = g$  for initial coherent state and Schrodinger cat state

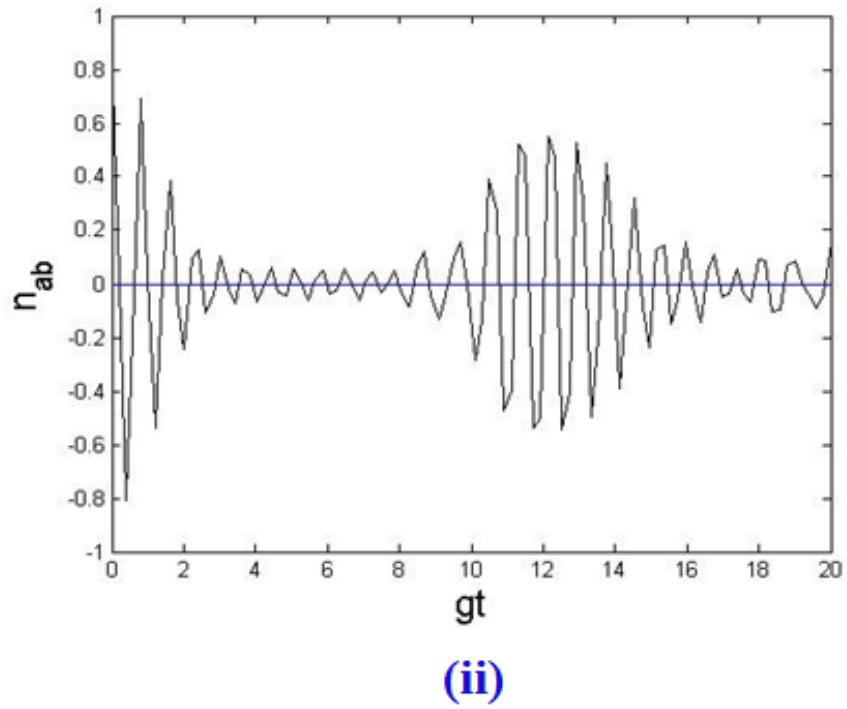
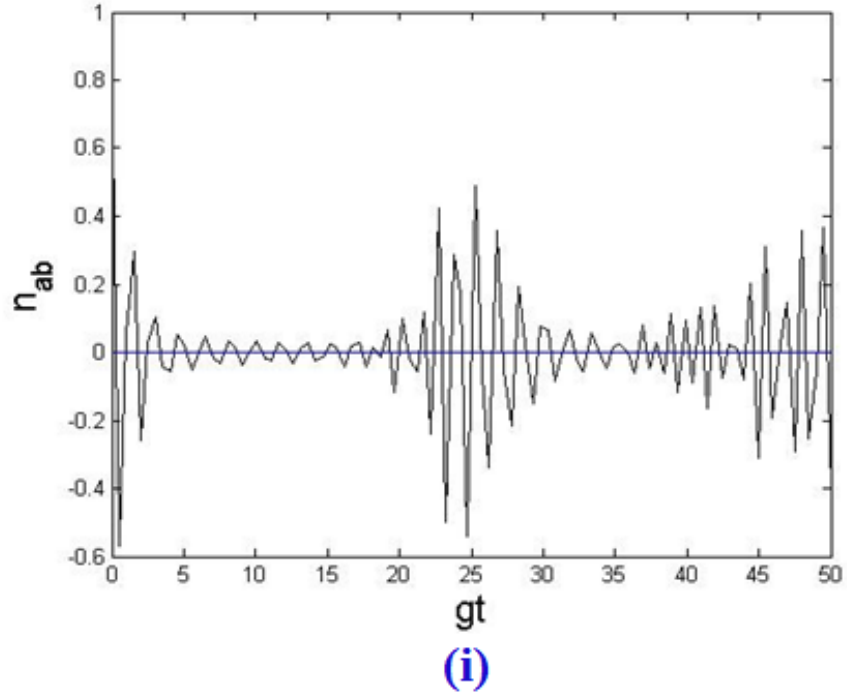
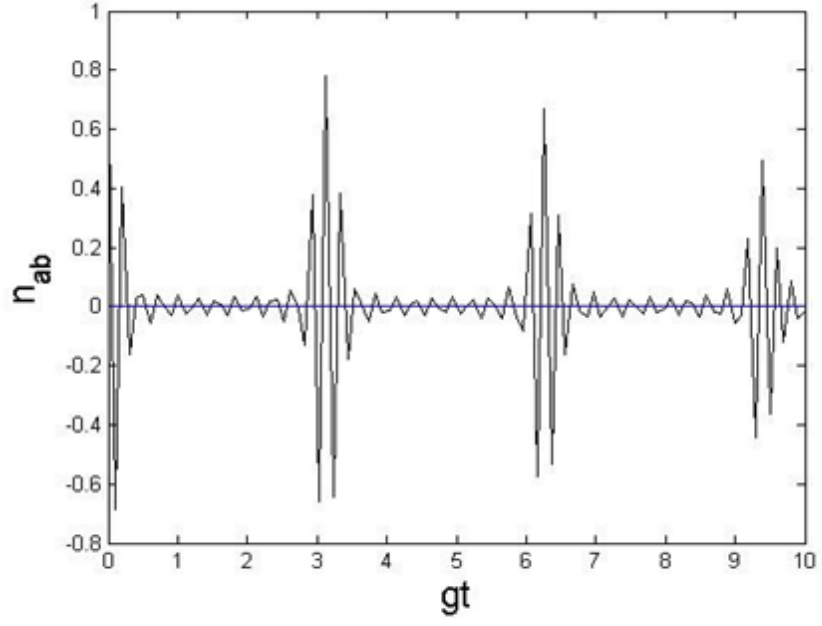


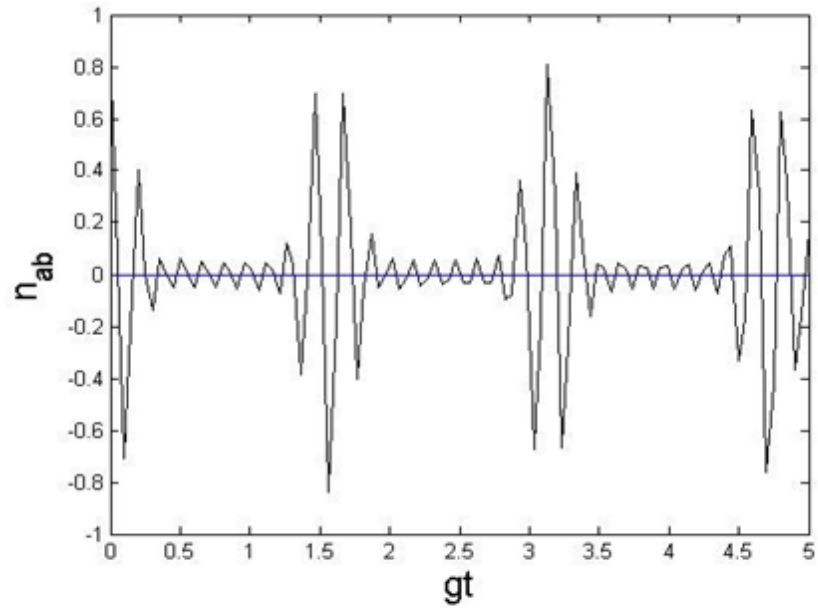
Figure 4.4: Comparison of inversion plots of  $g(t) = g$  for intensity independent coupling between initial (i) coherent state and (ii) Schrodinger cat state.

cases. In term of collapse duration, it appears shorter time interval when intensity dependent is applied in coupling function. This feature shows an analogy of the quantum Zeno effect.

The generalization from constant coupling  $g$  to arbitrary time dependent coupling



(i)



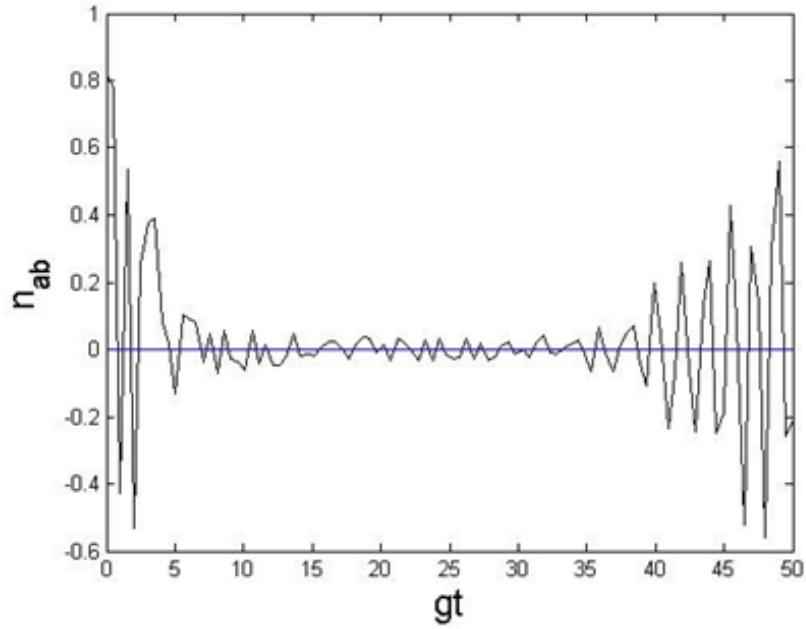
(ii)

Figure 4.5: Comparison of inversion plots of  $g(t) = g$  for intensity dependent coupling between initial (i) coherent state and (ii) Schrodinger cat state.

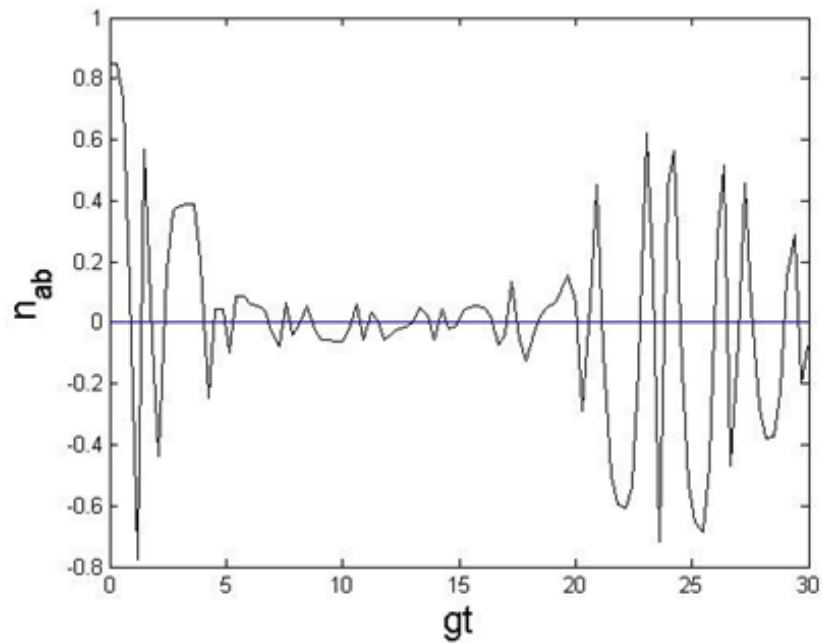
$g(t)$  through numerical computations enables us to model the dynamics of the atomic system not studied before. Interesting features are found for sinusoidal and hat pulse coupling function which will discuss in the next section.

#### 4.4.2 Sinusoidal Coupling Function

For an atom oscillating back and forth across a narrow cavity within a square well trap (illustrated in Fig.4.2b), the coupling is modelled approximately to be sinusoidal  $g(t) = g \sin^2 xgt$  where  $x$  is arbitrary.



(i)



(ii)

Figure 4.6: Comparison of inversion plots of  $g(t) = g \sin^2(xgt)$  for intensity independent coupling between initial (i) coherent state and (ii) Schrodinger cat state.

The Wigner function evolves like the previous constant case where the single peak

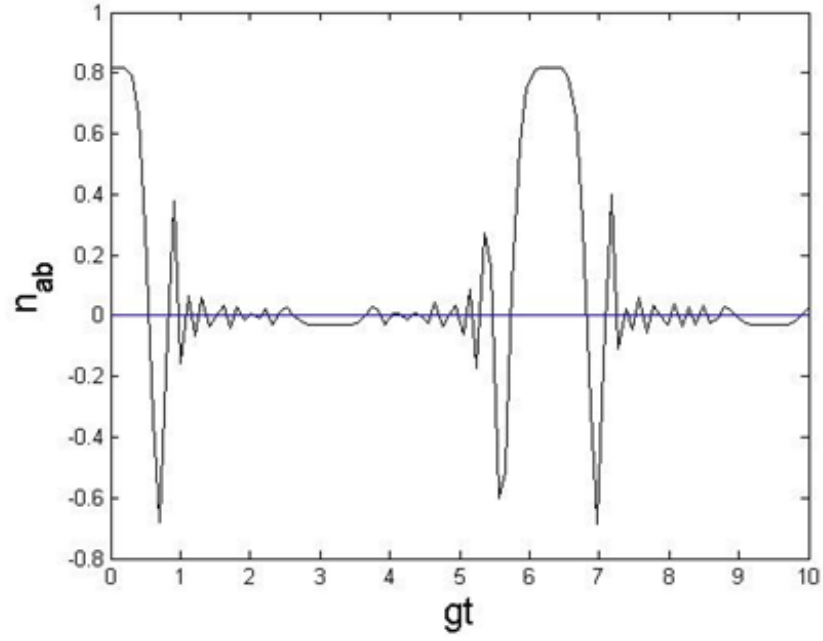


appear corespond to revival phase and split into two peaks to indicate it enters the collapse phase in CS. It evolves very rapidly corresponds to the frequent generation of collapse and revival which 2 peaks opposite to each other appear in SS case and split into 4 peaks when collapse phase takes turn. The inversion plots for both initial field state demonstrate the same style with constant coupling case where it show the zeno-like effect when intensity dependent is applied to the coupling. This can be seen if we compare the intensity independent case in Fig.4.6 with the case of intensity dependent in Fig4.7.

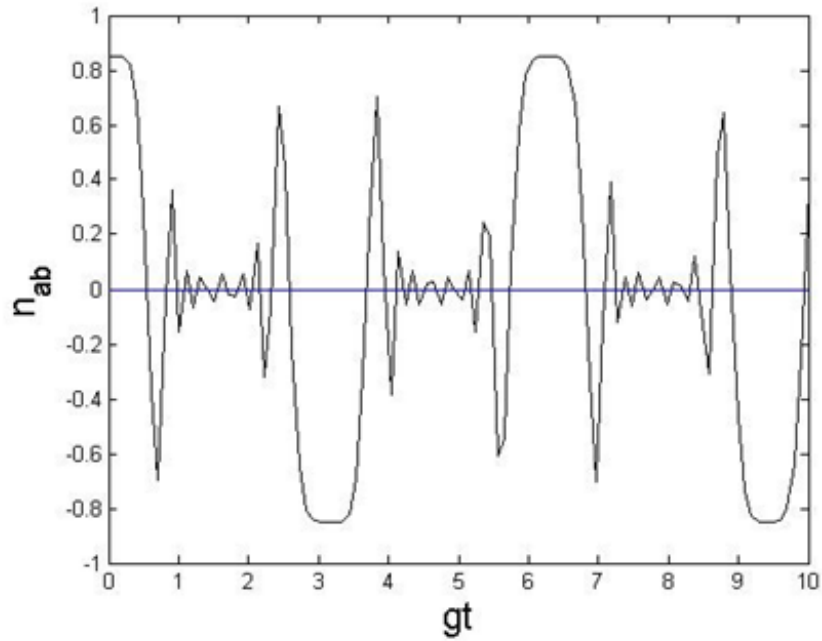
Quite an interesting pattern of inversion is found for sinusoidal function if compared with the constant coupling inversion. The atomic inversion exhibits the usual periodic collapse and revival phenomenon but in intensity dependent for sinusoidal case (Fig. 4.7), the highest amplitude of the fluctuation oscillates in longer period with a constant value of inversion about  $\Delta t = 1g^{-1}$  for a while before drop/rise. This corresponds to the freeze state of Wigner function evolution.

Another interesting feature in this coupling is for initial CS, the collapse duration is  $30g^{-1}$  as in Fig.4.6(i) and for intensity dependent case in Fig.4.7(i) is  $4g^{-1}$ . It is clearly been seen that the collapse duration of sinusoidal coupling function has longer collapse duration if compared to constant coupling case with  $15g^{-1}$  for intensity independent(Fig.4.6(i)) case and  $2g^{-1}$  for intensity dependent(Fig.4.7(i)). SS case also shows the increase in collapse duration for sinusoidal coupling compared to constant coupling. As an analogy with the Zeno effect, we call this anti Zeno-like effect (AZE) by modulation. Here, it is the increase of the collapse duration and not the decay/decoherence time as in the case of quantum Zeno effect. The modulated coupling field stretches the collapse duration by disturbing the rephasing process towards revival via quantum interference. Thus, its underlying mechanism is different from the recent work that uses the phase space tweezer approach (Raimond et al., 2010). The revival shows positive value in the intensity dependent coupling of CS case but alternately positive and negative value in SS case.

The corresponding coherence ( $\text{Imp}_{ab}$ ) is found to be maximum during the collapse phase, especially near the onset of revival. This has some relations to the recent work on controlling the purity (polarization) or mixing of NMR ensembles (Ivarez, Rao, Frydman, & Kurizki, 2010) and frequent measurements of the polarization to establish Zeno



(i)



(ii)

Figure 4.7: Comparison of inversion plots of  $g(t) = g \sin^2(xgt)$  for intensity dependent coupling between initial (i) coherent state and (ii) Schrodinger cat state.

and anti-Zeno effects (Kofman, Kurizki, & Opatrny, 2001). In intensity dependent case for both CS and SS show the same pattern but the number of revival oscillations in SS is doubled. This shows that when the coupling function depends on intensity, the collapse and revival occurs very rapid. The coherent interaction scheme does not show analogy with the anti-Zeno effect, first shown by Kofman and Kurizki using certain time-

dependent measurements in dissipative reservoir (Kofman & Kurizki, 2000). This implies that dissipation may be an important mechanism behind the anti-Zeno effect.

The present scheme applies to rapid change in the time-dependent weak coupling /excitation, related to the control of decay by weak time-dependent potential and time varying internal energies coupled to reservoir with arbitrary continuum (Kofman & Kurizki, 2001). The scheme may also describe coherent interaction with ultrashort laser pulse, if large value of  $g$  is used. This situation is connected to recent work of establishing the Zeno effect in decay and decoherence of qubits by using strong laser pulses in arbitrary thermal baths without rotating wave approximation (Kofman & Kurizki, 2004). Further studies of including dissipation in cavity/resonator would be interesting (Kofman & Kurizki, 1996).

#### 4.4.3 ‘Hat’ Pulse Function

The inversion plot with hat function  $g(t) = \frac{g}{\cosh((t-t_0)/t_m)^4}$  for intensity independent coupling shows the same value of collapse duration with constant  $g$  but it starts at a constant value of about 0.8 from  $gt = 0$  until about  $gt = 10$  as shown in Fig.4.8(i) and Fig.4.9(i) for CS and SS respectively. The constant value at the beginning and the end of inversion plots are consequence of atom movement. The inversion remain static as the cavity is empty and starts oscillate once the atom enters the cavity. The oscillation stops at the end corresponds to the atom exits the cavity so the cavity is emptied again. The Wigner peak also freezes a while at the time of constant value in the inversion as illustrates in Fig.4.8(ii-iii) for CS and Fig.4.9(ii-iii) for SS; and then oscillates as in  $g(t) = g$  plots. From  $gt = 40$  until  $gt = 50$ , once again the constant value appears in inversion plot but this time it is in the collapse phase. At this time, the Wigner function freezes, with 2 large peaks at the right and left edges of a circle on the plane of  $\text{Re}(\alpha)$  and  $\text{Im}(\alpha)$ , while 4 peaks appear in SS case. The maximum time taken is  $gt = 50$  and the revival appears twice in CS and trice in SS along the time interval. It can be seen that the collapse duration is decreases when initial SS is applied to the system of hat coupling function if compare with constant coupling case in Fig.4.4(i) and Fig.4.5(i). If refer to Fig.4.10(ii), for hat function of SS case, the Zeno-like effect also demonstrated here where the collapse duration is also decreases if compared to the case of intensity independent in Fig.4.10(i).

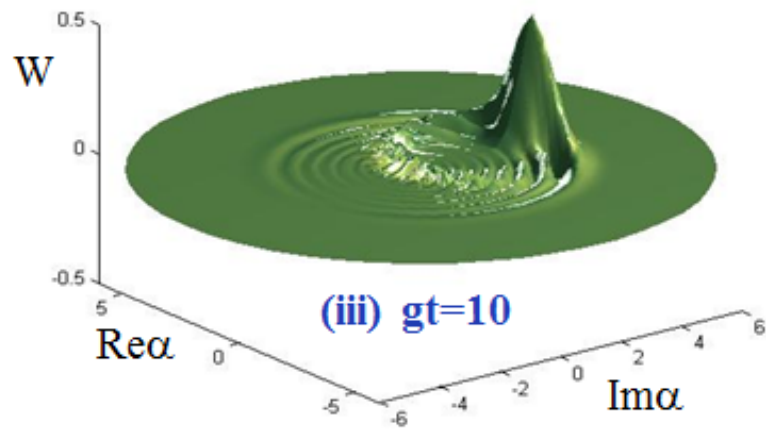
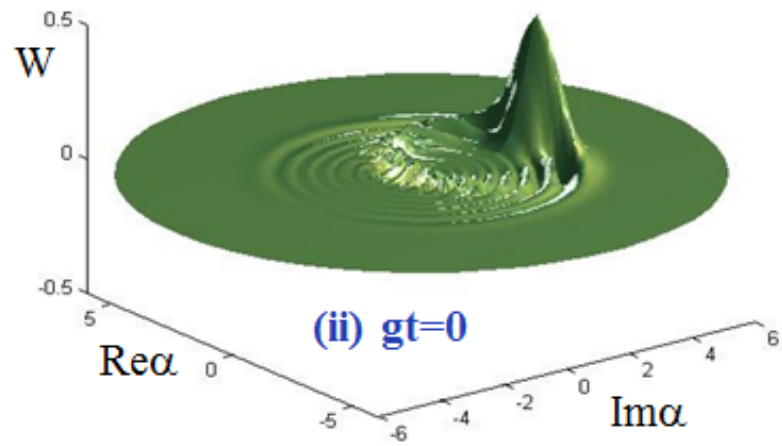
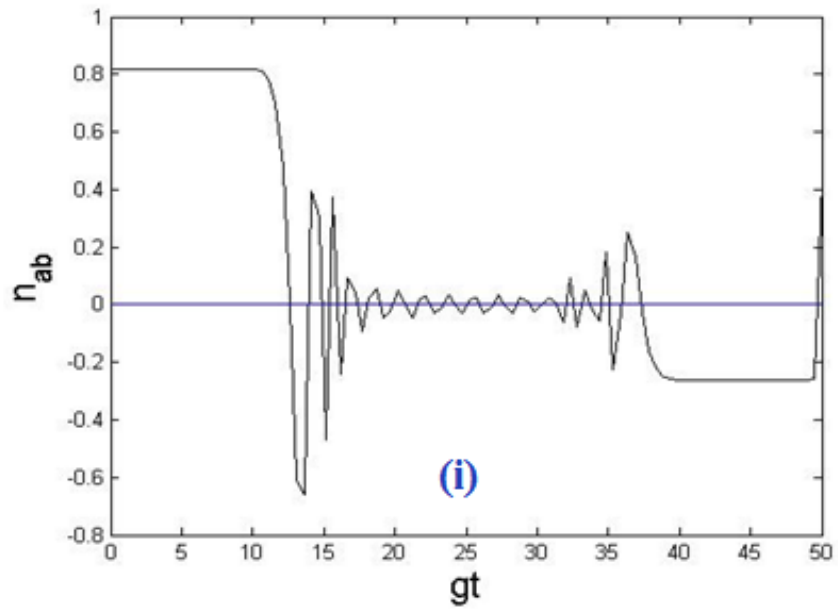


Figure 4.8: (i) Inversion and Wigner plot for intensity independent hat coupling function for initial coherent state at time (ii)  $gt = 0$  and (iii)  $gt = 10$

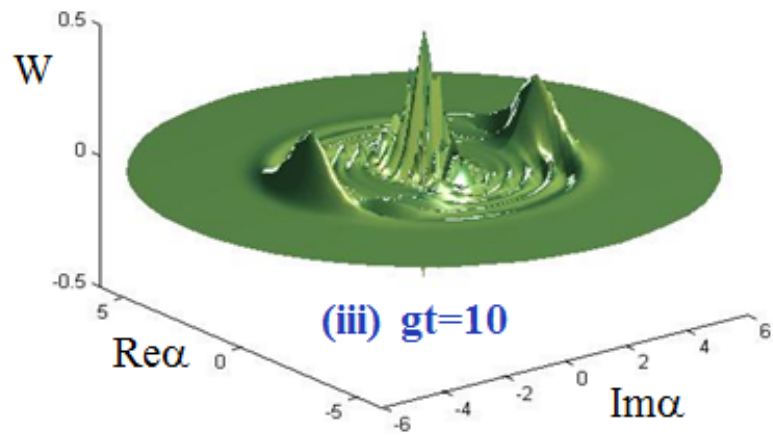
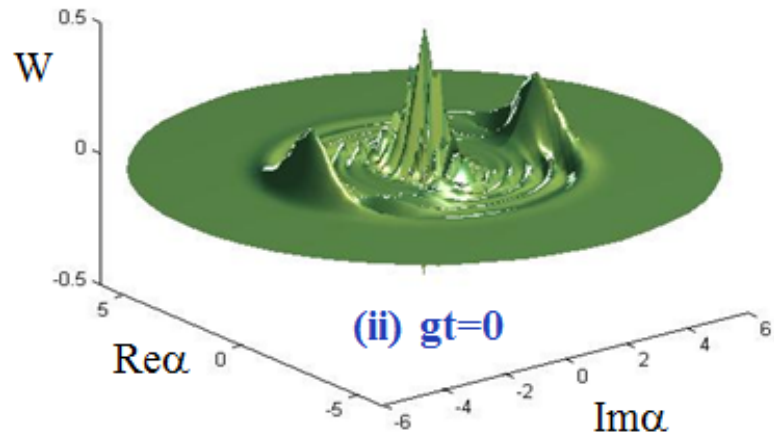
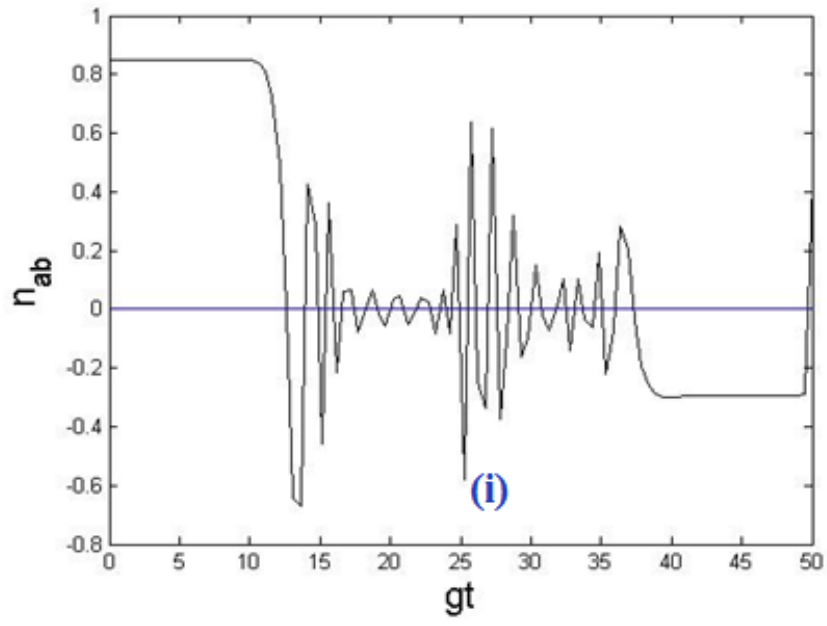


Figure 4.9: (i) Inversion and Wigner plot for intensity independent hat coupling function for initial Schrodinger cat state at time (ii)  $gt = 0$  and (iii)  $gt = 10$

When compare the hat function case from the constant case, it can be found that the collapse duration is almost equal.

The frozen populations depend on the hat duration  $t_m$ . This can be understood qualitatively by analyzing the function  $g(t) = \frac{g}{\cosh((t-t_0)/t_m)}$  which can be integrated as  $\lambda(t) = 2gt_m[\tan^{-1}(e^{\frac{t-t_0}{t_m}}) - \tan^{-1}(e^{-\frac{t_0}{t_m}})]$ . For  $t_0 \gg t_m$  the second term is negligible. At large  $t$  when the pulse is gone,  $\lambda(\infty) = \pi gt_m$ . Thus,  $t_m$  determines the value of the frozen inversion  $n_{ab}(\infty)$ . Thus, the duration of the hat function or atomic transit can be a control parameter for creating a frozen state of light in an empty cavity. This result is connected to the frozen cat state (Sherman et al., 1992) in photonic crystal.

In all cases, if we compare the inversion between the intensity-independent and intensity-dependent case, we find that the revival pattern appears more frequently in the latter case. For example, the inversion for sinusoidal function with initial CS in is plotted from  $gt = 0$  until  $gt = 50$  which is far longer than the intensity-dependent case which ended at  $gt = 10$ . However, the revival pattern appears 2 times in both cases. It can be concluded that within the same interval of time, the intensity-dependent case can generate more number collapse and revival.

#### 4.5 Extracting Nonclassical Photons

The Wigner function computed above describes the state of light inside the cavity. A desired state of light in the cavity can be frozen by controlling the presence (entrance and exit) of the atom in the cavity via the time-varying coupling  $g(t)$ , as illustrated in Figs.4.2a and b. In order to harness a desired state of light from the cavity, the reflectance of the cavity mirror has to be reduced. To study of the output field we need to consider the dissipation of the cavity field. The quantitative treatment is beyond the present scope and will be reported elsewhere. Here, we merely describe the mechanism qualitatively.

A desired quantum state of light can be coherently extracted on demand from the cavity by rapidly switching the reflectance  $R$  of the cavity mirrors at time  $t_s$  from  $R = 1$  to  $R = 0$ , like an inverse  $Q$ -switching. The field at time  $t_s$  would be "frozen". The nonclassical field can then be transmitted through one of the cavity mirrors, for example, into a waveguide/optical fiber. An optical switching can be employed for rapidly changing the cavity field decay rate. For example, electromagnetic induced transparency of the mirror

cavity (Boller, Imamoglu, & Harris, 1991) using a strong control laser can be used. Another option is using a photonic bandgap mirror or Bragg mirrors that can be optically switched within picosecond timescale through nonlinear optical process (Yanik, Fan, Soljacic, & Joannopoulos, 2003). Specific nonclassical light can be generated and harnessed on demand since we can predict the transient evolution of field through the atomic dynamic for the atom-cavity system. The time evolution of the cavity photons (Wigner function) can be experimentally mapped out using tomography technique (Lvovsky et al., 2001). Thus, the scheme provides an exciting possibility of producing heralded nonclassical light using the transient coherent coupling as well as timely switching of the cavity reflectance.

#### 4.6 Conclusions

We have studied the dynamics of a two-level particle or system coupled to any state of light in a cavity. This work focuses on field-state control through time dependent and intensity dependent coupling. The generalization to arbitrary time-dependent coupling  $g(t)$  enables the analysis of transient effects, such as particle oscillating through the cavity and particle transit duration. We have analyzed the time evolutions of the atomic states (through inversion) and the cavity field (through the Wigner function) for time-dependent and intensity-dependent atom-field coupling. Both quantities do not always show regular connection. For example, the collapse phase does not always correspond to the formation of the Schrodinger's cat. The atom and field dynamics, particularly the collapse duration and the time of collapse can be controlled by using simple oscillatory coupling. The former is called anti-Zeno effect while the latter bears analogy with the quantum Zeno effect, except that it does not involve a measurement nor dissipative mechanism. By using the hat function with certain duration for the coupling to simulate atomic transit through the cavity, the proportions of the frozen internal populations can be controlled, and the collapse phase can be locked/frozen inside the cavity even after the coupling ceases. Nonclassical light remains inside a high-Q cavity after the atom leaves the cavity. For initial superposition of states, the initial coherent field state has a weak effect on the inversion dynamics. In contrast, the initial cat field state is able to stimulate a much larger inversion amplitude. We derive an analytical expression to explain this effect. Each time-dependent coupling function with different initial field shows quantum Zeno effect when

the system include the intensity-dependent coupling. The anti-Zeno effect only occurs in oscillatory coupling compared with normal JCM with constant coupling.

Although we have considered atom, the scheme applies to other quantum systems such as quantum dot, superconducting qubit or Rydberg atom in a superconducting millimeter-wave cavity (Haroche & Raimond, 2006), where the transient coupling to the cavity can be realized more easily in practice. The above time-dependent analysis is not exhaustive since other profiles are possible. The effect of the center of mass motion along the cavity axis (Vernooy & Kimble, 1997) is important when the atomic motion is not entirely orthogonal to the cavity axis. This, along with the spatial-temporal dependent coupling can be considered in future works.



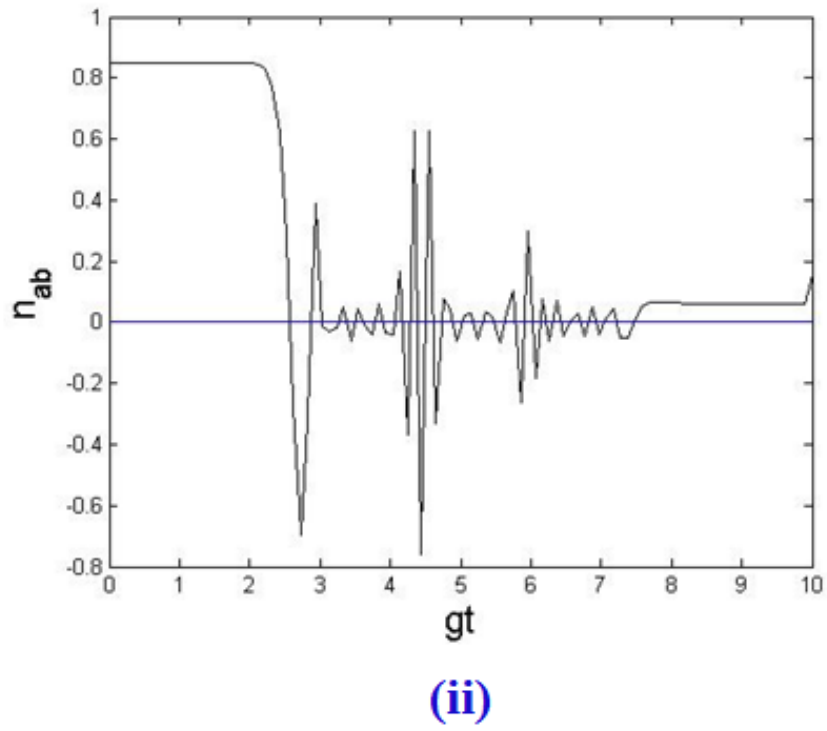
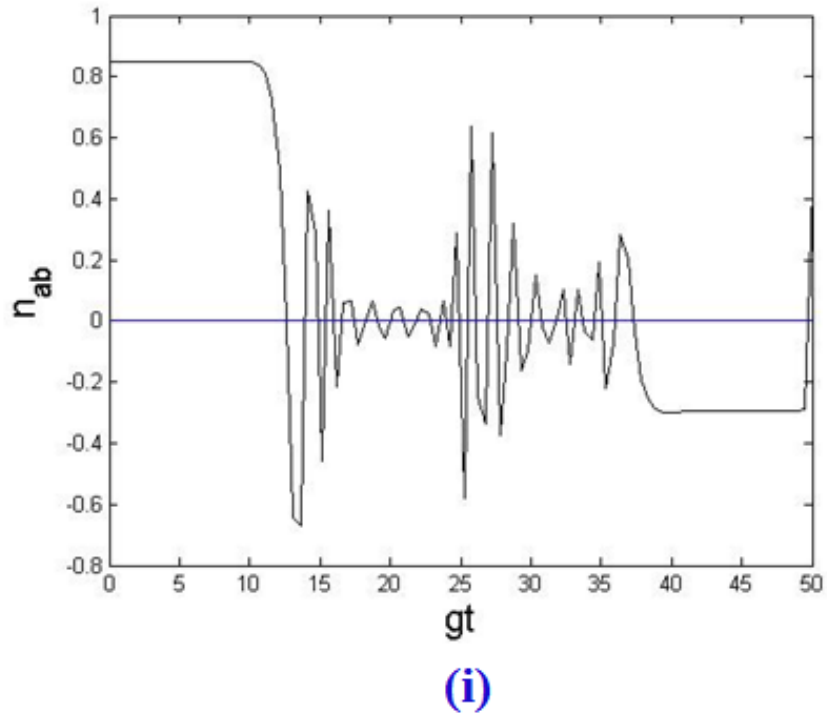


Figure 4.10: The Inversion plots of hat coupling function for initial Schrodinger cat state for (ii)intensity independent case and (iii)intensity dependent case

## CHAPTER 5

### ENTROPY OF A THREE-LEVEL ATOM WITH DAMPING

#### 5.1 Introduction

Past decades, atomic, molecular and optical physics has known spectacular developments in many fields, like nonlinear optics, laser cooling and trapping, quantum degenerate gases, and quantum information. Quantum entropies have played crucial role in quantum statistical mechanics and quantum information theory. The von Neumann entropy provides an important entropy functional used in thermodynamics (Breuer & Petruccione, 2002). Recently, scientists found its capability to develop quantum information science, where, it can describes a quantum state of an atom or photon to associate with the concept of information qubit. This will provide useful facts to determine how much quantum information is in a quantum system, measure quantum correlations and calculate the degree of quantum entanglement for the system. The negativity of the quantum entropy, called coherent information can only be explained quantum mechanically and it obeys a quantum data processing inequality. The powerful inequality of Araki–Lieb theorem (Araki & Lieb, 1970), reported that if the atom–field system is initially in a pure state, the field entropy and the atomic entropy are always the same.

In this chapter, we consider a  $\Lambda$ -type three-level atom interact with a single mode field and a laser coupling with the radiation reservoir. This system includes the dissipative mechanism due to interaction with reservoir. The effect of intensity dependent on the atom-field coupling and time dependent coupling function are also considered. Further investigation on the dynamics of atom(matter) and photon(light) and the connection between these two has been conducted. Nonclassical effects have been taken into account to gather more information and to get a better understanding of the system. The general overview of research methodology is as the following flow chart of Fig.5.1.

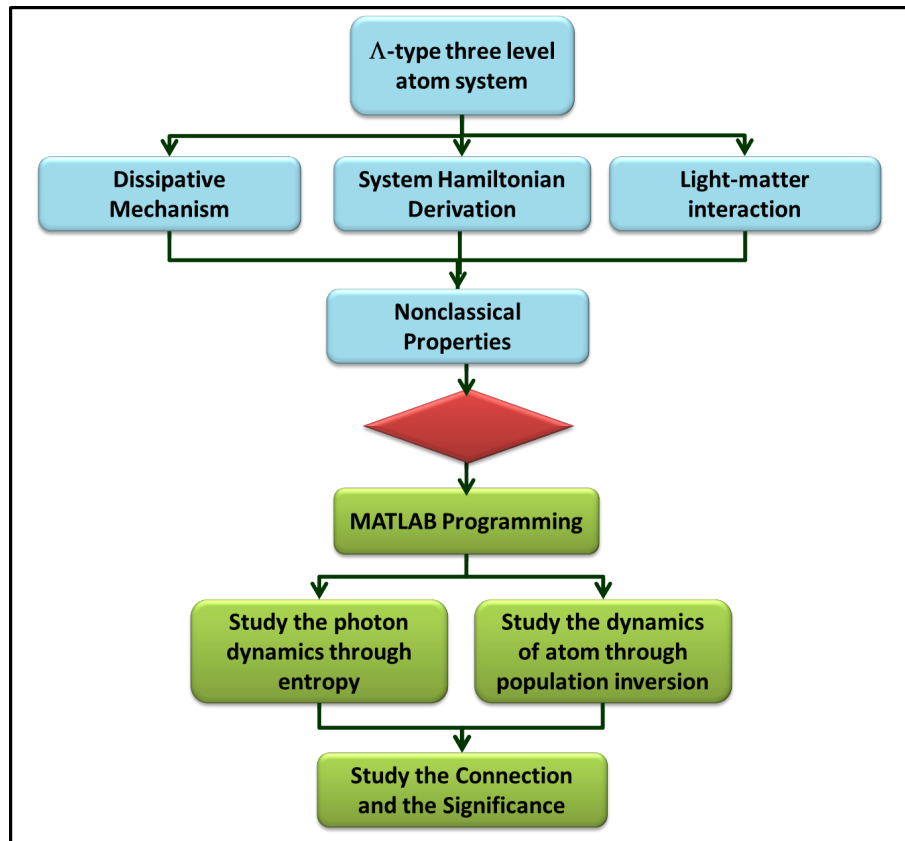


Figure 5.1: Overall research overview

## 5.2 Past Researches

Various research works have been extensively conducted to determine the entropy of a two-level system. The work of Buzek on quantum entanglement of a resonant interaction of two-level atom with a quantized field via two-photon transitions leads to a non-classical oscillations in the photon number distribution (Buzek & Hladky, 1993). They have studied the dynamics of the field by calculating the atomic inversion, entropy of the field, Q-function and photon number distribution.

The studies on two-level atom interaction carried out by Shore also ranges in non-classical properties and extended the investigation to three-level scheme to complete the findings (Shore & Knight, 1993). They present an overview of the theory of the Jaynes-Cumming Model and some of the many extensions and generalizations that have appeared in quantum problem. Scientists currently interested in three-level system, several research works are conducted by Abdel-Aty and Obada to understand the nonclassicality of light in three-level system. The entanglement of a general three-level system interacting with a correlated two-mode nonlinear coherent state has been presented with arbitrary forms of

nonlinearities of both the fields and the intensity-dependent atom-field coupling (Abdel-Aty & Obada, 2003). Their study showed that the entanglement can be significantly influenced by different kinds of nonlinearities. They have suggested that the nonlinear medium yields the superstructure of atomic Rabi oscillation and proposed a generation of Bell-type states of the system studied. Related study to clarify the role of quantum entanglement was carried out in a many-atom spontaneous emission process (Kim, Ooi, Ikram, & Lee, 2009). They have suggested that photons emitted spontaneously from a partially excited many-atom system exhibit strong directional correlations with the absorbed photons and also show strong directional correlations among the photons themselves.

Abdel-Aty reported that the evolution of the field quantum entropy and the entanglement of the atom field in a three-level atom has been investigated with an additional Kerr-like medium for one mode. The exact results are employed to perform a careful investigation of the temporal evolution of the entropy and analysed the effect of a Kerr-like medium on the entropy. It is shown that the addition of the Kerr medium has an important effect on the properties of the entropy and the entanglement (Abdel-Aty, 2000). He also extended his work to investigate the entanglement degree due to quasi-mutual entropy of an interaction between three-level atom and a single cavity field, with an initial field state were set to be coherent or a squeezed state (Abdel-Aty, 2004). He identified and numerically demonstrate the region of parameters where significantly large entanglement can be obtained and taking into account an arbitrary form of nonlinearity of the intensity-dependent coupling.

Another work related on entropy is a study by Zhao research team on determining the time evolution of the entropy of an initially coherent single-mode field interacting with a  $\Lambda$ -type degenerate quantum beat three-level atom in the strong field limit (Zhou & Zhu, 2005). They suggested that the initial atomic state and the detuning of the field play important roles in the evolution of the field entropy and the generation of a Schrodinger cat state. Faghihi et. al. have considered the nonlinear interaction between a  $\Lambda$ -type three-level atom and a single-mode field in a cavity containing a Kerr medium using the generalized JCM with intensity-dependent coupling (Faghihi & Tavassoly, 2012). They were investigating field entropy, quantum statistics and some nonclassical properties and compare their results with a three-level atom V-type studied by Huang group (Huang,

Tang, Kong, Fang, & Zhou, 2006). The studies also conducted on  $\Xi$ -type system which reported that the evolutions of the entropies of the atomic and field sub-systems exhibit multiperiodicity, as observed via the power spectrum of the entropy after an entanglement swapping with two cavity fields (Qiang, Cardoso, & Zhang, 2010).

In this work, a  $\Lambda$ -type three-level atom interacting with a single mode field driven by laser placed inside a multimode reservoir is studied. The interactions taking into account are the atom-field, the atom-laser, the atom-reservoir, and the cavity-reservoir interactions. The interaction with reservoir resulting the occurrence of dissipative mechanism in the system.

### 5.3 $\Lambda$ -type Three-Level Atom

Our system of interest is a single three-level  $\Lambda$ -type atom interacting with a single mode cavity field and driven by laser coupled to a multimode reservoir(5.2).

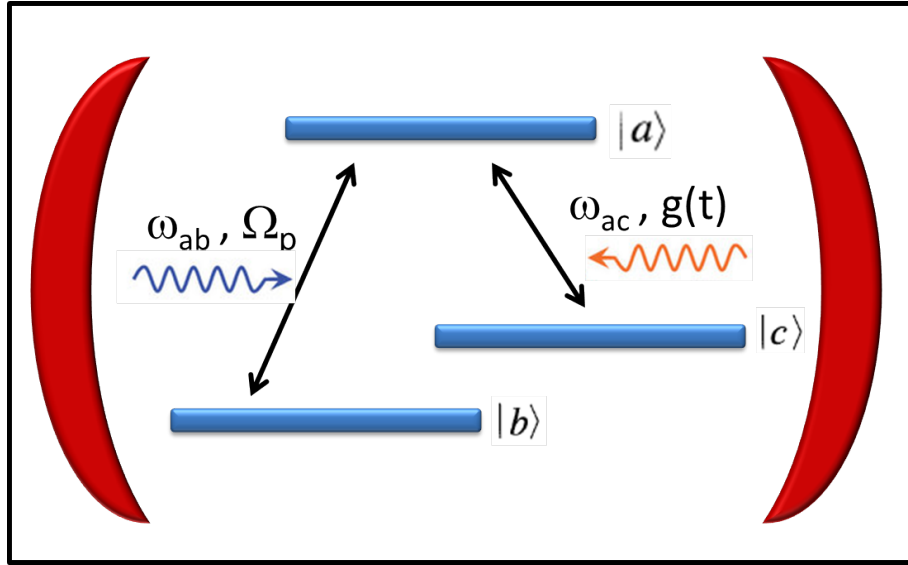


Figure 5.2: A  $\Lambda$ -type three-level atom interact with a single mode field and driven by a laser

The interactions taken into account are the atom-laser-cavity, the atom-reservoir, and the cavity-reservoir. If we denote the atomic lowering and raising operator by  $\hat{\sigma}_{ij} = |i\rangle \langle j|$  where  $i, j = a, b, c$  (referred to as atomic levels), free Hamiltonian consist of the atom( $\hat{H}_A$ ), cavity field( $\hat{H}_F$ ) and reservoir ( $\hat{H}_R$ ). The interaction Hamiltonian included are the atom-laser( $\hat{H}_{AL}$ ), the atom-cavity( $\hat{H}_{AF}$ ), the atom-reservoir( $\hat{H}_{AR}$ ) and the field-reservoir( $\hat{H}_{FR}$ ). The total Hamiltonian is given by:

$$\hat{H}_T = \hat{H}_A + \hat{H}_F + \hat{H}_R + \hat{H}_{AF} + \hat{H}_{AR} + \hat{H}_{FR} \quad (5.1)$$

where

$$\begin{aligned} \hat{H}_A &= \hbar\omega_a\hat{\sigma}_{aa} + \hbar\omega_b\hat{\sigma}_{bb} + \hbar\omega_c\hat{\sigma}_{cc} \\ \hat{H}_F &= \hbar\nu_F\hat{a}^\dagger\hat{a} \\ \hat{H}_R &= \hbar\sum_k \nu_R\hat{b}_k^\dagger\hat{b}_k \\ \hat{H}_{AL} &= \hbar\Omega_p\left(\hat{\sigma}_{ab}e^{-i\Delta_pt} + \hat{\sigma}_{ba}e^{i\Delta_pt}\right) \\ \hat{H}_{AF} &= \hbar g(t)\left(\hat{\sigma}_{ac}\hat{a}e^{-i\Delta_ct} + \hat{a}^\dagger\hat{\sigma}_{ca}e^{i\Delta_ct}\right) \\ \hat{H}_{AR} &= \hbar\sum_{\mathbf{k}}\left(g_{1,\mathbf{k}}^{(AR)}\left(\hat{\sigma}_{ac}\hat{b}_{\mathbf{k}} + \hat{b}_{\mathbf{k}}^\dagger\hat{\sigma}_{ca}\right) + g_{2,\mathbf{k}}^{(AR)}\left(\hat{\sigma}_{ab}\hat{b}_{\mathbf{k}} + \hat{b}_{\mathbf{k}}^\dagger\hat{\sigma}_{ba}\right)\right) \\ \hat{H}_{FR} &= \hbar\sum_{\mathbf{k}}g_{1,\mathbf{k}}^{(FR)}\left(\hat{a}^\dagger\hat{b}_{\mathbf{k}} + \hat{b}_{\mathbf{k}}^\dagger\hat{a}\right) \end{aligned}$$

with

$$\Omega_p = \mu_p E_p / 2\hbar$$

$\omega_i$  ( $i = a, b, c$ ) is level frequency,  $\nu_F$  denoted as field frequency, while  $\nu_R$  is the reservoir frequency.  $\Omega_p$  is the probe laser Rabi frequency coupled to level  $|a\rangle|b\rangle$ ,  $g(t)$  is the coupling function between cavity and level coupled to level  $|a\rangle|c\rangle$ , while  $\Delta_c = \omega_{ac} - \nu_f$  and  $\Delta_p = \omega_{ab} - \nu_p$  with  $\nu_c$  is cavity frequency and  $\nu_p$  is probe laser frequency.  $\hat{a}^\dagger$  ( $\hat{a}$ ) and  $\hat{b}_{\mathbf{k}}^\dagger$  ( $\hat{b}_{\mathbf{k}}$ ) are creation(annihilation) operator of field and reservoir respectively while  $g_{1,\mathbf{k}}^{(AR)}\left(g_{2,\mathbf{k}}^{(AR)}\right)$  and  $g_{1,\mathbf{k}}^{(FR)}$  are coupling between atom-reservoir and field-reservoir respectively.

The master equation of the whole system is given by:

$$\frac{d\hat{\rho}_T(t)}{dt} = \frac{1}{i\hbar} [\hat{V}_{AL} + \hat{V}_{AF}, \hat{\rho}(t)] + L\hat{\rho}_A + L\hat{\rho}_F \quad (5.2)$$

where

$$\begin{aligned} \hat{V}_{AL} &= \hbar\Omega_p\left(\hat{\sigma}_{ab}e^{i\Delta_pt} + \hat{\sigma}_{ba}e^{-i\Delta_pt}\right) \\ \hat{V}_{AF} &= \hbar g(t)\left(\hat{\sigma}_{ac}\hat{a}e^{i\Delta_ct} + \hat{a}^\dagger\hat{\sigma}_{ca}e^{-i\Delta_ct}\right) \\ L\hat{\rho}_F &= \gamma_F\left(2\hat{a}\hat{\rho}\hat{a}^\dagger - \hat{a}^\dagger\hat{a}\hat{\rho} - \hat{\rho}\hat{a}^\dagger\hat{a}\right) \end{aligned}$$

$$\begin{aligned}
L\hat{\rho}_A = & \Gamma_{ac}(2\hat{\sigma}_{ca}\hat{\rho}\hat{\sigma}_{ac} - \hat{\sigma}_{ac}\hat{\sigma}_{ca}\hat{\rho} - \hat{\rho}\hat{\sigma}_{ac}\hat{\sigma}_{ca}) \\
& + \Gamma_{ab}(2\hat{\sigma}_{ba}\hat{\rho}\hat{\sigma}_{ab} - \hat{\sigma}_{ab}\hat{\sigma}_{ba}\hat{\rho} - \hat{\rho}\hat{\sigma}_{ab}\hat{\sigma}_{ba})
\end{aligned}$$

with  $\Gamma_{ac}(\Gamma_{ab})$  is damping rate of individual atom transition between  $|a\rangle$  and  $|c\rangle(|a\rangle$  and  $|b\rangle)$  while  $\gamma_F$  is damping rate for field

The density matrix elements read

$$\dot{\rho}_{ij} = \sum_{i,j=a,b,c} \langle i | \dot{\rho}(t) | j \rangle \quad (5.3)$$

By projecting  $\langle i |$  and  $| j \rangle$  on the total density matrix derived, for  $\langle a | \dot{\rho}_T | a \rangle$  we obtain

$$\begin{aligned}
\langle a | \dot{\rho}_T | a \rangle = & -i\Omega_p \left( \langle a | a \rangle \langle b | e^{i\Delta_p t} \hat{\rho} | a \rangle + \langle a | b \rangle \langle a | e^{-i\Delta_p t} \hat{\rho} | a \rangle \right) \\
& + i\Omega_p \left( \langle a | \hat{\rho} | a \rangle \langle b | a \rangle e^{i\Delta_p t} + \langle a | \hat{\rho} | b \rangle \langle a | a \rangle e^{-i\Delta_p t} \right) \\
& - ig(t) \left( \langle a | a \rangle \langle c | \hat{a} \hat{\rho} | a \rangle e^{i\Delta_c t} + \langle a | \hat{a}^\dagger | c \rangle \langle a | \hat{\rho} | a \rangle e^{-i\Delta_c t} \right) \\
& + ig(t) \left( \langle a | \hat{\rho} | a \rangle \langle c | \hat{a} | a \rangle e^{i\Delta_c t} + \langle a | \hat{\rho} \hat{a}^\dagger | c \rangle \langle a | a \rangle e^{-i\Delta_c t} \right) \\
& + \gamma_F \langle a | \left( 2\hat{a} \hat{\rho} \hat{a}^\dagger - \hat{a}^\dagger \hat{a} \hat{\rho} - \hat{\rho} \hat{a}^\dagger \hat{a} \right) | a \rangle \\
& + \Gamma_{ac} (2 \langle a | c \rangle \langle a | \hat{\rho} | a \rangle \langle c | a \rangle - \langle a | a \rangle \langle c | c \rangle \langle a | \hat{\rho} | a \rangle - \langle a | \hat{\rho} | a \rangle \langle c | c \rangle \langle a | a \rangle) \\
& + \Gamma_{ab} (2 \langle a | b \rangle \langle a | \hat{\rho} | a \rangle \langle b | a \rangle - \langle a | a \rangle \langle b | b \rangle \langle a | \hat{\rho} | a \rangle - \langle a | \hat{\rho} | a \rangle \langle b | b \rangle \langle a | a \rangle) \\
= & -i\Omega_p \langle b | e^{i\Delta_p t} \hat{\rho} | a \rangle \langle n \rangle + i\Omega_p \langle m | \langle a | \hat{\rho} | b \rangle \langle n \rangle e^{-i\Delta_p t} \\
& - ig(t) \langle c | \hat{a} \hat{\rho} | a \rangle e^{i\Delta_c t} + ig(t) \langle a | \hat{\rho} \hat{a}^\dagger | c \rangle e^{-i\Delta_c t} + \gamma_F L(\hat{\rho}_{aa}) \\
& + \Gamma_{ac} (-\langle a | \hat{\rho} | a \rangle - \langle a | \hat{\rho} | a \rangle) + \Gamma_{ab} (-\langle a | \hat{\rho} | a \rangle - \langle a | \hat{\rho} | a \rangle) \\
= & -i\Omega_p \rho_{ba} e^{i\Delta_p t} + i\Omega_p \rho_{ab} e^{-i\Delta_p t} - ig(t) \hat{a} \rho_{ca} e^{i\Delta_c t} \\
& + ig(t) \rho_{ac} \hat{a}^\dagger e^{-i\Delta_c t} + \gamma_F L(\rho_{aa}) - 2(\Gamma_{ac} + \Gamma_{ab}) \rho_{aa}
\end{aligned} \quad (5.4)$$

the same method is applied to the rest of elements of density matrix and resulting at

$$\dot{\rho}_{aa} = -i\Omega_p \rho_{ba} e^{i\Delta_p t} + i\Omega_p \rho_{ab} e^{-i\Delta_p t} - ig(t) \hat{a} \rho_{ca} e^{i\Delta_c t} \quad (5.5)$$

$$+ ig(t) \rho_{ac} \hat{a}^\dagger e^{-i\Delta_c t} + \gamma_F L(\rho_{aa}) - 2(\Gamma_{ac} + \Gamma_{ab}) \rho_{aa} \quad (5.6)$$

$$\dot{\rho}_{bb} = -i\Omega_p \rho_{ab} e^{-i\Delta_p t} + i\Omega_p \rho_{ba} e^{i\Delta_p t} + \gamma_F L(\rho_{bb}) + 2\Gamma_{ab} \rho_{aa}$$

$$\dot{\rho}_{cc} = -ig(t) \hat{a}^\dagger \rho_{ac} e^{-i\Delta_c t} + ig(t) \rho_{ca} \hat{a} e^{i\Delta_c t} + \gamma_F L(\rho_{cc}) + 2\Gamma_{ac} \rho_{aa}$$

$$\dot{\rho}_{ca} = i\Omega_p \rho_{cb} e^{-i\Delta_p t} + ig(t) \rho_{cc} \hat{a}^\dagger e^{-i\Delta_c t} - ig(t) \hat{a}^\dagger \rho_{aa} e^{-i\Delta_c t} + \gamma_F L(\rho_{ca}) - (\Gamma_{ac} + \Gamma_{ab}) \rho_{ca}$$

$$\begin{aligned}
\dot{\rho}_{ac} &= -i\Omega_p \rho_{bc} e^{i\Delta_p t} - ig(t) \hat{a} \rho_{cc} e^{i\Delta_c t} + ig(t) \rho_{aa} \hat{a} e^{i\Delta_c t} + \gamma_F L(\rho_{ac}) - (\Gamma_{ac} + \Gamma_{ab}) \rho_{ac} \\
\dot{\rho}_{ba} &= -i\Omega_p \rho_{aa} e^{-i\Delta_p t} + i\Omega_p \rho_{bb} e^{-i\Delta_p t} + ig(t) \rho_{bc} \hat{a}^\dagger e^{-i\Delta_c t} + \gamma_F L(\rho_{ba}) - (\Gamma_{ac} + \Gamma_{ab}) \rho_{ba} \\
\dot{\rho}_{ab} &= -i\Omega_p \rho_{bb} e^{i\Delta_p t} + i\Omega_p \rho_{aa} e^{i\Delta_p t} - ig(t) \hat{a} \rho_{cb} e^{i\Delta_c t} + \gamma_F L(\rho_{ab}) - (\Gamma_{ac} + \Gamma_{ab}) \rho_{ab} \\
\dot{\rho}_{bc} &= -i\Omega_p \rho_{ac} e^{-i\Delta_p t} + ig(t) \rho_{ba} \hat{a} e^{i\Delta_c t} + \gamma_F L(\rho_{bc}) \\
\dot{\rho}_{cb} &= i\Omega_p \rho_{ca} e^{i\Delta_p t} - ig(t) \hat{a}^\dagger \rho_{ab} e^{-i\Delta_c t} + \gamma_F L(\rho_{cb})
\end{aligned}$$

where for  $i, j = a, b, c$  and

$$L(\rho_{ij}) = \gamma_F \left( 2\hat{a} \rho_{ij} \hat{a}^\dagger - \hat{a}^\dagger \hat{a} \rho_{ij} - \rho_{ij} \hat{a}^\dagger \hat{a} \right) \quad (5.7)$$

In order to solve the matrix elements (see Appendix F), the equations of motion for a slowly varying amplitude are introduced. Then the density matrix equation is used with  $\hat{R} = \hat{a} \sqrt{\hat{a}^\dagger \hat{a}}$  and  $\hat{R}^\dagger = \sqrt{\hat{a}^\dagger \hat{a}} \hat{a}^\dagger$  to include the intensity dependent on the system. From the previous chapter, the intensity dependent coupling is known has a great relevance in understanding the interaction since the coupling is proportional to the amplitude of the field. So the matrix elements become

$$\begin{aligned}
\frac{d}{dt} \rho_{aa} &= i\Omega_p [\tilde{\rho}_{ab} - \tilde{\rho}_{ba}] + ig(t) [\tilde{\rho}_{ac} \hat{R}^\dagger - \hat{R} \tilde{\rho}_{ca}] \\
&\quad + \gamma_F L(\rho_{aa}) - 2(\Gamma_{ac} + \Gamma_{ab}) \rho_{aa} \\
\frac{d}{dt} \rho_{bb} &= i\Omega_p [\tilde{\rho}_{ba} - \tilde{\rho}_{ab}] + \gamma_F L(\rho_{bb}) + 2\Gamma_{ab} \rho_{aa} \\
\frac{d}{dt} \rho_{cc} &= ig(t) [\tilde{\rho}_{ca} \hat{R} - \hat{R}^\dagger \tilde{\rho}_{ac}] + \gamma_F L(\rho_{cc}) + 2\Gamma_{ac} \rho_{aa} \\
\frac{d}{dt} \tilde{\rho}_{ca} &= i\Delta_c \tilde{\rho}_{ca} + i\Omega_p \tilde{\rho}_{cb} + ig(t) [\rho_{cc} \hat{R}^\dagger - \hat{R}^\dagger \rho_{aa}] \\
&\quad + \gamma_F L(\tilde{\rho}_{ca}) - (\Gamma_{ac} + \Gamma_{ab}) \tilde{\rho}_{ca} \\
\frac{d}{dt} \tilde{\rho}_{ba} &= i\Delta_p \rho_{ba} + i\Omega_p [\rho_{bb} - \rho_{aa}] + ig(t) \tilde{\rho}_{bc} \hat{R}^\dagger \\
&\quad + \gamma_F L(\tilde{\rho}_{ba}) - (\Gamma_{ac} + \Gamma_{ab}) \tilde{\rho}_{ba} \\
\frac{d}{dt} \tilde{\rho}_{bc} &= -i(\Delta_c - \Delta_p) \tilde{\rho}_{bc} - i\Omega_p \tilde{\rho}_{ac} \\
&\quad + ig(t) \tilde{\rho}_{ba} \hat{R} + \gamma_F L(\tilde{\rho}_{bc})
\end{aligned} \quad (5.8)$$

with

$$L\tilde{\rho}_{ij} = \left( 2\hat{R} \rho_{ij} \hat{R}^\dagger - \hat{R}^\dagger \hat{R} \rho_{ij} - \rho_{ij} \hat{R}^\dagger \hat{R} \right) \quad (5.9)$$



Taking the matrix elements we have the diagonal element for photon number as following

$$\begin{aligned} \frac{d}{dt}\rho_{aa}(n,n) = & i\Omega_p\tilde{\rho}_{ab}(n,n) - i\Omega_p\tilde{\rho}_{ba}(n,n) + ig(t)(n+1)\tilde{\rho}_{ac}(n,n+1) \quad (5.10) \\ & - ig(t)(n+1)\tilde{\rho}_{ca}(n+1,n) + 2\gamma_F(n+1)^2\rho_{aa}(n+1,n+1) \\ & - (2\gamma_F n^2 + 2\Gamma_{ac} + 2\Gamma_{ab})\rho_{aa}(n,n) \end{aligned}$$

$$\begin{aligned} \frac{d}{dt}\rho_{bb}(n,n) = & i\Omega_p\tilde{\rho}_{ba}(n,n) - i\Omega_p\tilde{\rho}_{ab}(n,n) + 2\gamma_F(n+1)^2\rho_{bb}(n+1,n+1) \quad (5.11) \\ & - 2\gamma_F n^2\rho_{bb}(n,n) + 2\Gamma_{ab}\rho_{aa}(n,n) \end{aligned}$$

$$\begin{aligned} \frac{d}{dt}\rho_{cc}(n,n) = & ig(t)(n)\tilde{\rho}_{ca}(n,n-1) - ig(t)(n)\tilde{\rho}_{ac}(n-1,n) \quad (5.12) \\ & + 2\gamma_F(n+1)^2\rho_{cc}(n+1,n+1) - 2\gamma_F n^2\rho_{cc}(n,n) \\ & + 2\Gamma_{ac}\rho_{aa}(n,n) \end{aligned}$$

$$\begin{aligned} \frac{d}{dt}\tilde{\rho}_{ca}(n+1,n) = & \left(i\Delta_c - (n+1)^2 - (n)^2\right)\gamma_F\tilde{\rho}_{ca}(n+1,n) \quad (5.13) \\ & + i\Omega_p\tilde{\rho}_{cb}(n+1,n) + ig(t)(n+1)\rho_{cc}(n+1,n+1) \\ & - ig(t)(n+1)\rho_{aa}(n,n) - (\Gamma_{ac} + \Gamma_{ab})\tilde{\rho}_{ca}(n+1,n) \\ & + 2(n+2)(n+1)\gamma_F\tilde{\rho}_{ca}(n+2,n+1) \end{aligned}$$

$$\begin{aligned} \frac{d}{dt}\tilde{\rho}_{ba}(n,n) = & [i\Delta_p - 2\gamma_F n^2 - (\Gamma_{ac} + \Gamma_{ab})]\tilde{\rho}_{ba}(n,n) \quad (5.14) \\ & + i\Omega_p\rho_{bb}(n,n) - i\Omega_p\rho_{aa}(n,n) \\ & + ig(t)(n+1)\tilde{\rho}_{bc}(n,n+1) + 2\gamma_F(n+1)^2\hat{\rho}_{ba}(n+1,n+1) \end{aligned}$$

$$\begin{aligned} \frac{d}{dt}\tilde{\rho}_{bc}(n,n+1) = & - \left[i(\Delta_c - \Delta_p) + \gamma_F(n)^2 + \gamma_F(n+1)^2\right]\tilde{\rho}_{bc}(n,n+1) \quad (5.15) \\ & - i\Omega_p\tilde{\rho}_{ac}(n,n+1) + ig(t)(n+1)\tilde{\rho}_{ba}(n,n) \\ & + 2\gamma_F(n+1)(n+2)\tilde{\rho}_{bc}(n+1,n+2) \end{aligned}$$

So far  $\rho_{xx}(n,n)$  and the coherences have already been computed previously. In order to compute the Wigner function, the matrix elements diagonal in atomic states by off diagonal in photon number such as  $\rho_{xx}(n,m)$  where  $m \neq n$  were needed to be solved.

That means the matrix elements were found for the following

$$\begin{aligned}
\frac{d}{dt}\rho_{aa}(n,m) = & i\Omega_p\tilde{\rho}_{ab}(n,m) - i\Omega_p\tilde{\rho}_{ba}(n,m) \\
& +ig(t)(m+1)\tilde{\rho}_{ac}(n,m+1) - ig(t)(n+1)\tilde{\rho}_{ca}(n+1,m) \\
& +2\gamma_F(n+1)(m+1)\rho_{aa}(n+1,m+1) \\
& - ((n^2+m^2)\gamma_F + 2(\Gamma_{ac} + \Gamma_{ab}))\rho_{aa}(n,m)
\end{aligned} \tag{5.16}$$

$$\begin{aligned}
\frac{d}{dt}\rho_{bb}(n,m) = & i\Omega_p\tilde{\rho}_{ba}(n,m) - i\Omega_p\tilde{\rho}_{ab}(n,m) + 2\Gamma_{ab}\rho_{aa}(n,m) \\
& +2\gamma_F(n+1)(m+1)\rho_{bb}(n+1,m+1) \\
& - (n^2+m^2)\gamma_F\rho_{bb}(n,m)
\end{aligned} \tag{5.17}$$

$$\begin{aligned}
\frac{d}{dt}\rho_{cc}(n,m) = & ig(t)(m)\tilde{\rho}_{ca}(n,m-1) - ig(t)(n)\tilde{\rho}_{ac}(n-1,m) \\
& +2\Gamma_{ac}\rho_{aa}(n,m) - (n^2+m^2)\gamma_F\rho_{cc}(n,m) \\
& +2(n+1)\gamma_F(m+1)\rho_{cc}(n+1,m+1)
\end{aligned} \tag{5.18}$$

$$\begin{aligned}
\frac{d}{dt}\tilde{\rho}_{ca}(n,m) = & (i\Delta_c - \Gamma_{ac} - \Gamma_{ab})\tilde{\rho}_{ca}(n,m) - (n^2+m^2)\gamma_F\hat{\rho}_{ca}(n,m) \\
& +i\Omega_p\tilde{\rho}_{cb} + ig(t)(m+1)\rho_{cc}(n,m+1) \\
& -ig(t)(n)\rho_{aa}(n-1,m) \\
& +2(n+1)\gamma_F(m+1)\rho_{ca}(n+1,m+1)
\end{aligned} \tag{5.19}$$

$$\begin{aligned}
\frac{d}{dt}\tilde{\rho}_{ba}(n,m) = & (i\Delta_p - \Gamma_{ac} - \Gamma_{ab})\tilde{\rho}_{ba}(n,m) + i\Omega_p\rho_{bb}(n,m) \\
& -i\Omega_p\rho_{aa}(n,m) + ig(t)\tilde{\rho}_{bc}(n,m+1)(m+1) \\
& +2(n+1)\gamma_F(m+1)\rho_{ba}(n+1,m+1) \\
& - (n^2+m^2)\gamma_F\rho_{ba}(n,m)
\end{aligned} \tag{5.20}$$

$$\begin{aligned}
\frac{d}{dt}\tilde{\rho}_{bc}(n,m) = & - [i(\Delta_c - \Delta_p) + (n^2+m^2)\gamma_F]\tilde{\rho}_{bc}(n,m) \\
& -i\Omega_p\tilde{\rho}_{ac}(n,m) + ig(t)(m)\tilde{\rho}_{ba}(n,m-1) \\
& +2(n+1)(m+1)\gamma_F\rho_{bc}(n+1,m+1)
\end{aligned} \tag{5.21}$$

The derived elements will be used to plot the inversion and the entropy of the system.

## 5.4 Inversion and Entropy

Atomic inversion for three-level atom lambda type can be obtained by

$$n_{abc}(t) = \rho_{aa}(n, m) - \rho_{bb}(n, m) - \rho_{cc}(n, m) \quad (5.22)$$

which is used to determine the population of atomic states to show the probability of finding the system in excited state. As discussed in chapter 3, entropy  $S$  is a measure of the uncertainty of a quantum state. Using the Von-Neumann entropy equation,

$$S(\rho) = -Tr(\hat{\rho} \ln \hat{\rho}) \quad (5.23)$$

the partial entropy can be calculated for field alone and for atom entropy given by

$$S_A = -Tr_F(\hat{\rho}_F \ln \hat{\rho}_F) \quad (5.24)$$

$$S_F = -Tr_A(\hat{\rho}_A \ln \hat{\rho}_A) \quad (5.25)$$

Then  $S(\rho)$  expresses our uncertainty, or lack of knowledge about the realization of a particular state in the mixture (Breuer & Petruccione, 2002) and it offers a quantitative measure of the disorder of a system and of the purity of a quantum state. The time evolution of the atomic (field) entropy carries information about the degree of atom-field entanglement (Hessian et al., 2009). For diagonal number state,  $m = n$ , the inversion and entropy plot are illustrated in figures 5.3 until 5.15 below and will be discussed in detailed.

The inversion plot for the interaction between a three-level atom with a single mode field driven by a laser without considering the damping mechanism is shown in Fig.5.3 with the usual collapse and revival oscillations.

If we include the damping term into the system, the inversion plot obtained is as illustrated in Fig.5.4 It can be seen that, when damping is included, the revival is lost at large times and the oscillations cease after two cycles. The atomic entropy is zero in the absence of damping while the field damping shows rapid oscillations. The atomic entropy increases rapidly and after two oscillations, dies away. The field entropy rises and after two oscillations, rises and saturates at a constant value.

When damping is reduced, let say to  $\Gamma_{ab} = \Gamma_{ac} = 10^6 s^{-1}$  it can be found that the times for the inversion to reduce to  $-1$  as seen in Fig.5.5 and the entropy to reduce to

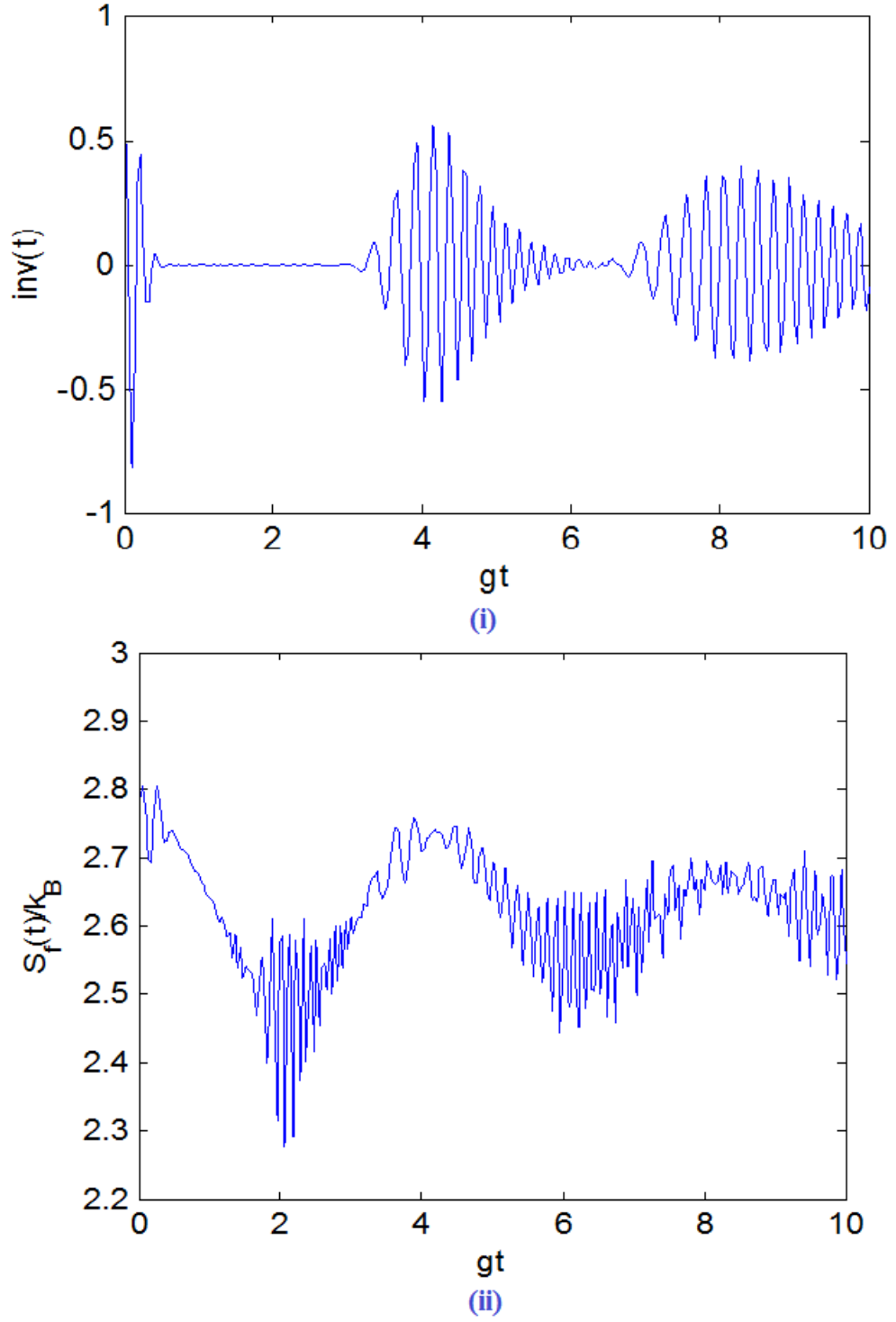


Figure 5.3: (i) Inversion and (ii) field entropy plot for  $g = 2 \times 10^6 s^{-1}$  with  $\alpha_0 = \sqrt{15}$ , and no damping mechanism considered for time duration  $gt = 0$  until  $gt = 15$

zero had become longer. More oscillations can be seen in the plot. Interestingly the introduction of cavity damping reduces the field entropy nearly to zero.

When the laser drives one of the transitions ( $|a\rangle - |c\rangle$ ), oscillations can be seen on the inversion as shown in Fig.5.7 and Fig.5.8.

Now if we consider a smaller  $\alpha_o = \sqrt{3}$ , we find that there are less rapid oscillations but the collapse time is shorter(Fig.5.9). When atomic damping mechanism is considered by having  $\Gamma_{ab} = \Gamma_{ac} = 10^7 s^{-1}$ , we got plots as in Fig.5.10 where the oscillations in field entropy plot is reduced and the atom entropy is nonzero. The results for inversion, atom entropy and field entropy has been plotted for smaller  $\alpha_o$  and we find that it is identical to the case of  $\alpha_o = \sqrt{15}$ , which means that the initial condition of the field has little effect when the driving field is significant. This can be shown in Fig.5.11 and Fig.5.12. When we include the driving field to the system of  $\alpha_o = \sqrt{3}$ , the results obtained are as illustrate in Fig.5.13 Fig.5.14 shows that the inversion oscillates when the population is transferred to excited state during the coupling pulse and then being transferred to the ground state  $|b\rangle$  by the pump pulse. Here, in Fig.5.15 the inversion increases slowly following the profile of the (subsequent) coupling pulse. The peak inversion almost corresponds to the peak atomic entropy and field entropy. Actually, they correspond to the maximum overlap between the two pulses.

We have extended the density matrix formalism to three-level system with intensity dependent coupling. The master equations have been solved numerically for density matrix elements diagonal in number states. The diagonal matrix elements are extracted by a numerical code which we have developed to compute the dynamics of inversion, atomic entropy and the field entropy, The results provide insights on how the atomic damping, cavity damping and the laser pump affect these quantities in different regimes of the ratios  $\gamma_F/g$ ,  $\Gamma/g$  and  $\Omega_p/g$ . Our formalism and numerical algorithm allow the coupling function to take arbitrary time dependent coupling function  $g(t)$  and pump field  $\Omega(t)$ . We have plotted the results for Gaussian pulses, that simulate the well-known transition of Raman adiabatic passage(Fig.5.14 and Fig.5.15). It is much more challenging to extend the work to compute the density matrix off-diagonal in number state as the computation is much more demanding. This may be explored in future work. It would allow the Wigner function to be computed to study how the Wigner function and nonclassical light can be controlled by an arbitrary laser pulse.

## 5.5 Conclusion

We have reviewed the concepts of entropy and inversion of a system of three-level  $\Lambda$ -type atom interact with a single mode field driven by a laser and interact with a reservoir which causes the atomic damping as well as field damping. The entropy can connected to the entanglement and described the behaviour of the system. We have presented the time evolution density matrix element for the system and the plots of inversion for different value of coupling constant along with the plot of entropy.

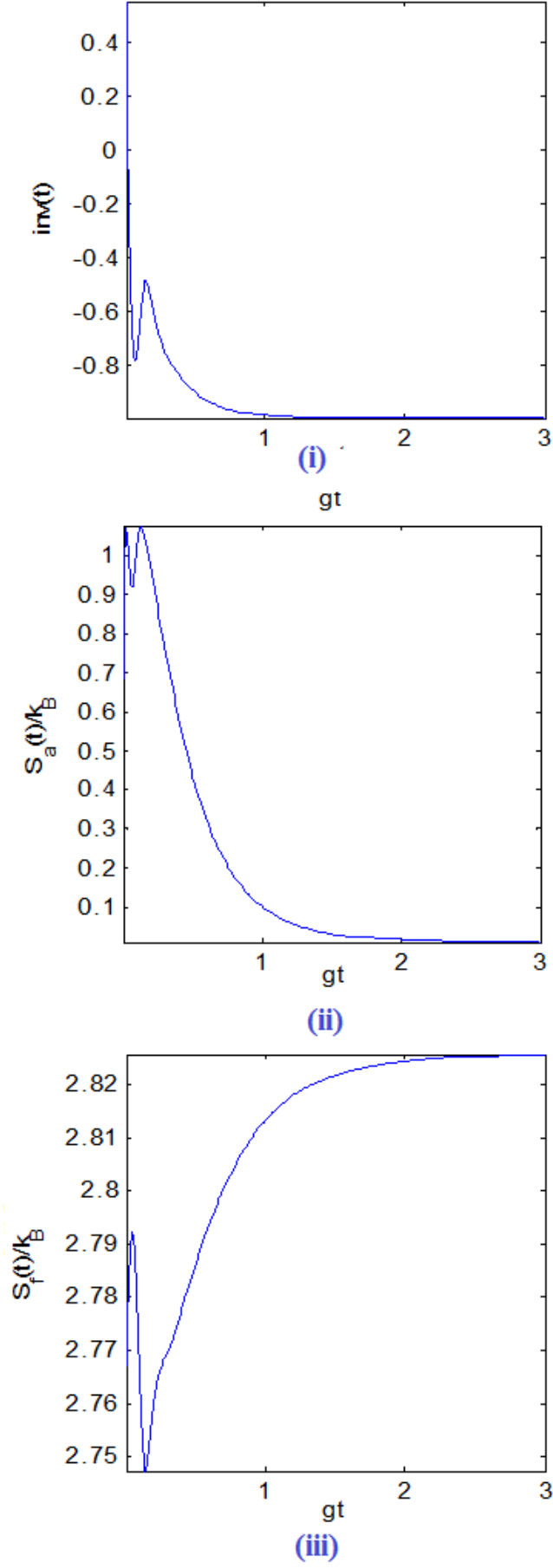


Figure 5.4: (i) Inversion, (ii) atom entropy and (iii) field entropy plot for  $g = 2 \times 10^6 s^{-1}$  with  $\alpha_0 = \sqrt{15}$ ,  $\Gamma_{ab} = \Gamma_{ac} = 10^7 s^{-1}$  for time duration  $gt = 0$  until  $gt = 3$

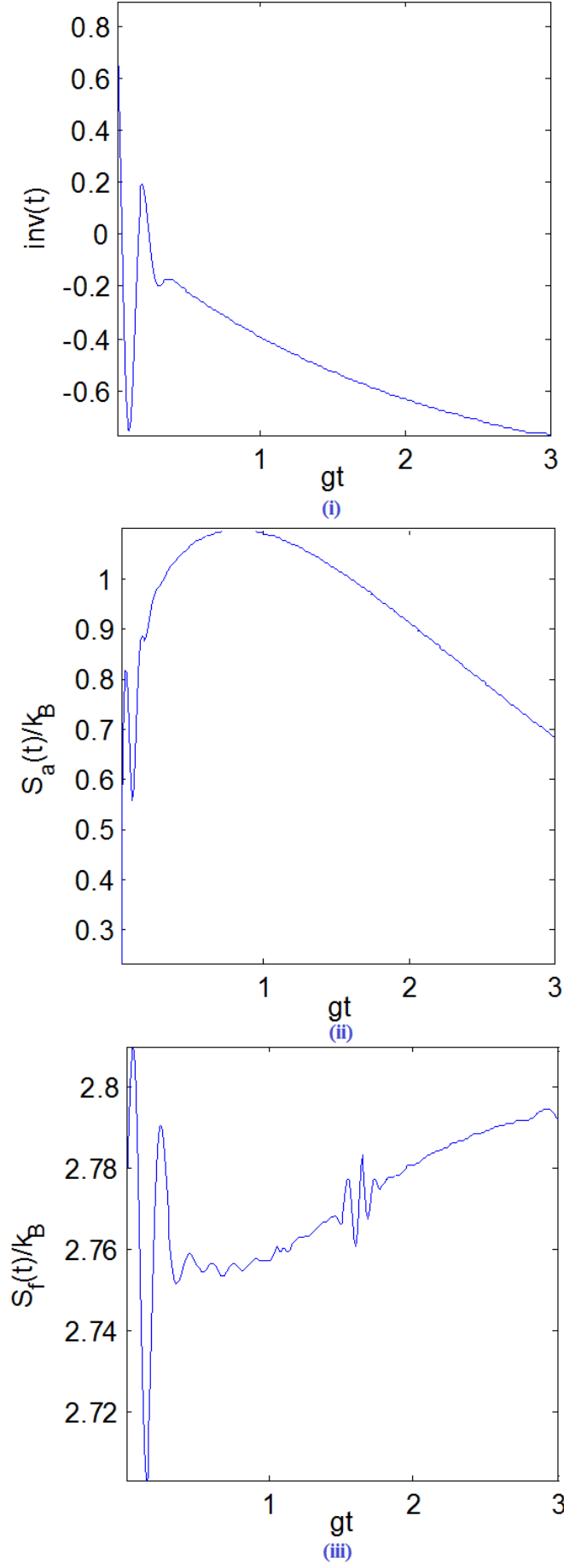


Figure 5.5: (i) Inversion, (ii) atom entropy and (iii) field entropy plots for  $g = 2 \times 10^6 s^{-1}$  with  $\alpha_0 = \sqrt{15}$ , and  $\Gamma_{ab} = \Gamma_{ac} = 10^6 s^{-1}$  within time duration  $gt = 0$  until  $gt = 3$



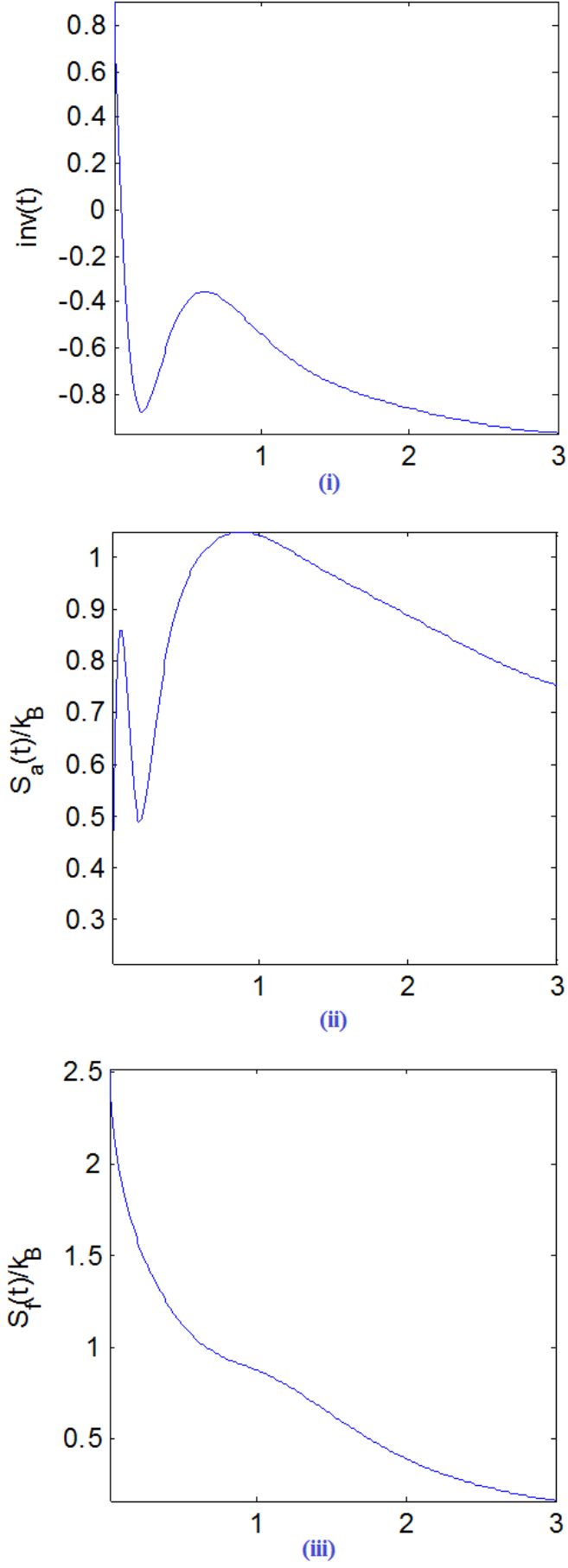


Figure 5.6: (i) Inversion, (ii) atom entropy and (iii) field entropy plots for  $g = 2 \times 10^6 s^{-1}$  with  $\alpha_0 = \sqrt{15}$ ,  $\Gamma_{ab} = \Gamma_{ac} = 10^6 s^{-1}$  and  $\gamma_F = 10^6 s^{-1}$  within time duration  $gt = 0$  until  $gt = 3$

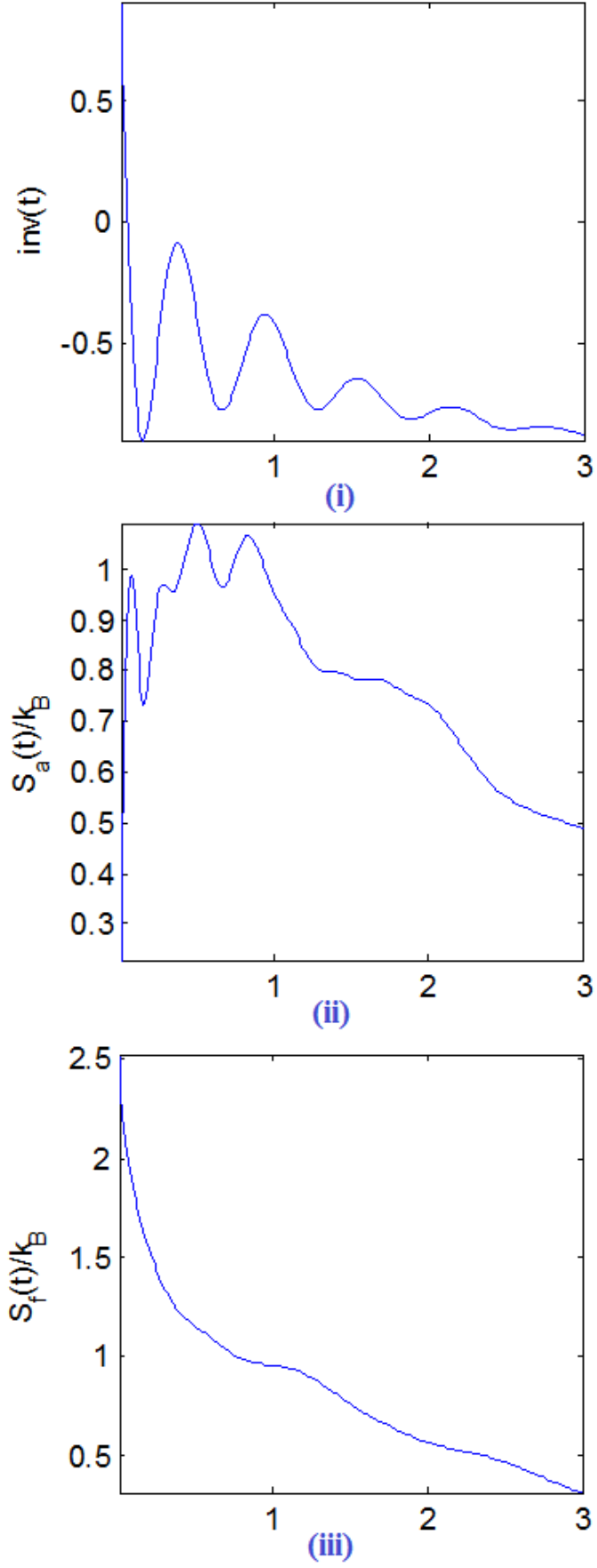


Figure 5.7: (i) Inversion, (ii) atom entropy and (iii) field entropy plots for  $g = 2 \times 10^6 s^{-1}$  with  $\alpha_0 = \sqrt{15}$ ,  $\Gamma_{ab} = \Gamma_{ac} = 10^6 s^{-1}$ ,  $\gamma_F = 10^6 s^{-1}$  and  $\Omega_p = 10^7 s^{-1}$  within time duration  $gt = 0$  until  $gt = 3$

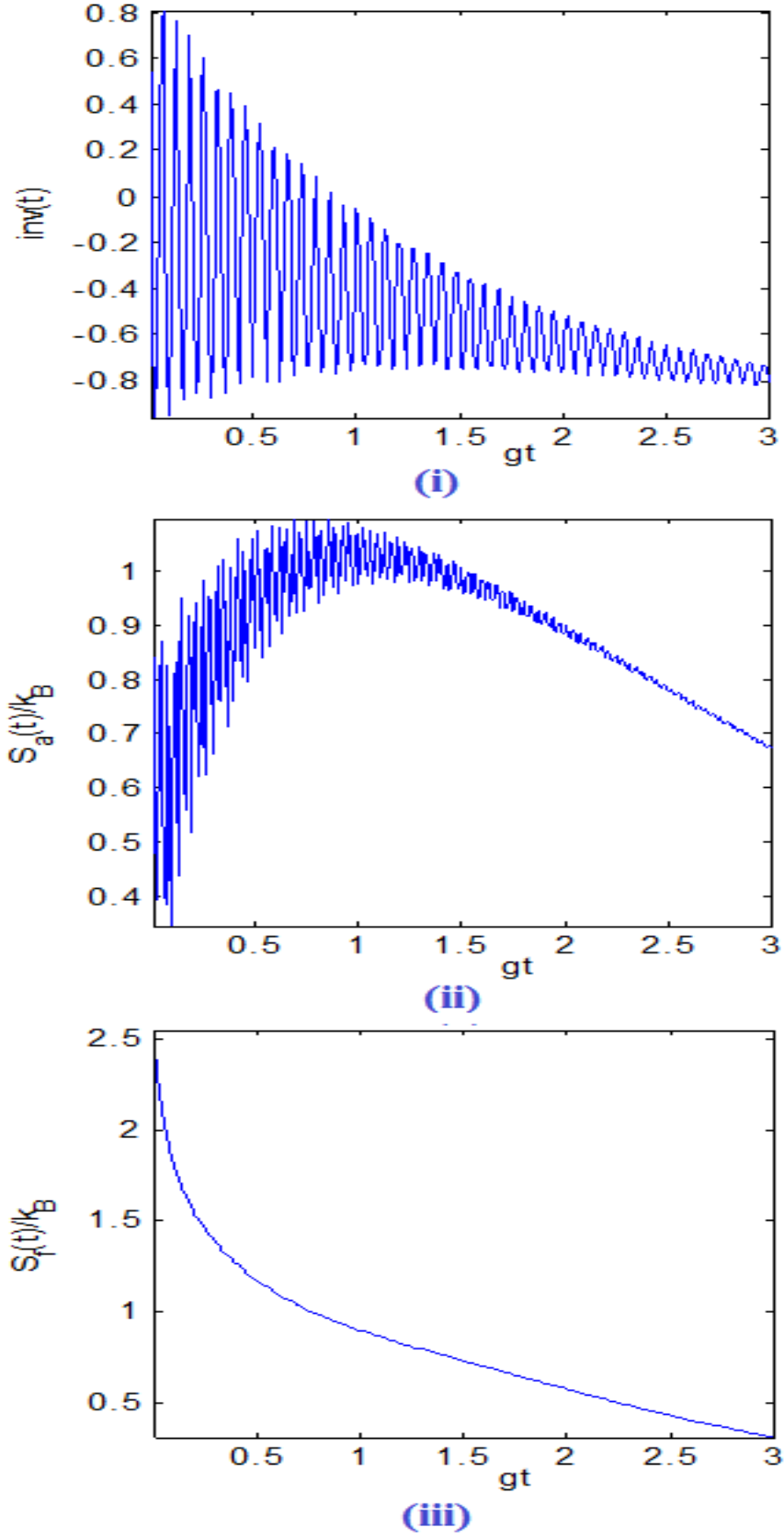
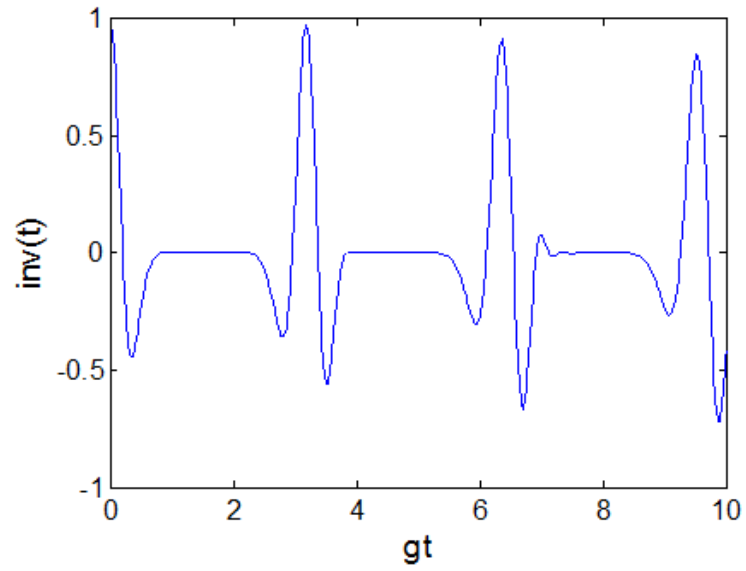
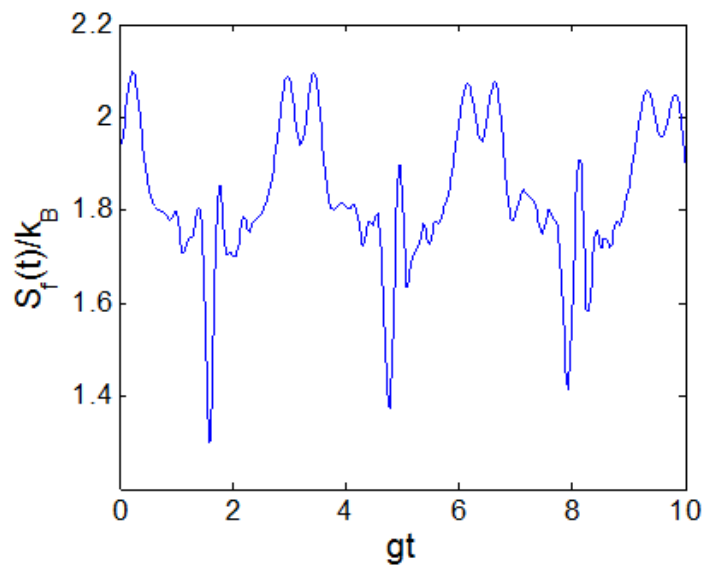


Figure 5.8: (i) Inversion, (ii) atom entropy and (iii) field entropy plots for  $g = 2 \times 10^6 s^{-1}$  with  $\alpha_0 = \sqrt{15}$ ,  $\Gamma_{ab} = \Gamma_{ac} = 10^6 s^{-1}$ ,  $\gamma_F = 10^6 s^{-1}$  and  $\Omega_p = 10^8 s^{-1}$  within time duration  $gt = 0$  until  $gt = 3$

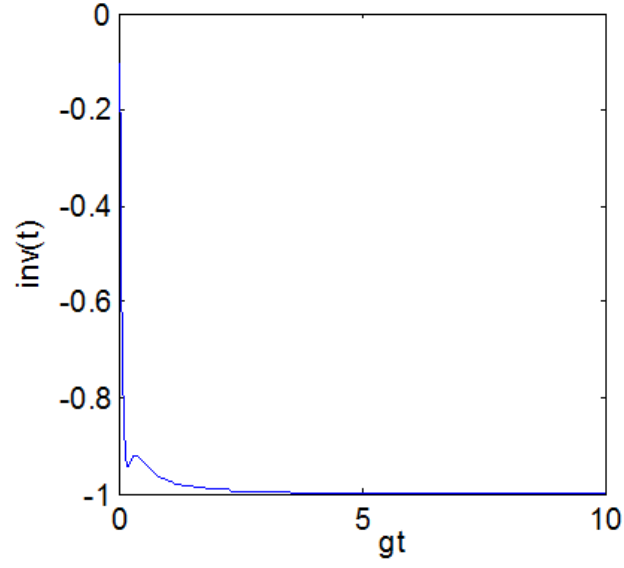


(i)

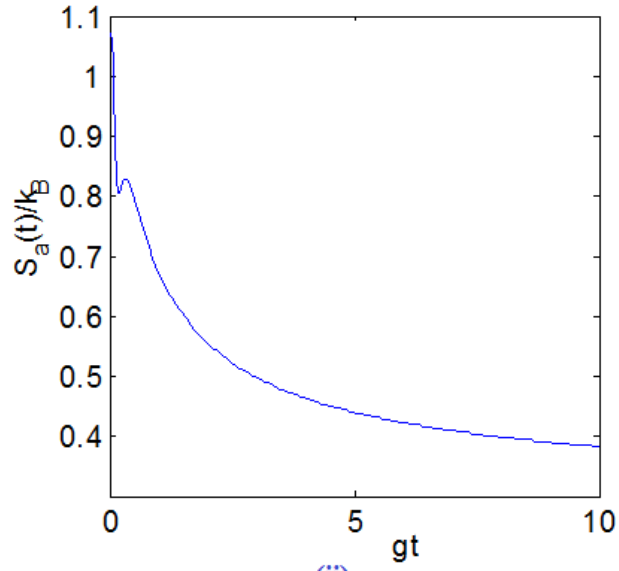


(ii)

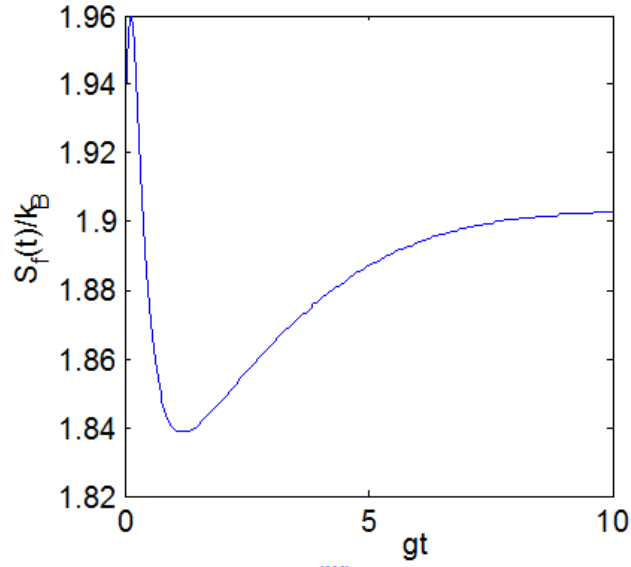
Figure 5.9: (i) Inversion, (ii) field entropy plots for  $g = 2 \times 10^6 s^{-1}$  with  $\alpha_0 = \sqrt{3}$ , with no damping within time duration  $gt = 0$  until  $gt = 10$



(i)



(ii)



(iii)

Figure 5.10: (i) Inversion, (ii) atom entropy and (iii) field entropy plots for  $g = 2 \times 10^6 s^{-1}$  with  $\alpha_0 = \sqrt{3}$ , with  $\Gamma_{ab} = \Gamma_{ac} = 10^7 s^{-1}$  within time duration  $gt = 0$  until  $gt = 10$

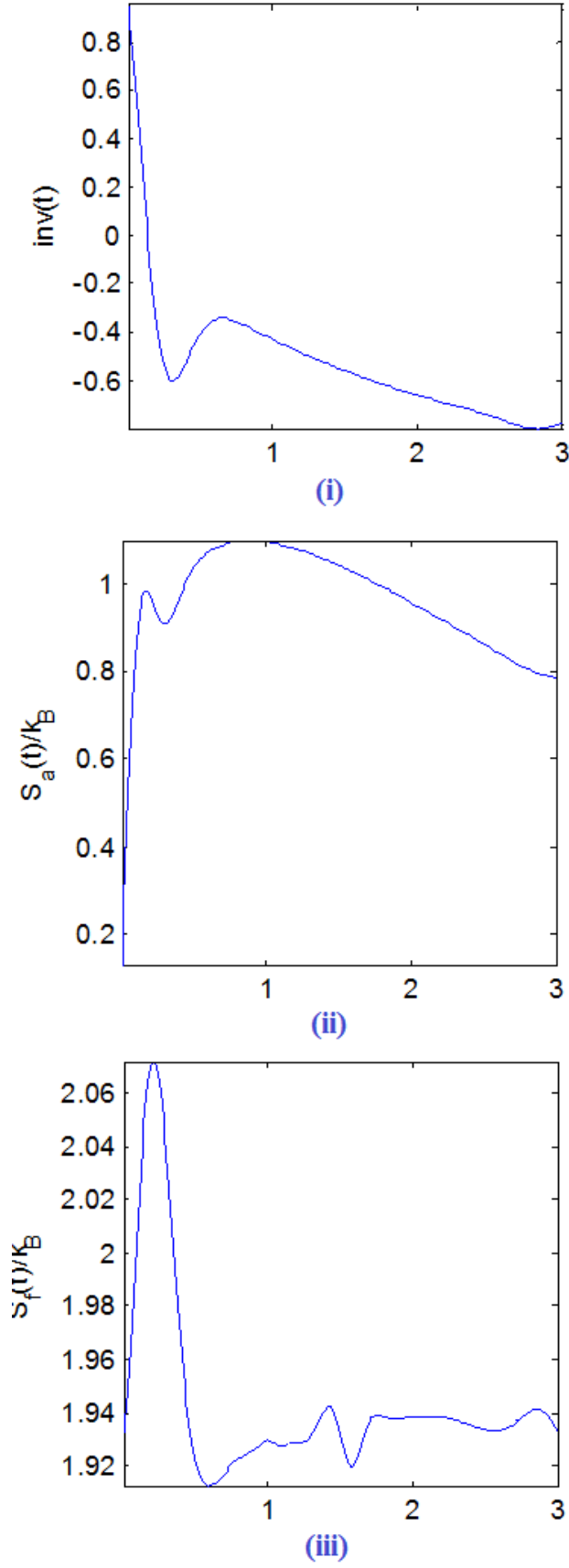


Figure 5.11: (i) Inversion, (ii) atom entropy and (iii) field entropy plots for  $g = 2 \times 10^6 s^{-1}$  with  $\alpha_0 = \sqrt{3}, \Gamma_{ab} = \Gamma_{ac} = 10^6 s^{-1}$  with no field damping within time duration  $gt = 0$  until  $gt = 3$

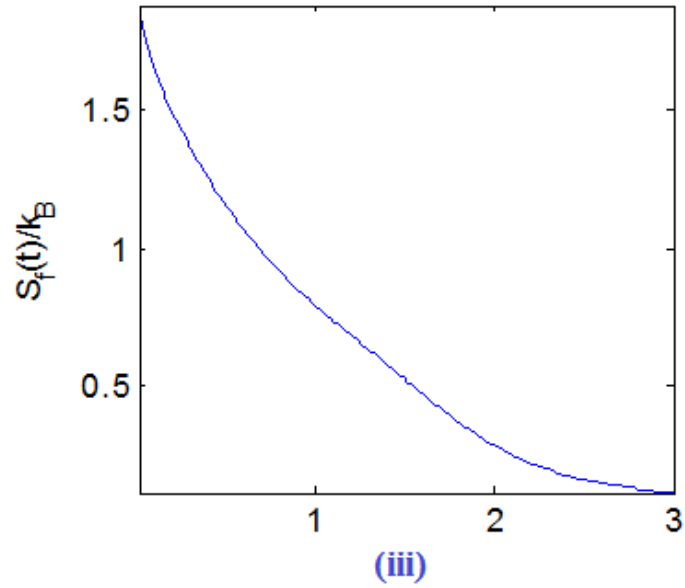
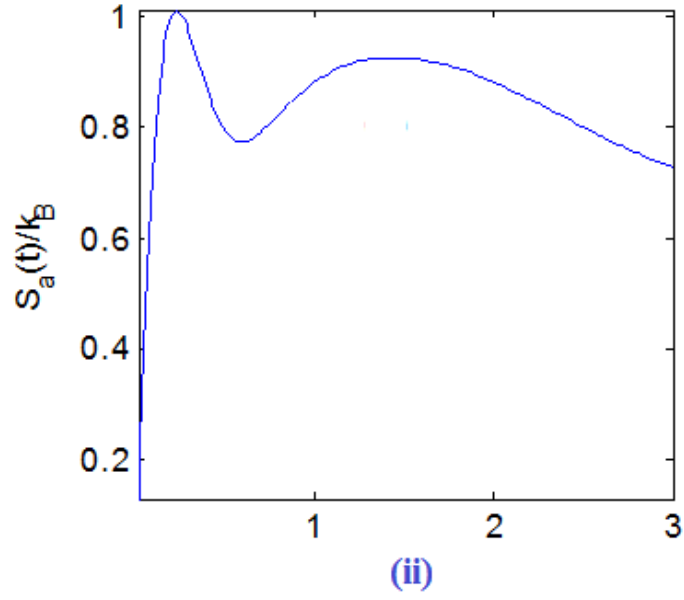
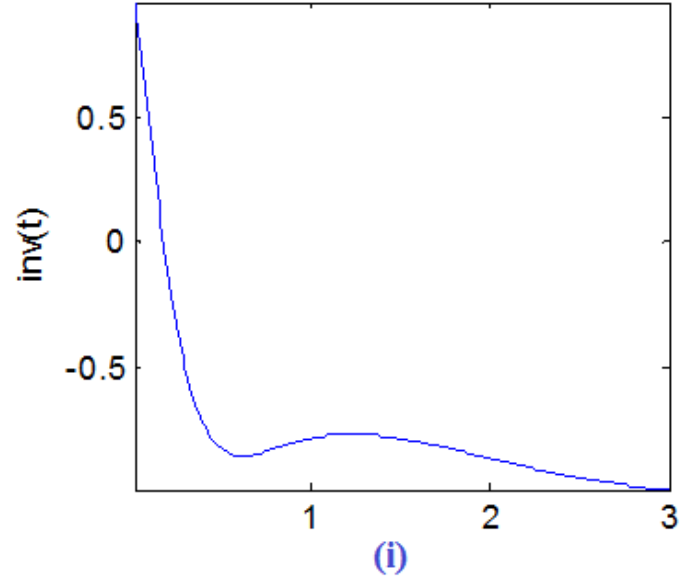


Figure 5.12: (i) Inversion, (ii) atom entropy and (iii) field entropy plots for  $g = 2 \times 10^6 s^{-1}$  with  $\alpha_0 = \sqrt{3}, \Gamma_{ab} = \Gamma_{ac} = 10^6 s^{-1}$  with  $\gamma_F = 10^6 s^{-1}$  within time duration  $gt = 0$  until  $gt = 3$

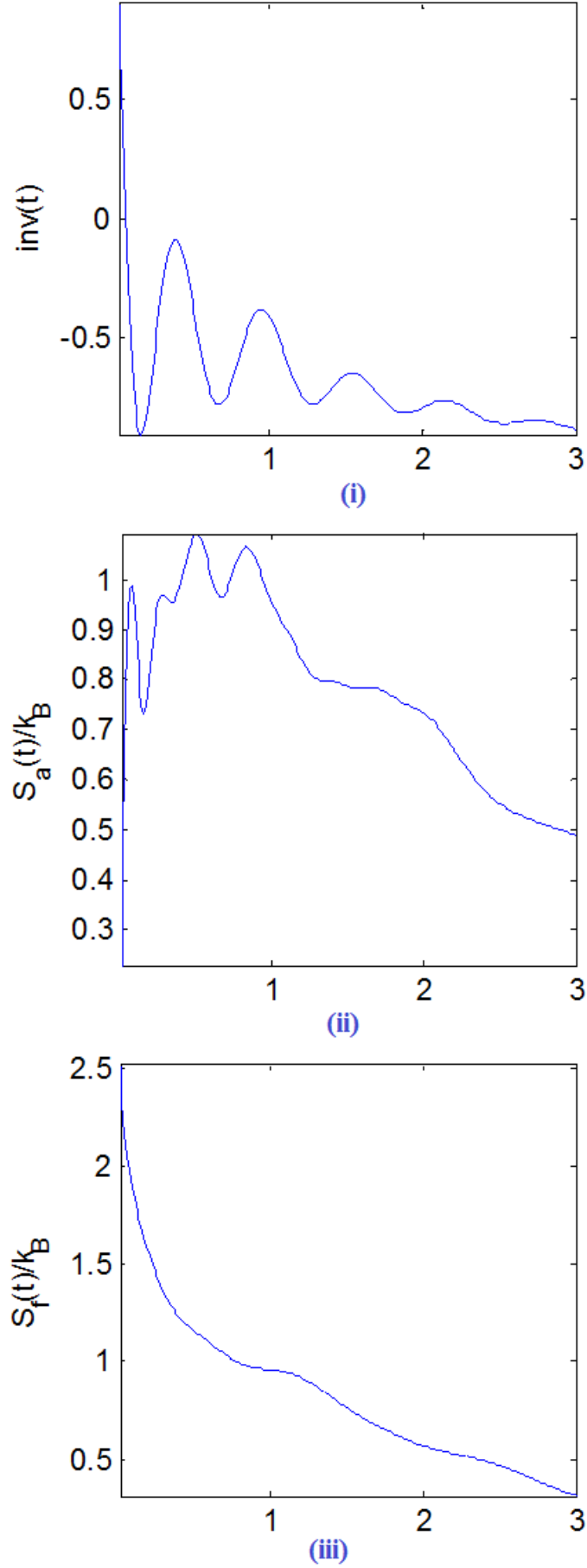


Figure 5.13: (i) Inversion, (ii) atom entropy and (iii) field entropy plots for  $g = 2 \times 10^6 s^{-1}$  with  $\alpha_0 = \sqrt{3}$ ,  $\Gamma_{ab} = \Gamma_{ac} = 10^6 s^{-1}$ ,  $\gamma_F = 10^6 s^{-1}$  with  $\Omega_p = 10^7 s^{-1}$  within time duration  $gt = 0$  until  $gt = 3$



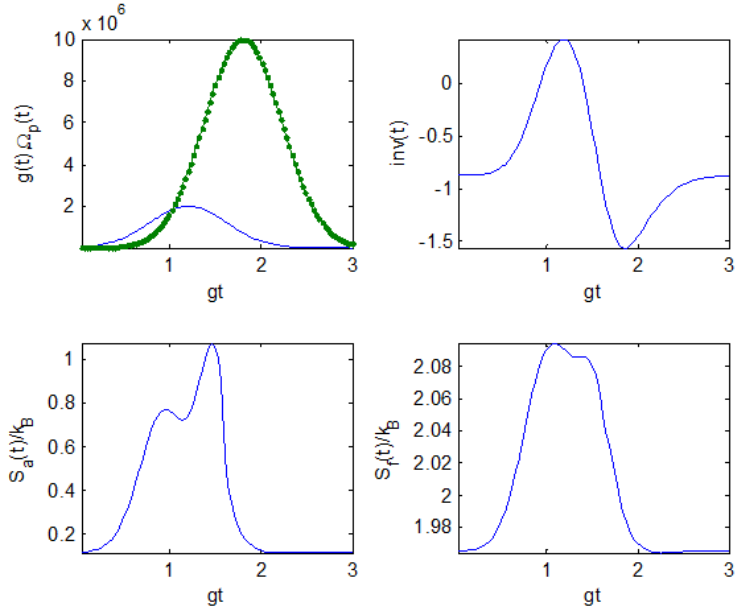


Figure 5.14: Intuitive sequence of pulses for atom initially in level  $|c\rangle$  (i) Inversion, (ii) atom entropy and (iii) field entropy plots for  $g = 2 \times 10^6 s^{-1}$  with  $\alpha_0 = \sqrt{3}, \Gamma_{ab} = \Gamma_{ac} = 10^6 s^{-1}, \gamma_F = 10^6 s^{-1}$  with  $\Omega_p = 10^7 s^{-1}$  within time duration  $gt = 0$  until  $gt = 3$

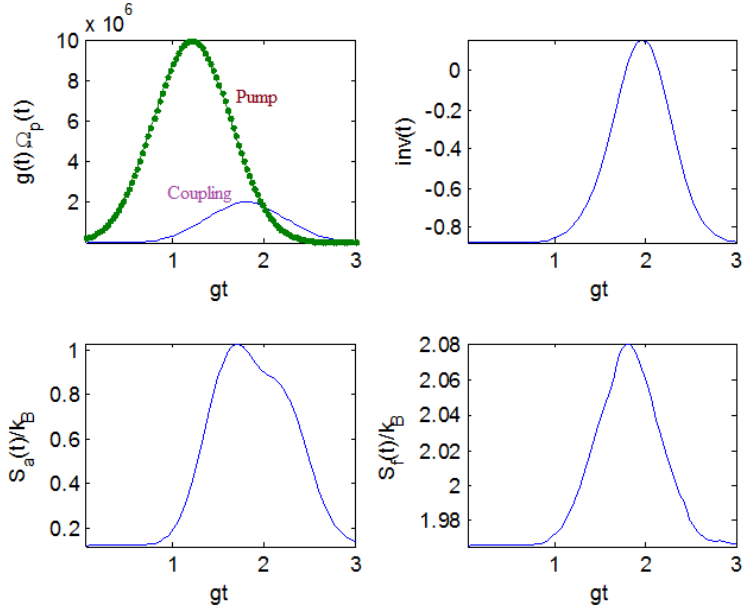


Figure 5.15: Counter-intuitive sequence for atom initially at  $|c\rangle$  with (i) Inversion, (ii) atom entropy and (iii) field entropy plots for  $g = 2 \times 10^6 s^{-1}, \alpha_0 = \sqrt{3}, \Gamma_{ab} = \Gamma_{ac} = 10^6 s^{-1}, \gamma_F = 10^6 s^{-1}$  and  $\Omega_p = 10^7 s^{-1}$  within time duration  $gt = 0$  until  $gt = 3$

## CHAPTER 6

### CONCLUSION AND OUTLOOK

#### 6.1 Introduction

In recent years, the fastest growing nano-technology leads to the development of quantum technologies and devices. The state-of-the-art research conducted involves the studies of novel quantum optical phenomena that can alter the properties of light in several interesting ways. The research requires quantum theoretical formalisms and advanced mathematical methods to study the effects of interaction between light and matter and the generation of nonclassical light. It involves analytical calculations and numerical computation of physical variables expressed as quantum operators.

#### 6.2 Research Significances

The research involves the field of quantum optics and quantum electrodynamics that includes the major fundamental effects at the quantum level. The theory would be applicable to optical characterization of a wide variety of nanostructures. Analytical and computational techniques will provide understanding and solutions that are needed to compute quantities that determine the nonclassical properties of light. The findings and theory developed will provide useful physical insights to analyze experimental works. It will lead to significant knowledge on nanostructures, particularly in enhancing the understanding of the connection between nonclassical properties of light and the particular atom system. This research will advance the field of quantum nanophotonics.

The interactions at atomic level need to be modelled using quantum optics since classical phenomenological models are inapplicable. The master equation is formulated for describing the spatial and temporal evolutions of electric field of nonclassical light produced by atom system interacting with laser fields. Desirable nonclassical optical effects can then be tailored to develop quantum information technology using nonclassical light sources. Current schemes in quantum information that rely on atomic ensembles to produce single photon source requires bulky and complicated setup involving optical

trapping. The new theoretical formalism and published results from this research will stimulate further theoretical and experimental works and facilitate progress on nanophotonic technology. The research results will particularly benefit quantum information technology.

### **6.3 Future works**

In present works, a system of two-level atom interacting with a quantized field in a high quality cavity is studied. The time- and intensity-dependent atom-field coupling are applied to the system, with different initial atomic states and also different initial field states: coherent states and Schrodinger cat states. The dynamics of the atom in the collapse-revival pattern of inversion and the dynamics of photon through Wigner function are investigated. In this study, the dissipative mechanism is excluded since the quality of the cavity is very high. In the future, for the case of two-level atom, the dissipation should be counted since most of the interaction system experience damping effect due to the coupling with each other. A system of multi-photon and multi-level may also give good results and interesting features.

The study has been extended to a system of three-level  $\Lambda$ -type atom interact with a single mode field driven by a laser. The dissipation due to coupling with reservoir is also included. The time- and intensity dependent are remain of interest with different pulse parameters and different initial state in good and bad cavity. The entropy of the system, the inversion, Wigner function and Q parameter are calculated. A challenging future studies have been planned. The more complex system will be considered such as N-atom system, various reservoir coupling, dipole-dipole approximation and many more.

The interaction of many-body system could be more interesting to study because more phenomenon will occur during the interaction and more classical and nonclassical effects will get involved. The findings must be essential to provide useful information to understand the nature of the system and to enhance future technologies such as in quantum information science. More interesting nonclassical properties of light are expected to be included later in the future research, to have a complete view and an established knowledge on the behaviour of light.

As a conclusion, this research will bring the realization of quantum information tech-

nology closer to reality and enhance the field of quantum optics and photonic. The theoretical results obtained could also provide basic predictions and understanding the system as a preparation for experimental research.

# **Appendices**

## APPENDIX A

### LIST OF PUBLICATIONS

#### Journal Articles

##### *Published*

C.H.Raymond Ooi, **S. N. Hazmin**, Sudha Singh. Nonclassical Dynamics with Time- and Intensity-Dependent Coupling, *Quantum Information Processing*. Springer US, (2012). ISSN 1573-1332. (DOI: 10.1007/s11128-012-0512-6).

S. Aini Shahida, **S. N. Hazmin**, C. H. Raymond Ooi. Quantum Entanglement Criteria. *Journal of Modern Optics*. Taylor & Francis. (2013). ISSN 1362-3044. (DOI: 10.1080/09500340.2013.796016)

##### *Will Be Submitted*

C. H .Raymond Ooi, **S. N. Hazmin**, S. Aini Shahida. The Dynamics of a Damped  $\Lambda$ -type Three-Level Atom with Time- and Intensity-Dependent Coupling. (2013)

#### Proceeding

##### *International Conference*

**S. N. Hazmin** & C. H. Raymond Ooi. Nonclassical Photons via Time- and Intensity-Dependent Coupling of Jaynes-Cumming Model. Proceeding of Asia Pacific Conference & Workshop in Quantum Information Science 2012 (APCWQIS). (2012).

##### *National Conference*

**S. N. Hazmin** & C. H. Raymond Ooi. The Study of Nonclassical Optical Properties of Light in Low Dimensional Structures. Proceeding of UMT Postgraduate Seminar. (2012). ISBN: 978-967-5366-88-8

#### Public Talk

##### *PhD Seminar*

**S. N. Hazmin**. Nonclassical Optical Properties of Light in Atom-Cavity Interaction Scheme with Time- and Intensity- Dependent Coupling. PhD Seminar. DKF, Physics Department, University of Malaya. (2012).

## APPENDIX B

### COUPLED EQUATION DERIVATION FOR TWO-LEVEL ATOM

Interaction Hamiltonian of single two level atom interact with a single mode field is given by:

$$V(t) = \hbar g(t)(\sigma_+ \hat{R} e^{i\Delta t} + \sigma_- \hat{R}^\dagger e^{-i\Delta t}) \quad (\text{B.1})$$

The evolution of the atom-field system can be described by the state vector

$$|\psi(t)\rangle = \sum_n [C_{a,n}(t)|a, n\rangle + C_{b,n}(t)|b, n\rangle] \quad (\text{B.2})$$

with the time dependent atom-field coefficients  $C_{x,n}$  for level  $x (= a, b)$  with  $n$  photons. The equation of motion for  $|\psi(t)\rangle$

$$i\hbar \frac{d}{dt} |\psi(t)\rangle = V(t) |\psi(t)\rangle \quad (\text{B.3})$$

So

$$i\hbar \frac{d}{dt} [C_{a,n}(t)|a, n\rangle + C_{b,n}(t)|b, n\rangle] \quad (\text{B.4})$$

$$= \hbar g(t)(\sigma_+ \hat{R} e^{i\Delta t} + \sigma_- \hat{R}^\dagger e^{-i\Delta t}) [C_{a,n}(t)|a, n\rangle + C_{b,n}(t)|b, n\rangle] \quad (\text{B.5})$$

where  $\sigma_+ = |a\rangle\langle b|$ ,  $\sigma_- = |b\rangle\langle a|$ , and  $\hat{R}$  as a function of  $\hat{a}$  and  $\hat{a}^\dagger$  given by:

$$\hat{R} = \hat{a}\sqrt{\hat{n}}$$

$$\hat{R}^\dagger = \sqrt{\hat{n}}\hat{a}^\dagger$$

$$\hat{n} = \hat{a}^\dagger \hat{a}$$

$$\hat{R}\hat{R}^\dagger = \hat{a}\sqrt{\hat{n}}\sqrt{\hat{n}}\hat{a}^\dagger$$

$$= \hat{a}\hat{a}^\dagger \hat{a}\hat{a}^\dagger$$

$$\begin{aligned}
&= \left(\hat{a}\hat{a}^\dagger\right)^2 \\
&= (\hat{n}+1)^2 \\
\hat{R}^\dagger \hat{R} &= \sqrt{\hat{a}^\dagger \hat{a}} \hat{a}^\dagger \hat{a} \sqrt{\hat{a}^\dagger \hat{a}} \\
&= \left(\hat{a}^\dagger \hat{a}\right)^2 \\
&= \hat{n}^2
\end{aligned}$$

Interaction energy can only cause transition between  $|a, n\rangle$  and  $|b, n+1\rangle$  so we have

$$i\hbar \frac{d}{dt} [C_{a,n}(t)|a, n\rangle + C_{b,n+1}(t)|b, n+1\rangle] \quad (\text{B.6})$$

$$= \hbar g(t)(\sigma_+ \hat{R} e^{i\Delta t} + \sigma_- \hat{R}^\dagger e^{-i\Delta t})[C_{a,n}(t)|a, n\rangle + C_{b,n+1}(t)|b, n+1\rangle] \quad (\text{B.7})$$

$$\frac{d}{dt} [C_{a,n}(t)|a, n\rangle + C_{b,n+1}(t)|b, n+1\rangle] \quad (\text{B.8})$$

$$= -ig(t)(\sigma_+ \hat{R} e^{i\Delta t} + \sigma_- \hat{R}^\dagger e^{-i\Delta t})C_{a,n}(t)|a, n\rangle \quad (\text{B.9})$$

$$-ig(t)(\sigma_+ \hat{R} e^{i\Delta t} + \sigma_- \hat{R}^\dagger e^{-i\Delta t})C_{b,n+1}(t)|b, n+1\rangle \quad (\text{B.10})$$

$$= -ig(t)\sigma_+ \hat{R} e^{i\Delta t} C_{a,n}(t)|a, n\rangle \quad (\text{B.11})$$

$$-ig(t)\sigma_- \hat{R}^\dagger e^{-i\Delta t} C_{a,n}(t)|a, n\rangle \quad (\text{B.12})$$

$$-ig(t)\sigma_+ \hat{R} e^{i\Delta t} C_{b,n+1}(t)|b, n+1\rangle \quad (\text{B.13})$$

$$-ig(t)\sigma_- \hat{R}^\dagger e^{-i\Delta t} C_{b,n+1}(t)|b, n+1\rangle \quad (\text{B.14})$$

$$= -ig(t)|a\rangle\langle b|\hat{a}\sqrt{\hat{n}}e^{i\Delta t}C_{a,n}(t)|a\rangle|n\rangle - \quad (\text{B.15})$$

$$ig(t)|b\rangle\langle a|\sqrt{\hat{n}}\hat{a}^\dagger e^{-i\Delta t}C_{a,n}(t)|a\rangle|n\rangle \quad (\text{B.16})$$

$$-ig(t)|a\rangle\langle b|\hat{a}\sqrt{\hat{n}}e^{i\Delta t}C_{b,n+1}(t)|b\rangle|n+1\rangle \quad (\text{B.17})$$

$$-ig(t)|b\rangle\langle a|\sqrt{\hat{n}}\hat{a}^\dagger e^{-i\Delta t}C_{b,n+1}(t)|b\rangle|n+1\rangle \quad (\text{B.18})$$

$$= -ig(t)\sqrt{\hat{n}}\hat{a}^\dagger e^{-i\Delta t}C_{a,n}(t)|b\rangle|n\rangle - ig(t)\hat{a}\sqrt{\hat{n}}e^{i\Delta t}C_{b,n+1}(t)|a\rangle|n+1\rangle \quad (\text{B.19})$$

$$\frac{d}{dt} [C_{a,n}(t)|a, n\rangle + C_{b,n+1}(t)|b, n+1\rangle] \quad (\text{B.20})$$

$$= -ig(t)\sqrt{\hat{n}}\sqrt{n+1}e^{-i\Delta t}C_{a,n}(t)|b\rangle|n+1\rangle \quad (\text{B.21})$$

$$-ig(t)\hat{a}\sqrt{n+1}e^{i\Delta t}C_{b,n+1}(t)|a\rangle|n+1\rangle \quad (\text{B.22})$$

$$= -ig(t)\sqrt{n+1}\sqrt{n+1}e^{-i\Delta t}C_{a,n}(t)|b\rangle|n+1\rangle \quad (\text{B.23})$$



$$-ig(t)\sqrt{n+1}\sqrt{n+1}e^{i\Delta t}C_{b,n+1}(t)|a\rangle|n\rangle \quad (\text{B.24})$$

$$= -ig(t)(n+1)e^{-i\Delta t}C_{a,n}(t)|b\rangle|n+1\rangle \quad (\text{B.25})$$

$$-ig(t)(n+1)e^{i\Delta t}C_{b,n+1}(t)|a\rangle|n\rangle \quad (\text{B.26})$$

Now by projecting the resulting equation with  $\langle a, n|$  and  $\langle b, n+1|$  we get coupled equations

$$\frac{d}{dt}C_{a,n}(t) = -ig(t)(n+1)e^{i\Delta t}C_{b,n+1}(t) \quad (\text{B.27})$$

$$\frac{d}{dt}C_{b,n+1}(t) = -ig(t)(n+1)e^{-i\Delta t}C_{a,n}(t) \quad (\text{B.28})$$

where  $g(t)$  is the atom-field coupling factor and  $|C_{x,n}|^2$  being the probability with  $n$  photons and atom in state  $|a\rangle$ .

## APPENDIX C

### SOLVING THE COUPLED EQUATION

Given coupled equation:

$$\begin{aligned}\frac{d}{dt}C_{a,n}(t) &= -ig(t)(n+1)e^{i\Delta t}C_{b,n+1}(t) \\ \frac{d}{dt}C_{b,n+1}(t) &= -ig(t)(n+1)e^{-i\Delta t}C_{a,n}(t)\end{aligned}$$

Coupled equation above can be solved by Laplace transform

$$L[F'(t)] = sf(s) - F(0)$$

where  $c_{a,n}(s)$  is used as the Laplace transform of  $C_{a,n}(t)$ . Using the general differentiation rule:

$$\frac{d}{dx}(uv) = u\frac{dv}{dx} + v\frac{du}{dx} \quad (\text{C.1})$$

for  $\frac{d}{dt}C_{a,n}(t)$ , we denote

$$\begin{aligned}u &= C_{a,n}(t) \\ v &= e^{-i\Delta t}\end{aligned} \quad (\text{C.2})$$

.By substituting into eq.C.1, we get

$$\begin{aligned}\frac{d}{dt}[C_{a,n}(t)e^{-i\Delta t}] &= C_{a,n}(t)\frac{d}{dt}(e^{-i\Delta t}) + e^{-i\Delta t}\frac{d}{dt}(C_{a,n}(t)) \\ &= -i\Delta C_{a,n}(t)e^{-i\Delta t} + e^{-i\Delta t}\left[\frac{d}{dt}(C_{a,n}(t))\right] \\ &= -i\Delta C_{a,n}(t)e^{-i\Delta t} + e^{-i\Delta t}\left[-ig(t)(n+1)e^{i\Delta t}C_{b,n+1}(t)\right] \\ &= -i\Delta C_{a,n}(t)e^{-i\Delta t} - ig(t)(n+1)C_{b,n+1}(t)\end{aligned}$$

The equation is then transformed to have the form of  $L[F'(t)] = sf(s) - F(0)$  then become

$$\begin{aligned}L\left[\frac{d}{dt}[C_{a,n}(t)e^{-i\Delta t}]\right] &= s[c_{a,n}(s)e^{-i\Delta t}] - c_{a,n}(0) \\ c_{a,n}(s)e^{-i\Delta t} &= \frac{1}{s}c_{a,n}(0) - i\frac{1}{s}\Delta c_{a,n}(s)e^{-i\Delta t} - i\frac{1}{s}g(t)(n+1)c_{b,n+1}(s)\end{aligned}$$

$$\begin{aligned}
c_{a,n}(s)e^{-i\Delta t} + \frac{i\Delta}{s}c_{a,n}(s)e^{-i\Delta t} &= \frac{1}{s}c_{a,n}(0) - i\frac{1}{s}g(t)(n+1)c_{b,n+1}(s) \\
\left[ \frac{se^{-i\Delta t} + i\Delta e^{-i\Delta t}}{s} \right] c_{a,n}(s) &= \frac{1}{s}c_{a,n}(0) - i\frac{1}{s}g(t)(n+1)c_{b,n+1}(s) \\
&= \left[ \frac{1}{se^{-i\Delta t} + i\Delta e^{-i\Delta t}} \right] c_{a,n}(0) \\
&\quad - i \left[ \frac{1}{se^{-i\Delta t} + i\Delta e^{-i\Delta t}} \right] g(t)(n+1)c_{b,n+1}(s) \\
c_{a,n}(s) &= \left[ \frac{e^{i\Delta t}}{(s+i\Delta)} \right] c_{a,n}(0) - \left[ \frac{e^{i\Delta t}}{(s+i\Delta)} \right] ig(t)(n+1)c_{b,n+1}(s)
\end{aligned}$$

$$\begin{aligned}
\frac{d}{dt} [C_{b,n+1}(t)e^{i\Delta t}] &= i\Delta C_{b,n+1}(t)e^{i\Delta t} - ig(t)(n+1)C_{a,n}(t) \\
L \left[ \frac{d}{dt} [C_{b,n+1}(t)e^{i\Delta t}] \right] &= s [c_{b,n+1}(s)e^{-i\Delta t}] - c_{b,n+1}(0) \\
s [c_{b,n+1}(s)e^{-i\Delta t}] &= c_{b,n+1}(0) + i\Delta c_{b,n+1}(s)e^{i\Delta t} - ig(t)(n+1)c_{a,n}(s) \\
c_{b,n+1}(s) - \frac{1}{s}i\Delta c_{b,n+1}(s)e^{2i\Delta t} &= \frac{1}{s}c_{b,n+1}(0)e^{i\Delta t} - \frac{1}{s}ig(t)(n+1)c_{a,n}(s)e^{i\Delta t} \\
\left[ \frac{s - i\Delta e^{2i\Delta t}}{s} \right] c_{b,n+1}(s) &= \frac{1}{s}c_{b,n+1}(0)e^{i\Delta t} - \frac{1}{s}ig(t)(n+1)c_{a,n}(s)e^{i\Delta t} \\
c_{b,n+1}(s) &= \left[ \frac{1}{s - i\Delta e^{2i\Delta t}} \right] c_{b,n+1}(0)e^{i\Delta t} \\
&\quad - \left[ \frac{1}{s - i\Delta e^{2i\Delta t}} \right] ig(t)(n+1)c_{a,n}(s)e^{i\Delta t}
\end{aligned}$$

$$\begin{aligned}
c_{a,n}(s) &= \left[ \frac{e^{i\Delta t}}{(s+i\Delta)} \right] c_{a,n}(0) - \left[ \frac{e^{i\Delta t}}{(s+i\Delta)} \right] ig(t)(n+1)c_{b,n+1}(s) \\
c_{a,n}(s) &= \left[ \frac{e^{i\Delta t}}{(s+i\Delta)} \right] c_{a,n}(0) - \left[ \frac{ig(t)(n+1)}{(s+i\Delta)(s-i\Delta)} \right] c_{b,n+1}(0) \\
&\quad - \left[ \frac{g^2(t)(n+1)^2}{(s+i\Delta)(s-i\Delta)} \right] c_{a,n}(s) \\
c_{a,n}(s) &= \left[ \frac{(s-i\Delta)e^{i\Delta t}}{(s+i\Delta)(s-i\Delta) + g^2(t)(n+1)^2} \right] c_{a,n}(0) \\
&\quad - \left[ \frac{ig(t)(n+1)}{(s+i\Delta)(s-i\Delta) + g^2(t)(n+1)^2} \right] c_{b,n+1}(0) \\
&= \left( \frac{s}{s^2 + \left( \sqrt{\Delta^2 + g^2(t)(n+1)^2} \right)^2} \right) e^{i\Delta t} c_{a,n}(0)
\end{aligned}$$

$$\begin{aligned}
& - \left( \frac{i\Delta}{s^2 + \left( \sqrt{\Delta^2 + g^2(t)(n+1)^2} \right)^2} \right) e^{i\Delta t} c_{a,n}(0) \\
& - i \frac{g(t)(n+1)}{\sqrt{\Delta^2 + g^2(t)(n+1)^2}} \left[ \frac{\sqrt{\Delta^2 + g^2(t)(n+1)^2}}{s^2 + \left( \sqrt{\Delta^2 + g^2(t)(n+1)^2} \right)^2} \right] c_{b,n+1}(0) \\
c_{a,n}(s) = & c_{a,n}(0) \left[ \cos(\Omega_R t) - \frac{i\Delta}{\Omega_R} \sin(\Omega_R t) \right] e^{i\Delta t} \\
& - \frac{ig(t)(n+1)}{\Omega_R} [\sin(\Omega_R t)] c_{b,n+1}(0)
\end{aligned}$$

where

$$\begin{aligned}
\Omega_R &= \sqrt{\Delta^2 + g^2(t)(n+1)^2} \\
\sin \Omega_R t &= \frac{\Omega_R}{s^2 + \Omega_R^2} \\
\cos \Omega_R t &= \frac{s}{s^2 + \Omega_R^2}
\end{aligned}$$

## APPENDIX D

### DENSITY MATRIX ELEMENTS FOR TWO-LEVEL ATOM

From Appendix B, we get coupled equation for a system of two-level atom interact with a single mode field in a high quality cavity (as discussed in Chapter 4). coupled equations

$$\frac{d}{dt}C_{a,n}(t) = -ig(t)(n+1)e^{i\Delta t}C_{b,n+1}(t) \quad (D.1)$$

$$\frac{d}{dt}C_{b,n+1}(t) = -ig(t)(n+1)e^{-i\Delta t}C_{a,n}(t) \quad (D.2)$$

A step by step calculation for a density matrix element is given by

$$\begin{aligned} \langle n|\rho_{aa}(t)|m\rangle &= C_{a,n}(t)C_{a,m}^*(t) \quad (D.3) \\ &= \left[ e^{i\Delta t/2}[C_{a,n}(0)r_n(t) - iC_{b,n+1}(0)q_n(t)] \right] \\ &\quad \left[ e^{-i\Delta t/2}[C_{a,m}^*(0)r_m^*(t) + iC_{b,m+1}^*(0)q_m(t)] \right] \\ &= e^{i\Delta t/2}C_{a,n}(0)r_n(t)e^{-i\Delta t/2}C_{a,m}^*(0)r_m^*(t) \\ &\quad + e^{i\Delta t/2}C_{a,n}(0)r_n(t)ie^{-i\Delta t/2}C_{b,m+1}^*(0)q_m(t) \\ &\quad - ie^{i\Delta t/2}C_{b,n+1}(0)q_n(t)e^{-i\Delta t/2}C_{a,m}^*(0)r_m^*(t) \\ &\quad - ie^{i\Delta t/2}C_{b,n+1}(0)q_n(t)ie^{-i\Delta t/2}C_{b,m+1}^*(0)q_m(t) \\ &= C_{a,n}(0)C_{a,m}^*(0)r_n(t)r_m^*(t) \\ &\quad + iC_{a,n}(0)C_{b,m+1}^*(0)r_n(t)q_m(t) \\ &\quad - iC_{b,n+1}(0)C_{a,m}^*(0)q_n(t)r_m^*(t) \\ &\quad + C_{b,n+1}(0)C_{b,m+1}^*(0)q_n(t)q_m(t) \\ &= \rho_{aa}(0)\rho_{n,m}(0)r_n(t)r_m^*(t) \\ &\quad + i\rho_{ab}(0)\rho_{n,m+1}(0)r_n(t)q_m(t) \\ &\quad - i\rho_{ba}(0)\rho_{n+1,m}(0)q_n(t)r_m^*(t) \\ &\quad + \rho_{bb}(0)\rho_{n+1,m+1}(0)q_n(t)q_m(t) \end{aligned}$$

$$\begin{aligned}
\langle n | \rho_{ab}(t) | m \rangle &= C_{a,n}(t) C_{b,m}^*(t) \tag{D.4} \\
&= \left[ e^{i\Delta t/2} [C_{a,n}(0) r_n(t) - i C_{b,n+1}(0) q_n(t)] \right] \\
&\quad \left[ e^{i\Delta t/2} [C_{b,m}^*(0) r_{m-1}(t) + i C_{a,m-1}^*(0) q_{m-1}(t)] \right] \\
&= [e^{i\Delta t/2} C_{a,n}(0) r_n(t) - i e^{i\Delta t/2} C_{b,n+1}(0) q_n(t)] \\
&\quad [e^{i\Delta t/2} C_{b,m}^*(0) r_{m-1}(t) + i e^{i\Delta t/2} C_{a,m-1}^*(0) q_{m-1}(t)] \\
&= e^{i\Delta t/2} C_{a,n}(0) r_n(t) e^{i\Delta t/2} C_{b,m}^*(0) r_{m-1}(t) \\
&\quad + e^{i\Delta t/2} C_{a,n}(0) r_n(t) i e^{i\Delta t/2} C_{a,m-1}^*(0) q_{m-1}(t) \\
&\quad - i e^{i\Delta t/2} C_{b,n+1}(0) q_n(t) e^{i\Delta t/2} C_{b,m}^*(0) r_{m-1}(t) \\
&\quad - i e^{i\Delta t/2} C_{b,n+1}(0) q_n(t) i e^{i\Delta t/2} C_{a,m-1}^*(0) q_{m-1}(t) \\
&= e^{i\Delta t} C_{a,n}(0) C_{b,m}^*(0) r_n(t) r_{m-1}(t) \\
&\quad + i e^{i\Delta t} C_{a,n}(0) C_{a,m-1}^*(0) r_n(t) q_{m-1}(t) \\
&\quad - i e^{i\Delta t} C_{b,n+1}(0) C_{b,m}^*(0) q_n(t) r_{m-1}(t) \\
&\quad + e^{i\Delta t} C_{b,n+1}(0) C_{a,m-1}^*(0) q_n(t) q_{m-1}(t) \\
&= e^{i\Delta t} \rho_{ab}(0) \rho_{n,m}(0) r_n(t) r_{m-1}(t) \\
&\quad + i e^{i\Delta t} \rho_{aa}(0) \rho_{n,m-1}(0) r_n(t) q_{m-1}(t) \\
&\quad - i e^{i\Delta t} \rho_{bb}(0) \rho_{n+1,m}(0) q_n(t) r_{m-1}(t) \\
&\quad + e^{i\Delta t} \rho_{ba}(0) \rho_{n+1,m-1}(0) q_n(t) q_{m-1}(t)
\end{aligned}$$

$$\begin{aligned}
\langle n | \rho_{ba}(t) | m \rangle &= C_{b,n}(t) C_{a,m}^*(t) \tag{D.5} \\
&= \left[ e^{-i\Delta t/2} [C_{b,n}(0) r_{n-1}^*(t) - i C_{a,n-1}(0) q_{n-1}(t)] \right] \\
&\quad \left[ e^{-i\Delta t/2} [C_{a,m}^*(0) r_m^*(t) + i C_{b,m+1}^*(0) q_m(t)] \right] \\
&= [e^{-i\Delta t/2} C_{b,n}(0) r_{n-1}^*(t) - i e^{-i\Delta t/2} C_{a,n-1}(0) q_{n-1}(t)] \\
&\quad [e^{-i\Delta t/2} C_{a,m}^*(0) r_m^*(t) + i e^{-i\Delta t/2} C_{b,m+1}^*(0) q_m(t)] \\
&= e^{-i\Delta t/2} C_{b,n}(0) r_{n-1}^*(t) e^{-i\Delta t/2} C_{a,m}^*(0) r_m^*(t) \\
&\quad + e^{-i\Delta t/2} C_{b,n}(0) r_{n-1}^*(t) i e^{-i\Delta t/2} C_{b,m+1}^*(0) q_m(t) \\
&\quad - i e^{-i\Delta t/2} C_{a,n-1}(0) q_{n-1}(t) e^{-i\Delta t/2} C_{a,m}^*(0) r_m^*(t)
\end{aligned}$$

$$\begin{aligned}
& -ie^{-i\Delta t/2}C_{a,n-1}(0)q_{n-1}(t)ie^{-i\Delta t/2}C_{b,m+1}^*(0)q_m(t) \\
= & e^{-i\Delta t}C_{b,n}(0)C_{a,m}^*(0)r_{n-1}^*(t)r_m^*(t) \\
& +ie^{-i\Delta t}C_{b,n}(0)C_{b,m+1}^*(0)r_{n-1}^*(t)q_m(t) \\
& -ie^{-i\Delta t}C_{a,n-1}(0)C_{a,m}^*(0)q_{n-1}(t)r_m^*(t) \\
& +e^{-i\Delta t}C_{a,n-1}(0)C_{b,m+1}^*(0)q_{n-1}(t)q_m(t) \\
= & e^{-i\Delta t}\rho_{ba}(0)\rho_{n,m}(0)r_{n-1}^*(t)r_m^*(t) \\
& +ie^{-i\Delta t}\rho_{bb}(0)\rho_{n,m+1}(0)r_{n-1}^*(t)q_m(t) \\
& -ie^{-i\Delta t}\rho_{aa}(0)\rho_{n-1,m}(0)q_{n-1}(t)r_m^*(t) \\
& +e^{-i\Delta t}\rho_{ab}(0)\rho_{n-1,m+1}(0)q_{n-1}(t)q_m(t)
\end{aligned}$$

$$\begin{aligned}
\langle n|\rho_{bb}(t)|m\rangle & = C_{b,n}(t)C_{b,m}^*(t) \tag{D.6} \\
& = \left[ e^{-i\Delta t/2}[C_{b,n}(0)r_{n-1}^*(t) - iC_{a,n-1}(0)q_{n-1}(t)] \right] \\
& \quad \left[ e^{i\Delta t/2}[C_{b,m}^*(0)r_{m-1}(t) + iC_{a,m-1}^*(0)q_{m-1}(t)] \right] \\
& = C_{b,n}(0)C_{b,m}^*(0)r_{n-1}^*(t)r_{m-1}(t) \\
& \quad +iC_{b,n}(0)C_{a,m-1}^*(0)r_{n-1}^*(t)q_{m-1}(t) \\
& \quad -iC_{a,n-1}(0)C_{b,m}^*(0)q_{n-1}(t)r_{m-1}(t) \\
& \quad +C_{a,n-1}(0)C_{a,m-1}^*(0)q_{n-1}(t)q_{m-1}(t) \\
& = \rho_{bb}(0)\rho_{n,m}(0)r_{n-1}^*(t)r_{m-1}(t) \\
& \quad +i\rho_{ba}(0)\rho_{n,m-1}(0)r_{n-1}^*(t)q_{m-1}(t) \\
& \quad -i\rho_{ab}(0)\rho_{n-1,m}(0)q_{n-1}(t)r_{m-1}(t) \\
& \quad +\rho_{aa}(0)\rho_{n-1,m-1}(0)q_{n-1}(t)q_{m-1}(t)
\end{aligned}$$

The atomic coherence is given by

$$\begin{aligned}
\rho_{nm}(t) & = \langle n|\{\hat{\rho}_{aa}(t) + \hat{\rho}_{bb}(t)\}|m\rangle \tag{D.7} \\
& = \rho_{aa}(0)\rho_{n,m}(0)r_n(t)r_m^*(t) + i\rho_{ab}(0)\rho_{n,m+1}(0)r_n(t)q_m(t) \\
& \quad -i\rho_{ba}(0)\rho_{n+1,m}(0)q_n(t)r_m^*(t) + \rho_{bb}(0)\rho_{n+1,m+1}(0)q_n(t)q_m(t) \\
& \quad +\rho_{bb}(0)\rho_{n,m}(0)r_{n-1}^*(t)r_{m-1}(t) + i\rho_{ba}(0)\rho_{n,m-1}(0)r_{n-1}^*(t)q_{m-1}(t)
\end{aligned}$$

$$\begin{aligned}
& -i\rho_{ab}(0)\rho_{n-1,m}(0)q_{n-1}(t)r_{m-1}(t) + \rho_{aa}(0)\rho_{n-1,m-1}(0)q_{n-1}(t)q_{m-1}(t) \\
= & \left\{ \rho_{aa}(0)r_n(t)r_m^*(t) + \rho_{bb}(0)r_{n-1}^*(t)r_{m-1}(t) \right\} \rho_{n,m}(0) \\
& + \rho_{bb}(0)q_n(t)q_m(t)\rho_{n+1,m+1}(0) + \rho_{aa}(0)q_{n-1}(t)q_{m-1}(t)\rho_{n-1,m-1}(0) \\
& + i\rho_{ab}(0) \left\{ r_n(t)q_m(t)\rho_{n,m+1}(0) - q_{n-1}(t)r_{m-1}(t)\rho_{n-1,m}(0) \right\} \\
& + i\rho_{ba}(0) \left\{ r_{n-1}^*(t)q_{m-1}(t)\rho_{n,m-1}(0) - q_n(t)r_m^*(t)\rho_{n+1,m}(0) \right\}
\end{aligned}$$

Where

$$C_{x,n}(0) = C_x(0)C_n(0)$$

$$\begin{aligned}
\rho_{xx}(0) &= \langle x | \hat{\rho}_s(0) | x \rangle \\
&= C_x(0)C_x^*(0)
\end{aligned}$$

$$\begin{aligned}
\rho_{nm}(0) &= \langle n | \hat{\rho}_f(0) | m \rangle \\
&= C_n(0)C_m^*(0)
\end{aligned}$$

$$C_{x,n}(0)C_{y,m}^*(0) = C_x(0)C_y^*(0)\rho_{nm}(0) \quad (\text{D.8})$$



## APPENDIX E

### DERIVATION OF INVERSION FOR TWO-LEVEL ATOM

Atomic inversion is given by

$$n_{ab} = \sum_{n=0}^{\infty} |C_{a,n}(t)|^2 - |C_{b,n}(t)|^2 \quad (\text{E.1})$$

For analytical solution,  $n_{ab}(t)$  can be written as

$$n_{ab}(t) = \sum_{n=0}^{\infty} (|C_{a,n}(t)|^2 - |C_{b,n+1}(t)|^2) - |C_{b,0}(t)|^2 \quad (\text{E.2})$$

Using the density matrix elements derived in Appendix D, we obtain

$$\begin{aligned} n_{ab}(t) &= \sum_{n=1}^{\infty} (|C_{a,n}(t)|^2 - |C_{b,n+1}(t)|^2) - |C_{b,1}(t)|^2 \quad (\text{E.3}) \\ &= \sum_{n=1}^{\infty} C_{a,n}(t)C_{a,n}^*(t) - C_{b,n+1}(t)C_{b,n+1}^*(t) - C_{b,1}(t)C_{b,1}^*(t) \\ &= \sum_{n=1}^{\infty} \left[ e^{i\Delta t/2} [C_{a,n}(0)r_n(t) - iC_{b,n+1}(0)q_n(t)] \right. \\ &\quad \left[ e^{-i\Delta t/2} [C_{a,n}^*(0)r_n^*(t) + iC_{b,n+1}^*(0)q_n(t)] \right] \\ &\quad - \left[ e^{-i\Delta t/2} [C_{b,n+1}(0)r_n^*(t) - iC_{a,n}(0)q_n(t)] \right] \\ &\quad \left[ e^{i\Delta t/2} [C_{b,n+1}^*(0)r_n(t) + iC_{a,n}^*(0)q_n(t)] \right] \\ &\quad - \left[ e^{-i\Delta t/2} [C_{b,1}(0)r_0^*(t) - iC_{a,0}(0)q_0(t)] \right] \\ &\quad \left. \left[ e^{i\Delta t/2} [C_{b,1}^*(0)r_0(t) + iC_{a,0}^*(0)q_0(t)] \right] \right] \\ &= \sum_{n=1}^{\infty} C_{a,n}(0)r_n(t)C_{a,n}^*(0)r_n^*(t) + C_{a,n}(0)r_n(t)iC_{b,n+1}^*(0)q_n(t) \\ &\quad - iC_{b,n+1}(0)q_n(t)C_{a,n}^*(0)r_n^*(t) - iC_{b,n+1}(0)q_n(t)iC_{b,n+1}^*(0)q_n(t) \\ &\quad - C_{b,n+1}(0)r_n^*(t)C_{b,n+1}^*(0)r_n(t) - C_{b,n+1}(0)r_n^*(t)iC_{a,n}^*(0)q_n(t) \\ &\quad + iC_{a,n}(0)q_n(t)C_{b,n+1}^*(0)r_n(t) + iC_{a,n}(0)q_n(t)iC_{a,n}^*(0)q_n(t) \\ &\quad - C_{b,1}(0)r_0^*(t)C_{b,1}^*(0)r_0(t) - C_{b,1}(0)r_0^*(t)iC_{a,0}^*(0)q_0(t) \\ &\quad + iC_{a,0}(0)q_0(t)C_{b,1}^*(0)r_0(t) + iC_{a,0}(0)q_0(t)iC_{a,0}^*(0)q_0(t) \\ &= \sum_{n=1}^{\infty} \rho_{aa}(0)\rho_{n,n}(0)r_n(t)r_n^*(t) + i\rho_{ab}(0)\rho_{n,n+1}(0)r_n(t)q_n(t) \end{aligned}$$

$$\begin{aligned}
& -i\rho_{ba}(0)\rho_{n+1,n}(0)q_n(t)r_n^*(t) + \rho_{bb}(0)\rho_{n+1,n+1}(0)q_n(t)q_n(t) \\
& -\rho_{bb}(0)\rho_{n+1,n+1}(0)r_n^*(t)r_n(t) - i\rho_{ba}(0)\rho_{n+1,n}(0)r_n^*(t)q_n(t) \\
& +i\rho_{ab}(0)\rho_{n,n+1}(0)q_n(t)r_n(t) - \rho_{aa}(0)\rho_{n,n}(0)q_n(t)q_n(t) \\
& -\rho_{bb}(0)\rho_{1,1}(0)r_0^*(t)r_0(t) - i\rho_{ba}(0)\rho_{1,0}(0)r_0^*(t)q_0(t) \\
& +i\rho_{ab}(0)\rho_{0,1}(0)q_0(t)r_0(t) - \rho_{aa}(0)\rho_{0,0}(0)q_0(t)q_0(t) \\
& \sum_{n=1}^{\infty} \{ \rho_{aa}(0)\rho_{n,n}(0) - \rho_{bb}(0)\rho_{n+1,n+1}(0) \} [r_n(t)r_n^*(t) - q_n(t)q_n(t)] \\
& +2i\rho_{ab}(0)\rho_{n,n+1}(0)r_n(t)q_n(t) - 2i\rho_{ba}(0)\rho_{n+1,n}(0)q_n(t)r_n^*(t) \\
& -\rho_{bb}(0)\rho_{1,1}(0)r_0^*(t)r_0(t) - i\rho_{ba}(0)\rho_{1,0}(0)r_0^*(t)q_0(t) \\
& +i\rho_{ab}(0)\rho_{0,1}(0)q_0(t)r_0(t) - \rho_{aa}(0)\rho_{0,0}(0)q_0(t)q_0(t)
\end{aligned}$$

So we can conclude that the atomic inversion is given by:

$$\begin{aligned}
n_{ab}(t) = & \sum_{n=1}^{\infty} \{ \rho_{aa}(0)\rho_{n,n}(0) - \rho_{bb}(0)\rho_{n+1,n+1}(0) \} [r_n(t)r_n^*(t) - q_n(t)q_n(t)] \quad (\text{E.4}) \\
& +2i\rho_{ab}(0)\rho_{n,n+1}(0)r_n(t)q_n(t) - 2i\rho_{ba}(0)\rho_{n+1,n}(0)q_n(t)r_n^*(t) \\
& -\rho_{bb}(0)\rho_{1,1}(0)r_0^*(t)r_0(t) - i\rho_{ba}(0)\rho_{1,0}(0)r_0^*(t)q_0(t) \\
& +i\rho_{ab}(0)\rho_{0,1}(0)q_0(t)r_0(t) - \rho_{aa}(0)\rho_{0,0}(0)q_0(t)q_0(t)
\end{aligned}$$

So if we substitute the term  $r_n(t)$  and  $q_n(t)$ , then it become:

$$\text{where } r_n(t) = \cos\left(\frac{\lambda(t)}{2}\right) - i\frac{\Delta}{\Omega_n} \sin\left(\frac{\lambda(t)}{2}\right), \quad q_n(t) = \frac{2g(t)(n+1)}{\Omega_n} \sin\left(\frac{\lambda(t)}{2}\right), \quad \Omega_n^2 = \Delta^2 + (2g(t)(n+1))^2$$

$$\text{and } \lambda_n(t) = \int_0^t \Omega_n(t') dt'.$$

$$\begin{aligned}
n_{ab}(t) = & \sum_{n=1}^{\infty} \{ \rho_{aa}(0)\rho_{n,n}(0) - \rho_{bb}(0)\rho_{n+1,n+1}(0) \} [r_n(t)r_n^*(t) - q_n(t)q_n(t)] \quad (\text{E.5}) \\
& +2i\rho_{ab}(0)\rho_{n,n+1}(0)r_n(t)q_n(t) - 2i\rho_{ba}(0)\rho_{n+1,n}(0)q_n(t)r_n^*(t) \\
& -\rho_{bb}(0)\rho_{1,1}(0)r_0^*(t)r_0(t) - i\rho_{ba}(0)\rho_{1,0}(0)r_0^*(t)q_0(t) \\
& +i\rho_{ab}(0)\rho_{0,1}(0)q_0(t)r_0(t) - \rho_{aa}(0)\rho_{0,0}(0)q_0(t)q_0(t) \\
= & \sum_{n=1}^{\infty} \{ \rho_{aa}(0)\rho_{n,n}(0) - \rho_{bb}(0)\rho_{n+1,n+1}(0) \} \\
& \left\{ \left( \cos\left(\frac{\lambda_n(t)}{2}\right) - i\frac{\Delta}{\Omega_n} \sin\left(\frac{\lambda_n(t)}{2}\right) \right) \left( \cos\left(\frac{\lambda_n(t)}{2}\right) + i\frac{\Delta}{\Omega_n} \sin\left(\frac{\lambda_n(t)}{2}\right) \right) \right. \\
& \left. - \left( \frac{2g(t)(n+1)}{\Omega_n} \sin\left(\frac{\lambda_n(t)}{2}\right) \right)^2 \right\}
\end{aligned}$$

$$\begin{aligned}
& +2i\rho_{ab}(0)\rho_{n,n+1}(0)\left(\cos\left(\frac{\lambda_n(t)}{2}\right)-i\frac{\Delta}{\Omega_n}\sin\left(\frac{\lambda_n(t)}{2}\right)\right) \\
& \left(\frac{2g(t)(n+1)}{\Omega_n}\sin\left(\frac{\lambda_n(t)}{2}\right)\right) \\
& -2i\rho_{ba}(0)\rho_{n+1,n}(0)\left(\frac{2g(t)(n+1)}{\Omega_n}\sin\left(\frac{\lambda_n(t)}{2}\right)\right) \\
& \left(\cos\left(\frac{\lambda_n(t)}{2}\right)+i\frac{\Delta}{\Omega_n}\sin\left(\frac{\lambda_n(t)}{2}\right)\right) \\
& -\rho_{bb}(0)\rho_{1,1}(0)\left(\cos\left(\frac{\lambda_0(t)}{2}\right)+i\frac{\Delta}{\Omega_0}\right)\left(\cos\left(\frac{\lambda_0(t)}{2}\right)-i\frac{\Delta}{\Omega_0}\right) \\
& -i\rho_{ba}(0)\rho_{1,0}(0)\left(\cos\left(\frac{\lambda_0(t)}{2}\right)+i\frac{\Delta}{\Omega_0}\right)\left(\frac{2g(t)}{\Omega_0}\sin\left(\frac{\lambda_0(t)}{2}\right)\right) \\
& +i\rho_{ab}(0)\rho_{0,1}(0)\left(\frac{2g(t)}{\Omega_0}\sin\left(\frac{\lambda_0(t)}{2}\right)\right)\left(\cos\left(\frac{\lambda_0(t)}{2}\right)-i\frac{\Delta}{\Omega_0}\right) \\
& -\rho_{aa}(0)\rho_{0,0}(0)\left(\frac{2g(t)}{\Omega_0}\sin\left(\frac{\lambda_0(t)}{2}\right)\right)^2 \\
& = \sum_{n=1}^{\infty} \left\{ \rho_{aa}(0)\rho_{n,n}(0) - \rho_{bb}(0)\rho_{n+1,n+1}(0) \right\} \left\{ \left( \cos\left(\frac{\lambda_n(t)}{2}\right) \right)^2 \right. \\
& \left. + \frac{\Delta^2}{\Omega_n^2} \left( \sin\left(\frac{\lambda_n(t)}{2}\right) \right)^2 - \frac{4g^2(t)(n+1)^2}{\Omega_n^2} \left( \sin\left(\frac{\lambda_n(t)}{2}\right) \right)^2 \right\} \\
& + 2i\rho_{ab}(0)\rho_{n,n+1}(0)\frac{2g(t)(n+1)}{\Omega_n} \left\{ \left( \sin\left(\frac{\lambda_n(t)}{2}\right) \cos\left(\frac{\lambda_n(t)}{2}\right) \right) \right. \\
& \left. - i\Delta \frac{2g(t)(n+1)}{\Omega_n^2} \left( \sin\left(\frac{\lambda_n(t)}{2}\right) \right)^2 \right\} \\
& - 2i\rho_{ba}(0)\rho_{n+1,n}(0) \left\{ \frac{2g(t)(n+1)}{\Omega_n} \left( \sin\left(\frac{\lambda_n(t)}{2}\right) \cos\left(\frac{\lambda_n(t)}{2}\right) \right) \right. \\
& \left. + i\Delta \frac{2g(t)(n+1)}{\Omega_n^2} \left( \sin\left(\frac{\lambda_n(t)}{2}\right) \right)^2 \right\} \\
& - \rho_{bb}(0)\rho_{1,1}(0) \left[ \left( \cos\left(\frac{\lambda_0(t)}{2}\right) \right)^2 + \left( \frac{\Delta^2}{\Omega_0^2} \right) \right] \\
& - \rho_{aa}(0)\rho_{0,0}(0) \frac{4g^2(t)}{\Omega_0^2} \left( \sin\left(\frac{\lambda_0(t)}{2}\right) \right)^2 \\
& - i\rho_{ba}(0)\rho_{1,0}(0) \left( \left( \frac{g(t)}{\Omega_0} \sin\lambda_0(t) \right) + i\Delta \frac{2g(t)}{\Omega_0^2} \left( \sin\left(\frac{\lambda_0(t)}{2}\right) \right) \right) \\
& + i\rho_{ab}(0)\rho_{0,1}(0) \left( \left( \frac{g(t)}{\Omega_0} \sin\lambda_0(t) \right) - i\Delta \frac{2g(t)}{\Omega_0^2} \left( \sin\left(\frac{\lambda_0(t)}{2}\right) \right) \right)
\end{aligned}$$

where the trigonometric function give  $\sin 2\phi = 2 \sin \phi \cos \phi$  and  $\cos^2 \phi + \sin^2 \phi = 1$ .

while  $r_0(t) = \cos\left(\frac{\lambda_0(t)}{2}\right) - i\frac{\Delta}{\Omega_0} \sin\left(\frac{\lambda_0(t)}{2}\right)$ ,  $q_0(t) = \frac{2g(t)}{\Omega_0} \sin\left(\frac{\lambda_0(t)}{2}\right)$ ,  $\Omega_0^2 = \Delta^2 + 4g^2(t)$

and  $\lambda_0(t) = \int_0^t \Omega_0(t') dt'$ .

$$\begin{aligned}
n_{ab}(t) &= \sum_{n=1}^{\infty} \{ \rho_{aa}(0) \rho_{n,n}(0) - \rho_{bb}(0) \rho_{n+1,n+1}(0) \} \\
&\quad \left[ \left( \cos\left(\frac{\lambda_n(t)}{2}\right) \right)^2 + \left( \frac{\Delta^2 - 4g^2(t)(n+1)^2}{\Omega_n^2} \right) \left( \sin\left(\frac{\lambda_n(t)}{2}\right) \right)^2 \right] \\
&\quad + 2i\rho_{ab}(0) \rho_{n,n+1}(0) \left( \frac{g(t)(n+1)}{\Omega_n} \sin(\lambda_n(t)) - i\Delta \frac{2g(t)(n+1)}{\Omega_n^2} \left( \sin\left(\frac{\lambda_n(t)}{2}\right) \right)^2 \right) \\
&\quad - 2i\rho_{ba}(0) \rho_{n+1,n}(0) \left( \frac{g(t)(n+1)}{\Omega_n} \sin(\lambda_n(t)) + i\Delta \frac{2g(t)(n+1)}{\Omega_n^2} \left( \sin\left(\frac{\lambda_n(t)}{2}\right) \right)^2 \right) \\
&\quad - \rho_{bb}(0) \rho_{1,1}(0) \left[ \left( \cos\left(\frac{\lambda_0(t)}{2}\right) \right)^2 + \frac{\Delta^2}{\Omega_0^2} \right] - \rho_{aa}(0) \rho_{0,0}(0) \frac{4g^2(t)}{\Omega_0^2} \left( \sin\left(\frac{\lambda_0(t)}{2}\right) \right)^2 \\
&\quad - i\rho_{ba}(0) \rho_{1,0}(0) \left( \left( \frac{g(t)}{\Omega_0} \sin \lambda_0(t) \right) + i\Delta \frac{2g(t)}{\Omega_0^2} \left( \sin\left(\frac{\lambda_0(t)}{2}\right) \right) \right) \\
&\quad + i\rho_{ab}(0) \rho_{0,1}(0) \left( \left( \frac{g(t)}{\Omega_0} \sin \lambda_0(t) \right) - i\Delta \frac{2g(t)}{\Omega_0^2} \left( \sin\left(\frac{\lambda_0(t)}{2}\right) \right) \right) \\
&= \sum_{n=1}^{\infty} \{ \rho_{aa}(0) \rho_{n,n}(0) - \rho_{bb}(0) \rho_{n+1,n+1}(0) \} \\
&\quad \left[ 1 + \left( \frac{-8(g(t)(n+1))^2}{\Omega_n^2} \right) \left( \sin\left(\frac{\lambda(t)}{2}\right) \right)^2 \right] \\
&\quad + 2i\rho_{ab}(0) \rho_{n,n+1}(0) D_n^* - 2i\rho_{ba}(0) \rho_{n+1,n}(0) D_n \\
&\quad - \rho_{bb}(0) \rho_{1,1}(0) \left[ \left( \cos\left(\frac{\lambda_0(t)}{2}\right) \right)^2 + \frac{\Delta^2}{\Omega_0^2} \right] \\
&\quad - \rho_{aa}(0) \rho_{0,0}(0) \frac{4g^2(t)}{\Omega_0^2} \left( \sin\left(\frac{\lambda_0(t)}{2}\right) \right)^2 - i\rho_{ba}(0) \rho_{1,0}(0) D_0 + i\rho_{ab}(0) \rho_{0,1}(0) D_0^*
\end{aligned} \tag{E.6}$$

where  $D_n = \frac{g(t)(n+1)}{\Omega_n} \sin(\lambda(t)) + i\Delta \frac{2g(t)(n+1)}{\Omega_n^2} \left( \sin\left(\frac{\lambda(t)}{2}\right) \right)^2$ .

Finally we obtain:

$$\begin{aligned}
n_{ab}(t) &= \sum_{n=1}^{\infty} \{ \rho_{aa}(0) \rho_{n,n}(0) - \rho_{bb}(0) \rho_{n+1,n+1}(0) \} \\
&\quad \left[ 1 + \left( \frac{-8(g(t)(n+1))^2}{\Omega_n^2} \right) \left( \sin\left(\frac{\lambda(t)}{2}\right) \right)^2 \right] \\
&\quad + 2i\rho_{ab}(0) \rho_{n,n+1}(0) D_n^* - 2i\rho_{ba}(0) \rho_{n+1,n}(0) D_n \\
&\quad - \rho_{bb}(0) \rho_{1,1}(0) \left[ \left( \cos\left(\frac{\lambda_0(t)}{2}\right) \right)^2 + \frac{\Delta^2}{\Omega_0^2} \right] \\
&\quad - \rho_{aa}(0) \rho_{0,0}(0) \frac{4g^2(t)}{\Omega_0^2} \left( \sin\left(\frac{\lambda_0(t)}{2}\right) \right)^2 \\
&\quad - i\rho_{ba}(0) \rho_{1,0}(0) D_0 + i\rho_{ab}(0) \rho_{0,1}(0) D_0^*
\end{aligned} \tag{E.7}$$

## APPENDIX F

### DENSITY MATRIX ELEMENTS FOR THREE-LEVEL ATOM

In order to solve the matrix elements in Chapter 5, the equations of motion for a slowly varying amplitude are introduced as

$$\begin{aligned}
 \tilde{\rho}_{ab} &= \hat{\rho}_{ab} e^{-i\Delta_p t} \\
 \tilde{\rho}_{ba} &= \hat{\rho}_{ba} e^{i\Delta_p t} \\
 \tilde{\rho}_{ac} &= \hat{\rho}_{ac} e^{-i\Delta_c t} \\
 \tilde{\rho}_{ca} &= \hat{\rho}_{ca} e^{i\Delta_c t} \\
 \tilde{\rho}_{cb} &= \hat{\rho}_{cb} e^{i(\Delta_c - \Delta_p)t} \\
 \tilde{\rho}_{bc} &= \hat{\rho}_{bc} e^{-i(\Delta_c - \Delta_p)t}
 \end{aligned} \tag{F.1}$$

By using the general differentiation rule,

$$\begin{aligned}
 \frac{d}{dt} \tilde{\rho}_{ab} &= \frac{d}{dt} \hat{\rho}_{ab} e^{-i\Delta_p t} \\
 &= \hat{\rho}_{ab} \frac{d}{dt} e^{-i\Delta_p t} + e^{-i\Delta_p t} \frac{d}{dt} \hat{\rho}_{ab}
 \end{aligned} \tag{F.2}$$

the elements then becomes:

$$\begin{aligned}
 \frac{d}{dt} \hat{\rho}_{aa} &= -i\Omega_p \tilde{\rho}_{ba} + i\Omega_p \tilde{\rho}_{ab} - ig(t) \hat{a} \tilde{\rho}_{ca} + ig(t) \tilde{\rho}_{ac} \hat{a}^\dagger \\
 &\quad + \gamma_F L(\hat{\rho}_{aa}) - 2(\Gamma_{ac} + \Gamma_{ab}) \hat{\rho}_{aa} \\
 \frac{d}{dt} \hat{\rho}_{bb} &= -i\Omega_p \tilde{\rho}_{ab} + i\Omega_p \tilde{\rho}_{ba} + \gamma_F L(\hat{\rho}_{bb}) + 2\Gamma_{ab} \hat{\rho}_{aa} \\
 \frac{d}{dt} \hat{\rho}_{cc} &= -ig(t) \hat{a}^\dagger \tilde{\rho}_{ac} + ig(t) \tilde{\rho}_{ca} \hat{a} + \gamma_F L(\hat{\rho}_{cc}) + 2\Gamma_{ac} \hat{\rho}_{aa} \\
 \frac{d}{dt} \tilde{\rho}_{ca} &= i\Delta_c \tilde{\rho}_{ca} + i\Omega_p \tilde{\rho}_{cb} + ig(t) \hat{\rho}_{cc} \hat{a}^\dagger - ig(t) \hat{a}^\dagger \hat{\rho}_{aa} \\
 &\quad + \gamma_F L(\tilde{\rho}_{ca}) - (\Gamma_{ac} + \Gamma_{ab}) \tilde{\rho}_{ca} \\
 \frac{d}{dt} \tilde{\rho}_{ac} &= -i\Delta_c \tilde{\rho}_{ac} - i\Omega_p \tilde{\rho}_{bc} - ig(t) \hat{a} \hat{\rho}_{cc} + ig(t) \hat{\rho}_{aa} \hat{a} \\
 &\quad + \gamma_F L(\tilde{\rho}_{ac}) - (\Gamma_{ac} + \Gamma_{ab}) \tilde{\rho}_{ac}
 \end{aligned} \tag{F.3}$$

$$\begin{aligned}
\frac{d}{dt}\tilde{\rho}_{ba} &= i\Delta_p\hat{\rho}_{ba} - i\Omega_p\hat{\rho}_{aa} + i\Omega_p\hat{\rho}_{bb} + ig(t)\tilde{\rho}_{bc}\hat{a}^\dagger \\
&\quad + \gamma_F L(\tilde{\rho}_{ba}) - (\Gamma_{ac} + \Gamma_{ab})\tilde{\rho}_{ba} \\
\frac{d}{dt}\tilde{\rho}_{ab} &= -i\Delta_p\tilde{\rho}_{ab} - i\Omega_p\hat{\rho}_{bb} + i\Omega_p\hat{\rho}_{aa} - ig(t)\hat{a}\tilde{\rho}_{cb} \\
&\quad + \gamma_F L(\tilde{\rho}_{ab}) - (\Gamma_{ac} + \Gamma_{ab})\tilde{\rho}_{ab} \\
\frac{d}{dt}\tilde{\rho}_{bc} &= -i(\Delta_c - \Delta_p)\tilde{\rho}_{bc} - i\Omega_p\tilde{\rho}_{ac} + ig(t)\tilde{\rho}_{ba}\hat{a} + \gamma_F L(\tilde{\rho}_{bc}) \\
\frac{d}{dt}\tilde{\rho}_{cb} &= i(\Delta_c - \Delta_p)\tilde{\rho}_{cb} + i\Omega_p\tilde{\rho}_{ca} - ig(t)\hat{a}^\dagger\tilde{\rho}_{ab} + \gamma_F L(\tilde{\rho}_{cb})
\end{aligned}$$

Rearrange the elements:

$$\begin{aligned}
\frac{d}{dt}\hat{\rho}_{aa} &= i\Omega_p[\tilde{\rho}_{ab} - \tilde{\rho}_{ba}] + ig(t)[\tilde{\rho}_{ac}\hat{a}^\dagger - \hat{a}\tilde{\rho}_{ca}] + \gamma_F L(\hat{\rho}_{aa}) \\
&\quad - 2(\Gamma_{ac} + \Gamma_{ab})\hat{\rho}_{aa} \\
\frac{d}{dt}\hat{\rho}_{bb} &= i\Omega_p[\tilde{\rho}_{ba} - \tilde{\rho}_{ab}] + \gamma_F L(\hat{\rho}_{bb}) + 2\Gamma_{ab}\hat{\rho}_{aa} \\
\frac{d}{dt}\hat{\rho}_{cc} &= ig(t)[\tilde{\rho}_{ca}\hat{a} - \hat{a}^\dagger\tilde{\rho}_{ac}] + \gamma_F L(\hat{\rho}_{cc}) + 2\Gamma_{ac}\hat{\rho}_{aa} \\
\frac{d}{dt}\tilde{\rho}_{ca} &= i\Delta_c\tilde{\rho}_{ca} + i\Omega_p\tilde{\rho}_{cb} + ig(t)[\hat{\rho}_{cc}\hat{a}^\dagger - \hat{a}^\dagger\hat{\rho}_{aa}] \\
&\quad + \gamma_F L(\tilde{\rho}_{ca}) - (\Gamma_{ac} + \Gamma_{ab})\tilde{\rho}_{ca} \\
\frac{d}{dt}\tilde{\rho}_{ac} &= -i\Delta_c\tilde{\rho}_{ac} - i\Omega_p\tilde{\rho}_{bc} + ig(t)[\hat{\rho}_{aa}\hat{a} - \hat{a}\hat{\rho}_{cc}] \\
&\quad + \gamma_F L(\tilde{\rho}_{ac}) - (\Gamma_{ac} + \Gamma_{ab})\tilde{\rho}_{ac} \\
\frac{d}{dt}\tilde{\rho}_{ba} &= i\Delta_p\hat{\rho}_{ba} + i\Omega_p[\hat{\rho}_{bb} - \hat{\rho}_{aa}] + ig(t)\tilde{\rho}_{bc}\hat{a}^\dagger \\
&\quad + \gamma_F L(\tilde{\rho}_{ba}) - (\Gamma_{ac} + \Gamma_{ab})\tilde{\rho}_{ba} \\
\frac{d}{dt}\tilde{\rho}_{ab} &= -i\Delta_p\tilde{\rho}_{ab} + i\Omega_p[\hat{\rho}_{aa} - \hat{\rho}_{bb}] - ig(t)\hat{a}\tilde{\rho}_{cb} \\
&\quad + \gamma_F L(\tilde{\rho}_{ab}) - (\Gamma_{ac} + \Gamma_{ab})\tilde{\rho}_{ab} \\
\frac{d}{dt}\tilde{\rho}_{bc} &= -i(\Delta_c - \Delta_p)\tilde{\rho}_{bc} - i\Omega_p\tilde{\rho}_{ac} + ig(t)\tilde{\rho}_{ba}\hat{a} + \gamma_F L(\tilde{\rho}_{bc}) \\
\frac{d}{dt}\tilde{\rho}_{cb} &= i(\Delta_c - \Delta_p)\tilde{\rho}_{cb} + i\Omega_p\tilde{\rho}_{ca} - ig(t)\hat{a}^\dagger\tilde{\rho}_{ab} + \gamma_F L(\tilde{\rho}_{cb})
\end{aligned} \tag{F.4}$$

For all equations above we can derive a system of coupled equations using the action of operator  $\hat{a}$  and  $\hat{a}^\dagger$  on a basis  $|n\rangle$  and  $\langle n|$  as discussed in chapter 1, then for the diagonal element for photon number we obtain

$$\frac{d}{dt}\hat{\rho}_{aa}(n, n) = i\Omega_p[\tilde{\rho}_{ab}(n, n) - \tilde{\rho}_{ba}(n, n)] \tag{F.5}$$

$$+ig(t)\sqrt{n+1}\tilde{\rho}_{ac}(n,n+1)$$

$$-ig(t)\sqrt{n+1}\tilde{\rho}_{ca}(n+1,n)$$

$$+2\gamma_F(n+1)\hat{\rho}_{aa}(n+1,n+1)$$

$$-2(\gamma_F n + \Gamma_{ac} + \Gamma_{ab})\hat{\rho}_{aa}(n,n)$$

$$\frac{d}{dt}\hat{\rho}_{bb}(n,n) = i\Omega_p[\tilde{\rho}_{ba}(n,n) - \tilde{\rho}_{ab}(n,n)] \quad (\text{F.6})$$

$$+2\gamma_F(n+1)\hat{\rho}_{bb}(n+1,n+1)$$

$$-2\gamma_F n\hat{\rho}_{bb}(n,n) + 2\Gamma_{ab}\hat{\rho}_{aa}(n,n)$$

$$\frac{d}{dt}\hat{\rho}_{cc}(n,n) = ig(t)[\sqrt{n}\tilde{\rho}_{ca}(n,n-1) - \sqrt{n}\tilde{\rho}_{ac}(n-1,n)] \quad (\text{F.7})$$

$$+2\gamma_F(n+1)\hat{\rho}_{cc}(n+1,n+1)$$

$$-2\gamma_F n\hat{\rho}_{cc}(n,n) + 2\Gamma_{ac}\hat{\rho}_{aa}(n,n)$$

$$\frac{d}{dt}\tilde{\rho}_{ca}(n+1,n) = i\Delta_c\tilde{\rho}_{ca}(n+1,n) + i\Omega_p\tilde{\rho}_{cb}(n+1,n) \quad (\text{F.8})$$

$$+ig(t)\sqrt{n+1}\hat{\rho}_{cc}(n+1,n+1)$$

$$-ig(t)\sqrt{n+1}\hat{\rho}_{aa}(n,n)$$

$$+2\gamma_F\sqrt{n+1}\sqrt{n+1}\hat{\rho}_{ca}(n+2,n+1)$$

$$-\gamma_F(n+1)\hat{\rho}_{ca}(n+1,n)$$

$$-\gamma_F n\hat{\rho}_{ca}(n+1,n) - (\Gamma_{ac} + \Gamma_{ab})\tilde{\rho}_{ca}(n+1,n)$$

$$\frac{d}{dt}\tilde{\rho}_{ac}(n,n+1) = \frac{d}{dt}\tilde{\rho}_{ca}^*(n+1,n) \quad (\text{F.9})$$

$$\frac{d}{dt}\tilde{\rho}_{ba}(n,n) = (i\Delta_p - 2\gamma_F n - \Gamma_{ac} - \Gamma_{ab})\tilde{\rho}_{ba}(n,n) \quad (\text{F.10})$$

$$+i\Omega_p[\hat{\rho}_{bb}(n,n) - \hat{\rho}_{aa}(n,n)]$$

$$+ig(t)\sqrt{n+1}\tilde{\rho}_{bc}(n,n+1)$$

$$+2\gamma_F(n+1)\hat{\rho}_{ba}(n+1,n+1)$$

$$\frac{d}{dt}\tilde{\rho}_{ab}(n,n) = \frac{d}{dt}\tilde{\rho}_{ba}^*(n,n) \quad (\text{F.11})$$

$$\frac{d}{dt}\tilde{\rho}_{cb}(n+1,n) = (i(\Delta_c - \Delta_p) - \gamma_F(2n+1))\hat{\rho}_{cb}(n+1,n) \quad (\text{F.12})$$

$$+i\Omega_p\tilde{\rho}_{ca}(n+1,n) - ig(t)\sqrt{n+1}\tilde{\rho}_{ab}(n,n)$$

$$+2\gamma_F\sqrt{n+1}\sqrt{n+1}\hat{\rho}_{cb}(n+2,n+1)$$

$$\tilde{\rho}_{bc}(n,n+1) = \frac{d}{dt}\tilde{\rho}_{cb}^*(n+1,n) \quad (\text{F.13})$$

## REFERENCES

- Abdel-Aty, M. (2000). Influence of a kerr-like medium on the evolution of field entropy and entanglement in a three-level atom. *J. Phys. B: At. Mol. Opt. Phys.*, 33(14), 2665.
- Abdel-Aty, M. (2004). Mixed-state entanglement of a three-level system with an intensity-dependent interaction. *J. Phys. A: Math. Gen.*, 37(5), 1759.
- Abdel-Aty, M., & Obada, A. S. F. (2003). Engineering entanglement of a general three-level system interacting with a correlated two-mode nonlinear coherent state. *THE EUROPEAN PHYSICAL JOURNAL D*, 23(1), 155-165.
- Agarwal, G. S., & Tara, K. (1992). Nonclassical character of states exhibiting no squeezing or sub-poissonian statistics. *Physical Review A*, 46, 485–488.
- Araki, H., & Lieb, E. H. (1970). Entropy inequalities. *Communication in Mathematical Physics*, 18(2), 160 - 170.
- Banaszek, K., & Wodkiewicz, K. (1996). Direct probing of quantum phase space by photon counting. *Physical Review Letters*, 76, 4344–4347.
- Barnett, S. M., & Radmore, P. M. (1997). *Methods in theoretical quantum optics*. Oxford University Press.
- Berman, P. R., & Ooi, C. H. R. (2012). Pulse propagation in a medium of  $\lambda$ -type atoms. *Physical Review A*, 86, 053812.
- Boller, J., Imamoglu, A., & Harris, S. E. (1991). Observation of electromagnetically induced transparency. *Physical Review Letters*, 66, 2593.
- Boto, A. N., Kok, P., Abrams, D. S., Braunstein, S. L., Williams, C. P., & Dowling, J. P. (2000). Quantum interferometric optical lithography: Exploiting entanglement to beat the diffraction limit. *Phys. Rev. Lett.*, 85, 2733-2736.
- Bouwmeester, D., Ekert, A. K., & Zeilinger, A. (2000). *The physics of quantum information: Quantum cryptography, quantum teleportation, quantum computation*. Springer.
- Breuer, H.-P., & Petruccione, F. (2002). *The theory of open quantum systems*. Oxford University Press.
- Buck, B., & Sukumar, C. V. (1981). Exactly soluble model of atom-phonon coupling showing periodic decay and revival. *Physics Letters A*, 81(2-3), 132 - 135. Retrieved from <http://www.sciencedirect.com/science/article/pii/0375960181900426> doi: 10.1016/0375-9601(81)90042-6
- Buzek, V., & Hladky, B. (1993). Macroscopic superposition states of light via two-photon resonant interaction of atoms with cavity field. *Journal of Modern Optics*, 40(7), 1309-1324.
- Cahill, K. E., & Glauber, R. J. (1969). Density operators and quasiprobability distributions. *Physical Review A*, 177, 1882–1902.
- Cohen-Tannoudji, C., Diu, B., & Laloe, F. (1977). *Quantum mechanics, vol 1*. Wiley.
- Cohen-Tannoudji, C., & Dupont-Roc, J. (1972). Experimental study of zeeman light shifts in weak magnetic fields. *Physical Review A*, 5(2), 968-984.
- Dakna, M., Anhut, T., Opatrny, T., Knoll, L., & Welsch, D.-G. (1997). Generating schrodinger-cat-like states by means of conditional measurements on a beam splitter. *Physical Review A*, 55, 3184–3194.
- D’Angelo, M., Chekhova, M. V., & Shih, Y. (2001). Two-photon diffraction and quantum lithography. *Phys. Rev. Lett.*, 87, 013602-013605.



- Dung, H., Tanas, R., & Shumovsky, A. S. (1990). Collapses, revivals, and phase properties of the field in jaynes-cummings type models. *Optics Communication*, 79, 462–468.
- Faghihi, M. J., & Tavassoly, M. K. (2012). Dynamics of entropy and nonclassical properties of the state of a  $\lambda$ -type three-level atom interacting with a single-mode cavity field with intensity-dependent coupling in a kerr medium. *J. Phys. B: At. Mol. Opt. Phys.*, 45, 035502.
- Feynman, R. P., Jr., F. L. V., & Hellwarth, R. W. (1957). Geometrical representation of the schrödinger equation for solving maser problems. *J. Appl. Phys.*, 28(1), 49-52. doi: 10.1063/1.1722572
- Fleischhauer, M., Imamoglu, A., & Marangos, J. P. (2005). Electromagnetically induced transparency: Optics in coherent media. *Reviews of Modern Physics*, 77(2), 633-673.
- Fox, M. (2006). *Quantum optics: An introduction*. Oxford University Press.
- Friedrich, B., & Herschbach, D. (1995). Alignment and trapping of molecules in intense laser fields. *Physical Review Letters*, 74, 4623–4626.
- Gatti, A., Brambilla, E., Bache, M., & Lugiato, L. A. (2004). Correlated imaging, quantum and classical. *Phys. Rev. A*, 70, 013802-013811.
- Gerry, C. C., & Knight, P. L. (2004). *Introductory quantum optics*. Cambridge University Press.
- Glauber, R. J. (1963). The quantum theory of optical coherence. *Phys. Rev.*, 130, 2529-2539.
- Glauber, R. J., & Lewenstein, M. (1991). Quantum optics of dielectric media. *Physical Review A*, 43, 467–491.
- Harel, G., Kurizk, G., McIver, J. K., & Coutias, E. (1996). Optimized preparation of quantum states by conditional measurements: Quantum optics of dielectric media. *Physical Review A*, 53, 4534–4538.
- Haroche, S., & Raimond, J. M. (2006). *Exploring the quantum*. Oxford University Press.
- Hessian, H., Mohammed, F., & Mohamed, A.-B. (2009). Entropy and entanglement in master equation of effective hamiltonian for jaynes-cummings model. *Communications in Theoretical Physics*, 51(4), 723-728.
- Huang, C., Tang, L., Kong, F., Fang, J., & Zhou, M. (2006). Entropy evolution of field interacting with v-type three-level atom via intensity-dependent coupling. *Physica A*, 368, 25-30.
- Jaynes, E. T., & Cummings, F. W. (1963). Comparison of quantum and semiclassical radiation theories with application to the beam maser. *Proceedings of the IEEE*, 51(1), 89 - 109. doi: 10.1109/PROC.1963.1664
- Jeong, H., & Ralph, T. (2007). Schrodinger cat states for quantum information processing. In N. J. Cerf, G. Leuchs, & E. S. Polzik (Eds.), *Quantum information with continuous variables of atoms and light*. London: Imperial College Press.
- Jones, G. N., Haight, J., & Lee, C. T. (1997). Nonclassical effects in photon-added thermal state. *Quantum Semiclassical Optic*, 9, 411–418.
- Kim, B.-G., Ooi, C. H. R., Ikram, M., & Lee, H.-W. (2009). Directional property of radiation emitted from entangled atoms. *Physics Letters A*, 373, 1658-1662.
- Kofman, A. G., & Kurizki, G. (1996). Quantum zeno effect on atomic excitation decay in resonators. *Physical Review A*, 54, R3750–R3753.
- Kofman, A. G., & Kurizki, G. (2000). Acceleration of quantum decay processes by frequent observation. *Nature*, 405, 546–550.
- Kofman, A. G., & Kurizki, G. (2001). Universal dynamical control of quantum mechanical decay: modu-

- lation of the coupling to the continuum. *Physical Review Letters*, 87, 270405.
- Kofman, A. G., & Kurizki, G. (2004). Unified theory of dynamically suppressed qubit decoherence in thermal baths. *Physical Review Letters*, 93, 130406.
- Kofman, A. G., Kurizki, G., & Opatrny, T. (2001). Zeno and anti-zeno effects for photon polarization dephasing. *Physical Review A*, 63, 042108.
- Lambropoulos, P., & Petrosyan, D. (2007). *Fundamentals of quantum optics and quantum information*. Springer-Verlag.
- Lee, C. T. (1991). Measure of the nonclassicality of nonclassical states. *Physical Review A*, 44, R2775–R2778.
- Leibfried, D., Knill, E., Seidlin, S., Britton, J., Blakestad, R. B., Chiaverini, J., . . . Wineland, D. J. (2005). Creation of a six-atom schrodinger cat state. *Nature*, 438, 639–642.
- Lutterbach, L. G., & Davidovich, L. (1997). Method for direct measurement of the wigner function in cavity qed and ion traps. *Physical Review Letters*, 78, 2547–2550.
- Ivarez, G. A., Rao, D. D. B., Frydman, L., & Kurizki, G. (2010). Zeno and anti-zeno polarization control of spin ensembles by induced dephasing. *Physical Review Letters*, 105, 160401.
- Lvovsky, A. I., Hansen, H., Aichele, T., Benson, O., Mlynek, J., & Schiller, S. (2001). Quantum state reconstruction of the single-photon fock state. *Physical Review A*, 63, 050402.
- Meystre, P., & Sargent, M. (2007). *Elements of quantum optics*. Springer.
- Milburn, G. J., & Walls, D. F. (2008). *Quantum optics*. Springer.
- Monroe, C., Meekhof, D. M., King, B. E., & Wineland, D. J. (1996). A ‘schrodinger cat’ superposition of an atom. *Science*, 272, 1131–1136.
- Nogues, G. G., Rauschenbeutel, A., Osnaghi, S., Bertet, P., Brune, M., Raimond, J. M., . . . Davidovich, L. (2000). Measurement of a negative value for the wigner function of radiation. *Physical Review A*, 62, 054101–054104.
- Ooi, C. H. R. (2007). Quenching the collective effects on the two-photon correlation from two double-raman atoms. *Phys. Rev. A*, 75, 043817.
- Ooi, C. H. R., & Gong, Q. (2012). Nonclassical photon correlation of nanoparticle in a microcavity. *Phys. Rev. A*, 85, 023803.
- Ooi, C. H. R., Hazmin, S. N., & Singh, S. (2012). Nonclassical dynamics with time- and intensity-dependent coupling. *Quantum Information Processing*, 1–18. Retrieved from <http://dx.doi.org/10.1007/s11128-012-0512-6> doi: 10.1007/s11128-012-0512-6
- Ooi, C. H. R., & Khoo, Y. Y. (2012). Controlling the repulsive casimir force with the optical kerr effect. *Physical Review A*, 86, 062509.
- Ooi, C. H. R., Kim, B.-G., & Lee, H.-W. (2007). Coherent effects on two-photon correlation and directional emission of two two-level atoms. *Phys. Rev. A*, 75, 063801.
- Ooi, C. H. R., Sun, Q., Zubairy, M. S., & Scully, M. O. (2007). Correlation of photon pairs from the double raman amplifier: Generalized analytical quantum langevin theory. *Phys. Rev. A*, 75, 013820.
- Ourjoumtsev, A., Jeong, H., Tualle-Brouiri, R., & Grangier, P. (2007). Generation of optical schrodinger cats from photon number states. *Nature*, 448, 784–786.
- Puri, R. R., & Agarwal, G. S. (2001). *Mathematical methods of quantum optics*. Springer.

- Qiang, W.-C., Cardoso, W., & Zhang, X.-H. (2010). The entropy of entangled three-level atoms interacting with entangled cavity fields: Entanglement swapping. *Physica A*, 389, 5109-5115.
- Raimond, J. M., Sayrin, C., Gleyzes, S., Dotsenko, I., Brune, M., Haroche, S., ... Pascazio, S. (2010). Phase space tweezers for tailoring cavity fields by quantum zeno dynamics. *Physical Review Letters*, 105, 213601.
- Ralph, T. C., Gilchrist, A., & Milburn, G. J. (2003). Quantum computation with optical coherent states. *Physical Review A*, 68, 042319.
- Schleich, W. P. (2001). *Quantum optics in phase space*. Wiley-VCH.
- Scully, M. O., & Drühl, K. (1982). Quantum eraser: A proposed photon correlation experiment concerning observation and "delayed choice" in quantum mechanics. *Phys. Rev. A*, 25, 2208-2213.
- Scully, M. O., & Ooi, C. H. R. (2004). Improving quantum microscopy and lithography via raman photon pairs: II. analysis. *Journal of Optics B: Quantum and Semiclassical Optics*, 6(8), S816.
- Scully, M. O., Rathe, U. W., Su, C., & Agarwal, G. S. (1997). On enhancing spectral resolution via correlated spontaneous emission. *Optics Communications*, 136, 39-43.
- Scully, M. O., & Zubairy, M. S. (1997). *Quantum optics*. Cambridge University Press.
- Sete, E. A., & Ooi, C. H. R. (2012). Continuous-variable entanglement and two-mode squeezing in a single-atom raman laser. *Phys. Rev. A*, 85, 063819.
- Sherman, B., Kurizki, G., & Kadyshevitch, A. (1992). Nonclassical field dynamics in photonic band structures: Atomic-beam resonant interaction with a spatially periodic field mode. *Physical Review Letter*, 69, 1927-1930.
- Shore, B. W., & Knight, P. L. (1993). The jaynes-cummings model. *Journal of Modern Optics*, 40(7), 1195-1238.
- Singh, S., Ooi, C. H. R., & Amrita. (2012). Dynamics for two atoms interacting with intensity-dependent two-mode quantized cavity fields in the ladder configuration. *Physical Review A*, 86, 023810.
- Sukumar, C. V., & Buck, B. (1981). Multi-phonon generalisation of the jaynes-cummings model. *Physics Letters A*, 83(5), 211 - 213. Retrieved from <http://www.sciencedirect.com/science/article/pii/0375960181908252> doi: 10.1016/0375-9601(81)90825-2
- Sumairi, A., Hazmin, S. N., & Ooi, C. H. R. (2013). Quantum entanglement criteria. *Journal of Modern Optics*, 60(7), 589-597.
- Vernooy, D. W., & Kimble, H. J. (1997). Well-dressed states for wave-packet dynamics in cavity qed. *Physical Review A*, 56, 4287-4295.
- Wallentowitz, S., & Vogel, W. (1996). Unbalanced homodyning for quantum state measurements. *Physical Review A*, 53, 4528-4533.
- Yamamoto, Y., & Imamoglu, A. (1999). *Mesoscopic quantum optics*. John Wiley and Sons.
- Yanik, M. F., Fan, S., Soljacic, M., & Joannopoulos, J. D. (2003). All-optical transistor action with bistable switching in a photonic crystal cross waveguide geometry. *Optic Letters*, 28, 2506.
- Zhou, Q.-C., & Zhu, S. N. (2005). Dynamics of a single-mode field interacting with a  $\lambda$ -type three-level atom. *Optics Communications*, 248, 437-448.